

p. 10
e-3 ka



elo. ↑

-Ka

Fig. 2, 3, 4, 5 (2 t. m)
18, 19, 20, 21, (1 t. m)
23, 24, 25, 26

Sensor and Simulation Notes

Note XLI
22 May 1967

Abis 411

The Multi-Gap Cylindrical Loop in Non-Conducting Media

Capt Carl E. Baum
Air Force Weapons Laboratory

straight on for some
of the ...

Abstract

The response characteristics of the multi-gap cylindrical loop are calculated for nonconducting media with certain restrictions on the loop design. The loop gaps are assumed to be evenly spaced around the loop and to have the same shape and identical resistive loads. As the number of loop gaps is increased the sensitivity to the direction of wave incidence is decreased and the upper frequency response (for sufficiently small cable conductance loading the loop) is increased.

Foreword

This note is a sequel to a previous note concerning the single-gap cylindrical loop. This note follows somewhat the same format as the previous note with the figures grouped together at the end. We would like to thank AIC Franklin Brewster, Jr. for programming the numerical calculations, and he and Mr. John N. Wood for preparing the graphs.

FOR PUBLIC RELEASE

PL/PA 10/27/94

PL 94-0911

Contents

<u>Section</u>	<u>Page</u>
I. Introduction	4
II. Short Circuit Currents	7
III. Admittances	11
IV. Frequency Response Characteristics	15
V. Summary	17

List of Illustrations

Figure 1. Multi-Gap Cylindrical Loop, Illustrated for N=4: Cross Section View	18
Figure 2. Short Circuit Current Transfer Function: N=1	19
Figure 3. Short Circuit Current Transfer Function: N=2	20
Figure 4. Short Circuit Current Transfer Function: N=4	21
Figure 5. Short Circuit Current Transfer Function: N=8	22
Figure 6. Normalized Internal Admittance: N=1	23
Figure 7. Normalized Internal Admittance: N=2	24
Figure 8. Normalized Internal Admittance: N=4	25
Figure 9. Normalized Internal Admittance: N=8	26
Figure 10. Normalized External Admittance: N=1	27
Figure 11. Normalized External Admittance: N=2	28
Figure 12. Normalized External Admittance: N=4	29
Figure 13. Normalized External Admittance: N=8	30
Figure 14. Effect of Admittances on Response: N=1, $\phi_o = .1$	31
Figure 15. Effect of Admittances on Response: N=2, $\phi_o = .1$	32
Figure 16. Effect of Admittances on Response: N=4, $\phi_o = .1$	33
Figure 17. Effect of Admittances on Response: N=8, $\phi_o = .1$	34

	<u>Page</u>
Figure 18. Artificial Response Characteristics: $N=1, \phi_o=.1$	35
Figure 19. Artificial Response Characteristics: $N=2, \phi_o=.1$	36
Figure 20. Artificial Response Characteristics: $N=4, \phi_o=.1$	37
Figure 21. Artificial Response Characteristics: $N=8, \phi_o=.1$	38
Figure 22. Dependence of Frequency Response on Cable Conductance: $\left T_{oy}^R(N) \right = 1/\sqrt{2}$	39
Figure 23. Response Characteristics: $N=1, \phi_o=.1, \frac{g_c^a}{Y_o} = 1$	40
Figure 24. Response Characteristics: $N=2, \phi_o=.1, \frac{g_c^a}{Y_o} = .6$	41
Figure 25. Response Characteristics: $N=4, \phi_o=.1, \frac{g_c^a}{Y_o} = .3$	42
Figure 26. Response Characteristics: $N=8, \phi_o=.1, \frac{g_c^a}{Y_o} = .07$	43

I. Introduction

In a previous note we considered the response characteristics of a single-gap cylindrical loop.¹ In a highly conducting external medium it was found advantageous to enclose the sensor in an insulator so as to increase the upper frequency response of the sensor for measuring \dot{B} . This use of an insulator to enclose the sensor also simplified the mathematical form of the sensor response by reducing an infinite sum to a single term for frequencies of interest. For what was termed the exposed cylindrical loop, the use of such an insulator then removes the dependence of the sensor response on the angle of wave incidence; so long as the direction of wave propagation is considered as perpendicular to the loop axis. For the case of a negligibly conducting external medium (with no added insulators) the response of the sensor is dependent on the angle of wave incidence for frequencies of interest, even with the direction of wave propagation perpendicular to the loop axis. However, in the previous note the variation of the sensor response with the angle of wave incidence was not considered; in this note it is considered, although still with the restriction that the wave is propagating perpendicular to the loop axis.

In this note we consider the response of a multi-gap cylindrical loop, one case of which is illustrated in figure 1. A previous note has considered some of the techniques for appropriately combining the signals from all the loop gaps for the case that the number of loop gaps is of the form 2^{M-1} where M is a positive integer.² For the present calculations we consider the case of N loop gaps, all of the same angular gap width, $2\phi_0$, and with each gap separated from the adjacent gaps by the angle, $\frac{2\pi}{N}$. For the graphs, however, we take N as 1, 2, 4, and 8. The loop axis^N is taken as the z axis and the x axis is taken as the direction of propagation of an incident plane wave. The angle of the center of the m th loop gap is ϕ_m . Choosing ϕ_1 and N then establishes the positions of all the loop gaps. Note that ϕ_1 is allowed to vary and as ϕ_1 is varied the loop response changes, at least for frequencies such that the radian wavelength, λ , is of the order of the loop radius, a . The magnetic field in the incident wave is taken parallel to the z axis. While the expressions for the loop response apply in the general case where the medium inside the loop has different parameters than the external medium, the graphs apply only to the case that both media have the same parameters. Also, for the numerical results in the graphs we only consider the case in which the conductivities in the two media are negligible.

The assumptions used for the calculations are essentially the same as those used for the single-gap cylindrical loop in nonconducting media in reference 1. Let the loop length, l , be sufficiently long so that $l \gg a$ and the solution involves only two spatial dimensions. Parameters such as the resistive gap loading are assumed independent of z . Practically, the resistive gap loading may be at discrete positions, uniformly spaced along the loop gaps, although the spacing between adjacent load positions on the

1. Capt Carl E. Baum, Sensor and Simulation Note XXX, The Single-Gap Cylindrical Loop in Non-Conducting and Conducting Media, January 1967.

2. Lt. Carl E. Baum, Sensor and Simulation Note XXIII, A Technique for the Distribution of Signal Inputs to Loops, July 1966.

same gap should be small compared to the loop radius and to the distance between the loop gaps so as to approximate a uniform distribution. The parameters, ϵ , μ , and σ , of the two media are assumed to be scalar constants, independent of position and time and have a subscript, l , applying to inside the loop and no subscript for the external medium. Other complications such as scattering of the fields from signal cables connected to the loop are not considered.

The electromagnetic field expansions for this problem are of the form³

$$H_z = H_{z_0} \sum_{n=0}^{\infty} a_n C_n^{(l)}(kr) \begin{cases} \cos(n\phi) \\ \sin(n\phi) \end{cases} \quad (1)$$

$$E_r = -jZH_z \sum_{n=0}^{\infty} a_n \frac{C_n^{(l)}(kr)}{kr} n \begin{cases} -\sin(n\phi) \\ \cos(n\phi) \end{cases} \quad (2)$$

and

$$E_\phi = jZH_z \sum_{n=0}^{\infty} a_n C_n^{(l)'}(kr) \begin{cases} \cos(n\phi) \\ \sin(n\phi) \end{cases} \quad (3)$$

where a time dependence of the form $e^{j\omega t}$ is assumed but is suppressed from all the expressions. One of the Bessel functions is denoted by $C_n^{(l)}(kr)$; a prime over a Bessel function denotes the derivative with respect to the argument. The braces with the trigonometric functions indicate a linear combination of these functions (the same combination for the three field components). The propagation constant is of the form

$$k = \sqrt{-j\omega\mu(\sigma + j\omega\epsilon)} \quad (4)$$

where for $\sigma \ll \omega\epsilon$ this reduces to

$$k = \omega\sqrt{\mu\epsilon} = \frac{1}{\lambda} \quad (5)$$

The wave impedance is of the form

$$Z = \sqrt{\frac{j\omega\mu}{\sigma + j\omega\epsilon}} \quad (6)$$

These two parameters are subscripted to apply to the two media. Since H_z and E_ϕ are sufficient to match the boundary conditions on the circular cylinder, then for convenience E_r is not listed with the field expansions.

3. Units are rationalized MKSA.

As with the case of the single-gap cylindrical loop previously considered, we first calculate the surface current density on the cylinder with the gaps shorted. The surface current density at the N gaps is averaged and normalized to the magnetic field in the incident wave. This averaging is appropriate since we assume that the signal connections to the loop gaps are such as to add the signals from each of the loop gaps and that each gap presents an identical impedance to that part of the signal common to all the loop gaps. The signal network connecting the loop gaps is also assumed to reject signals not common to all the loop gaps.⁴ The short circuit current transfer function obtained in this manner is an infinite series in which the index, n , (as in equations (1) through (3)) takes on values of zero and integer multiples of N , the number of loop gaps. The reduction of the short circuit current transfer function to this form, rejecting terms in the surface current density expansion, depends on symmetry in the spacing and dimensions of the loop gaps, and in the impedances at the loop gaps. Such symmetry is assumed for the calculations in this note. The short circuit current transfer function is a function of both the number of loop gaps and the angle of the first loop gap in relation to the direction of wave incidence. As N is increased the dependence of the loop response on ϕ_1 is decreased for frequencies of interest. The dependence of the loop response on ϕ_1 is contained in the terms for $n \geq 1$ in the field expansion and several of these terms are significant. One might think of the $n=1$ term as associated with the electric field near the sensor. Then the dependence of the response on ϕ_1 is not appropriately called an electric field sensitivity, at least for λ of the order of a , because terms for $n \geq 2$ are also rather significant. In fact, the two-gap loop has no contribution to its response from the $n=1$ term, but the response is still dependent on ϕ_1 . The dependence of the response on ϕ_1 can more appropriately be called a directional sensitivity.

Next the admittances per unit length at the loop gap are considered. There are three such admittances to consider, one associated with the interior of the loop, a second associated with the exterior of the loop, and a third associated with signal cables. The first two of these admittances per unit length require expansion of the electromagnetic fields inside and outside the loop structure. Since we are concerned with a loop structure which is periodic in ϕ with a period of $\frac{2\pi}{N}$, and since we are only interested (for the loop response) in signals common to all the loop gaps, these admittances can be calculated by driving all the gaps with the same voltage. Then we only use terms in the field expansions for which n is zero or an integer multiple of N to obtain the currents at the loop gaps. The symmetry of the loop structure simplifies the admittances somewhat. The boundary condition for the electric field at the loop gap which is used in calculating these admittances is the same quasi-static approximation used for the single-gap loop in the previously referenced note. All the admittances per unit length are normalized by dividing each by the low frequency form of the loop admittance, that associated with a simple inductance. The sum of the normalized admittances then conveniently goes to one in the low frequency limit.

4. For an example of such a signal connection network see reference 2.

As mentioned before, increasing the number of loop gaps has the effect of reducing the directional sensitivity of the sensor. Another effect of increasing the number of loop gaps is that of improving the high frequency response characteristics of the sensor. This latter effect is associated with the changes in the admittances as the number of loop gaps is increased. Thus, the multi-gap cylindrical loop has some distinct advantages over the single-gap cylindrical loop. Note that while the calculations in this note are made for a circular cylindrical loop, as illustrated in figure 1, they also apply to a half cylinder on a perfectly conducting infinite plane, providing that the conducting plane is symmetrically positioned with respect to the loop gaps. Then the image of the half cylindrical loop combines with the loop to give a full cylinder with uniformly spaced, identical loop gaps. In the case of such an image problem there is, of course, an additional wave to be considered which is the reflection of the incident wave off the conducting plane, or if one prefers, the image of the incident wave.

II. Short Circuit Currents

Consider the surface current density on the multi-gap cylindrical loop with all the gaps shorted along the full length of the loop. This leaves a continuous perfectly conducting cylinder of radius, a .

The incident plane wave is of the form (for the magnetic field)

$$H_{z_{inc}} = H_{z_0} e^{-jkx} = H_{z_0} e^{-jkr\cos(\phi)} \quad (7)$$

Note that the angle, ϕ , in figure 1 is defined as zero on the positive x axis in this note. In the previous note on the single-gap cylindrical loop ϕ was defined as zero on the positive y axis because of the fixed position of the loop gap as centered on the y axis. In this note the position of the loop gap is allowed to vary, making the present definition, as in figure 1, more convenient. Expanding equation (7) in the⁵ characteristic functions appropriate to cylindrical coordinates gives

$$H_{z_{inc}} = H_{z_0} \left[J_0(kr) + 2 \sum_{n=1}^{\infty} (-j)^n J_n(kr) \cos(n\phi) \right] \quad (8)$$

From equations (1) through (3) the associated azimuthal electric field is

$$E_{\phi_{inc}} = jZH_{z_0} \left[J'_0(kr) + 2 \sum_{n=1}^{\infty} (-j)^n J'_n(kr) \cos(n\phi) \right] \quad (9)$$

5. See AMS 55, Handbook of Mathematical Functions, National Bureau of Standards, 1964, for the expansions of $\cos[kr\cos(\phi)]$ and $\sin[kr\cos(\phi)]$.

Add. to this incident wave a reflected wave of the form

$$H_{z_{\text{refl}}} = H_{z_0} \left[a_0 H_0^{(2)}(kr) + 2 \sum_{n=1}^{\infty} (-j)^n a_n H_n^{(2)}(kr) \cos(n\phi) \right] \quad (10)$$

and

$$E_{\phi_{\text{refl}}} = jZH_{z_0} \left[a_0 H_0^{(2)'}(kr) + 2 \sum_{n=1}^{\infty} (-j)^n a_n H_n^{(2)'}(kr) \cos(n\phi) \right] \quad (11)$$

Setting the tangential electric field to zero at $r=a$ gives, from equations (9) and (11),

$$J_n'(ka) + a_n H_n^{(2)'}(ka) = 0 \quad (12)$$

or

$$a_n = - \frac{J_n'(ka)}{H_n^{(2)'}(ka)} \quad (13)$$

The short circuit surface current density is

$$J_{s_0}(\phi) = - \left[H_{z_{\text{inc}}} (a, \phi) + H_{z_{\text{refl}}} (a, \phi) \right] \quad (14)$$

For convenience we define a function of the form

$$T_n = J_n(ka) - \frac{J_n'(ka)}{H_n^{(2)'}(ka)} H_n^{(2)}(ka) \\ = \left[j \frac{\pi ka}{2} H_n^{(2)'}(ka) \right]^{-1} \quad (15)$$

where the last form is obtained by the application of a Wronskian relationship to the Bessel functions. From equations (8), (10), (13), (14), and (15) the short circuit surface current density is then

$$J_{s_0}(\phi) = -H_{z_0} \left[T_0 + 2 \sum_{n=1}^{\infty} (-j)^n T_n \cos(n\phi) \right] \quad (16)$$

Now define the short circuit current transfer function as the average of the short circuit surface current densities at the N loop gaps, divided by $-H_{z_0}$ to normalize the result. The short circuit current transfer function is then

$$\begin{aligned} T(\phi_1, N) &= -\frac{1}{NH_{z_0}} \sum_{m=1}^N J_{s_0}(\phi_m) \\ &= \frac{1}{N} \sum_{m=1}^N \left[T_0 + 2 \sum_{n=1}^{\infty} (-j)^n T_n \cos(n\phi_m) \right] \end{aligned} \quad (17)$$

Here we have ignored the variation of the surface current density over the angular width ($2\phi_0$) of the loop gap and have taken the value of the surface current density at the center, ϕ_m , of the loop gap. Thus, the width of the loop gap is assumed to be small compared to both the radius of the cylinder and the distance to the next loop gap. Again we take the average of the current densities at the N loop gaps because of the symmetry in the structure and in any signal cable network connected to the loop gaps.

Since the loop gaps are spaced a uniform angle, $\frac{2\pi}{N}$, apart the short circuit current transfer function simplifies to some extent. Equation (17) can be written, by interchanging the order of the summations, as

$$\begin{aligned} T(\phi_1, N) &= T_0 + 2 \sum_{n=1}^{\infty} (-j)^n T_n \left[\frac{1}{N} \sum_{m=1}^N \cos(n\phi_m) \right] \\ &= T_0 + 2 \sum_{n=1}^{\infty} (-j)^n T_n \left[\frac{1}{N} \sum_{m=1}^N \cos\left[n\left(\phi_1 + \frac{2\pi(m-1)}{N}\right)\right] \right] \end{aligned} \quad (18)$$

Solve for the inside sum as

$$\begin{aligned} \frac{1}{N} \sum_{m=1}^N \cos\left[n\left(\phi_1 + \frac{2\pi(m-1)}{N}\right)\right] &= \frac{1}{N} \operatorname{Re} \left[\sum_{m=1}^N e^{jn\left(\phi_1 + \frac{2\pi(m-1)}{N}\right)} \right] \\ &= \frac{1}{N} \operatorname{Re} \left[e^{jn\phi_1} \sum_{m=1}^N e^{j \frac{2\pi n(m-1)}{N}} \right] \\ &= \frac{1}{N} \operatorname{Re} \left[e^{jn\phi_1} \sum_{m=0}^{N-1} e^{j \frac{2\pi nm}{N}} \right] \end{aligned} \quad (19)$$

where Re indicates that only the real part of the complex number is taken. If $n = MN$ where M is a positive integer, then

$$\frac{1}{N} \sum_{m=1}^N \cos \left[n \left(\phi_1 + \frac{2\pi(m-1)}{N} \right) \right] = \frac{1}{N} \operatorname{Re} \left[e^{jn\phi_1} \sum_{m=0}^{N-1} 1 \right] = \cos(n\phi_1) \quad (20)$$

On the other hand if $n \neq MN$ we have a finite geometric series which can be summed giving

$$\frac{1}{N} \sum_{m=1}^N \cos \left[n \left(\phi_1 + \frac{2\pi(m-1)}{N} \right) \right] = \frac{1}{N} \operatorname{Re} \left[e^{jn\phi_1} \frac{1 - e^{j2\pi n}}{1 - e^{j\frac{2\pi n}{N}}} \right] = 0 \quad (21)$$

Thus, the only terms which contribute to the short circuit current transfer function are those for $n = MN$. The short circuit current transfer function can then be written as⁶

$$T(\phi_1, N) = T_0 + 2 \sum_{n=N}^{\infty, N} (-j)^n T_n \cos(n\phi_1) \quad (22)$$

giving a compact form for the result

This short circuit current transfer function is plotted versus λ/a in figures 2 through 5 for N equal to 1, 2, 4, and 8 for various values of ϕ_1 . Note that $T(\phi_1, N)$ is both even in ϕ_1 and periodic in ϕ_1 with a period of 2π . Thus, we choose ϕ_1 only in the range $0 \leq \frac{N\phi_1}{\pi} \leq 1$. For convenience we multiply $T(\phi_1, N)$ by e^{jka} for the plots. We also include this factor for any later plots which include $T(\phi_1, N)$ or T_0 as factors in the equations. This just adds ka to the phase since for the graphs only the case of $\sigma \ll \omega$ is considered. Note that $T(\phi_1, N)$ is independent of ϕ_1 for $\lambda/a \gg 1$, but that, progressing toward smaller λ/a , $T(\phi_1, N)$ departs from one and becomes more and more dependent on ϕ_1 . Note also that as N is increased $T(\phi_1, N)$ maintains its approximate independence of ϕ_1 to smaller and smaller values of λ/a . As a limiting case we define

$$T(\infty) = \lim_{N \rightarrow \infty} T(N, \phi_1) = T_0 \quad (23)$$

which is independent of ϕ_1 for all λ/a . This is included in the four figures for comparison.

The region of interest for the maximum frequency response of the loop is given by λ/a of the order of one. Looking at figures 2 through 5 we can see that the first several terms in the expansion of the surface current density are significant in the loop response. As N is increased more and more of the terms corresponding to $n \geq 1$ are removed and the directional sensitivity of the loop is decreased for frequencies of interest. As N is increased $T(\phi_1, N)$ behaves like $T(\infty)$ to smaller and smaller λ/a .

6. As in reference 1 the second term above the summation sign is the increment in n (starting at the lower limit) for the successive terms in the summation.

III. Admittances

Consider now the admittances associated with the multi-gap cylindrical loop. Since we are concerned only with signals common to all the loop gaps, then for the admittances we drive all the gaps with the same voltage, V_{gap}/N , and calculate the surface current densities produced. This gives three admittances per unit length, one associated with the loop interior, one associated with the loop exterior and one associated with the signal cables loading the loop gap. For these admittances the loop gaps are assumed to be electrically in series. If configurations other than series (but still with the necessary symmetry) are used the results still apply if proper factors are introduced to account for the changed number of turns, etc. Since for the admittance calculations there is no incident wave, then ϕ_1 is arbitrary and it is taken as zero for convenience. Also the loop gap widths are considered sufficiently small such that $2\phi_0 \ll 1$ and $2\phi_0 \ll \frac{2\pi}{N}$.

A. Boundary Conditions at Loop Gap

To calculate the admittances associated with the interior and exterior of the loop we use the same quasi-static approximation as in reference 1 for the electric field in the loop gaps. Then for $r=a$ and $|\phi - \phi_m| < \phi_0$ the azimuthal electric field in the m th loop gap is

$$E_\phi(a, \phi) = -\frac{V_{\text{gap}}}{Na\phi_0} f\left(\frac{\phi - \phi_m}{\phi_0}\right) \quad (24)$$

where

$$f(\xi) = \frac{1}{\pi} \left[1 - \xi^2\right]^{-1/2} \quad (25)$$

For $r=a$, but ϕ not in one of the loop gaps, $E_\phi(a, \phi)$ is zero.

Again this field distribution in the loop gaps is somewhat approximate, ignoring the presence of disturbing objects such as signal cable connections. Within the limitations of our assumption of z independent geometry, however, this is a reasonable field distribution to use.

B. Internal Admittance

Consider the internal admittance per unit length of the multi-gap cylindrical loop. The loop structure and the azimuthal electric field in the loop gaps are periodic in ϕ with a period, $\frac{2\pi}{N}$. The fields inside the loop then have the same periodicity, and thus the only terms in the field expansion are those with n an integer multiple of N . Since we take $\phi_1=0$ for these calculations the loop structure and the azimuthal electric field are also even in ϕ . Thus, we have the field expansion inside the loop as

$$H_z(r, \phi) = H_{z_0} \left[a_0 J_0(k_\perp r) + 2 \sum_{n=N}^{\infty} a_n J_n(k_\perp r) \cos(n\phi) \right] \quad (26)$$

and

$$E_\phi(r, \phi) = jZ_\ell H_{z_0} \left[a_0 J'_0(k_\ell r) + 2 \sum_{n=N}^{\infty, N} a_n J'_n(k_\ell r) \cos(n\phi) \right] \quad (27)$$

Equate $E_\phi(a, \phi)$ from equations (24) and (27). Multiply by $\cos(n\phi)$ and integrate from 0 to 2π giving

$$-\frac{V_{\text{gap}}}{Na\phi_0} \sum_{m=1}^N \left[\int_{\phi_m - \phi_0}^{\phi_m + \phi_0} f\left(\frac{\phi - \phi_m}{\phi_0}\right) \cos(n\phi) d\phi \right] = j2\pi Z_\ell H_{z_0} a_n J'_n(k_\ell a) \quad (28)$$

or, since $\phi_m = \frac{2\pi}{N}(m-1)$ and $\cos(n\phi)$ is periodic with a period of $\frac{2\pi}{N}$ (for n an integer multiple of N), this becomes

$$-\frac{V_{\text{gap}}}{a\phi_0} \int_{-\phi_0}^{\phi_0} f\left(\frac{\phi}{\phi_0}\right) \cos(n\phi) d\phi = j2\pi Z_\ell H_{z_0} a_n J'_n(k_\ell a) \quad (29)$$

This expression was evaluated in reference 1, giving

$$a_n = \frac{jV_{\text{gap}} J_0(n\phi_0)}{2\pi a Z_\ell F'_0 J'_n(k_\ell a)} \quad (30)$$

The surface current density associated with the internal admittance is

$$J_{s_\ell} = H_z(a, \phi_m \pm \phi_0) = H_z(a, \pm \phi_0) \quad (31)$$

Define

$$Y_{\ell n} = -\frac{J_n(k_\ell a)}{J'_n(k_\ell a)} \quad (32)$$

The admittance per unit length is then

$$y_\ell = \frac{J_{s_\ell}}{V_{\text{gap}}} = -\frac{i}{2\pi a Z_\ell} \left[Y_{\ell 0} + 2 \sum_{n=N}^{\infty, N} Y_{\ell n} J_0(n\phi_0) \cos(n\phi_0) \right] \quad (33)$$

Multiply this by $j\omega\mu_\ell \pi a^2$, the low frequency form of the loop admittance, to give the normalized internal admittance as

$$Y_\ell(N) = j\omega\mu_\ell \pi a^2 y_\ell = \frac{k_\ell a}{2} \left[Y_{\ell 0} + 2 \sum_{n=N}^{\infty, N} Y_{\ell n} J_0(n\phi_0) \cos(n\phi_0) \right] \quad (34)$$

Note that for $N=1$ this reduces to the result for a single-gap loop considered in reference 1.

The normalized internal admittance is plotted versus χ/a in figures 6 through 9 for N equal to 1, 2, 4, and 8 for a few values of ϕ_0 . For these plots $\epsilon_\ell = \epsilon$, $\mu_\ell = \mu$, and $\sigma_\ell = \sigma = 0$. For $\chi/a \gg 1$ the normalized internal admittance is approximately one. As χ/a is decreased $Y_\ell(N)$ departs from unity, but for the larger values of ϕ_0 the normalized internal admittance stays close to one to smaller values of χ/a . In the figures $Y_\ell(N)$ is plotted to small enough χ/a to include the first few infinities. These infinities are associated with the zeros of $J'_n(k_\ell a)$. As N is increased and terms are removed from the summation in equation (34), some of the infinities are removed from $Y_\ell(N)$. As a limiting case we define--

$$Y_\ell(\infty) = \lim_{N \rightarrow \infty} Y_\ell(N) = \frac{k_\ell a}{2} Y_{\ell 0} \quad (35)$$

which is independent of ϕ_0 and is included in the graphs for comparison. Note that as N is increased, $Y_\ell(N)$ approaches $Y_\ell(\infty)$, which we might consider the ideal case. There is a particularly noticeable improvement as N increases past 1 and 2 because the first two infinities, in order of decreasing χ/a , are removed, until we are left with the infinity at $\chi/a = .261$ associated with the $n=0$ term. Thus, increasing N decreases the χ/a to which $Y_\ell(N)$ is approximately 1, thereby possibly increasing the upper frequency response of the sensor.

C. External Admittance

The external admittance is calculated in a manner similar to the internal admittance. Expand the electromagnetic fields outside the loop as

$$H_z(r, \phi) = H_{z_0} \left[a_0 H_0^{(2)}(kr) + 2 \sum_{n=N}^{\infty, N} a_n H_n^{(2)}(kr) \cos(n\phi) \right] \quad (36)$$

and

$$E_\phi(r, \phi) = jZH_{z_0} \left[a_0 H_0^{(2)'}(kr) + 2 \sum_{n=N}^{\infty, N} a_n H_n^{(2)'}(kr) \cos(n\phi) \right] \quad (37)$$

These expressions are the same as those for the internal admittance except that the Bessel functions of the first kind have been replaced by Hankel functions of the second kind, and the parameters for the internal medium are replaced by those for the external medium. The coefficients are then

$$a_n = \frac{jV_{\text{gap}} J_0(n\phi_0)}{2\pi a Z H_{z_0} H_n^{(2)'}(ka)} \quad (38)$$

The surface current density associated with the external admittance is

$$J_{s_{\text{ext}}} = -H_z(a, \phi_m + \phi_o) = -H_z(a, \pm \phi_o) \quad (39)$$

Define

$$Y_{\text{ext}_n} = \frac{H_n^{(2)}(ka)}{H_n^{(2)'}(ka)} \quad (40)$$

The admittance per unit length is then

$$y_{\text{ext}} = \frac{J_{s_{\text{ext}}}}{V_{\text{gap}}} = -\frac{j}{2\pi a Z} \left[Y_{\text{ext}_o} + 2 \sum_{n=N}^{\infty, N} Y_{\text{ext}_n} \frac{J_o(n\phi_o) \cos(n\phi_o)}{J_o(n\phi_o) \cos(n\phi_o)} \right] \quad (41)$$

The normalized external admittance is given by

$$Y_{\text{ext}}(N) = j\omega\mu_\ell \pi a^2 y_{\text{ext}} = \frac{\mu_\ell}{\mu} \frac{ka}{2} \left[Y_{\text{ext}_o} + 2 \sum_{n=N}^{\infty, N} Y_{\text{ext}_n} \frac{J_o(n\phi_o) \cos(n\phi_o)}{J_o(n\phi_o) \cos(n\phi_o)} \right] \quad (42)$$

The normalized external admittance is plotted versus λ/a in figures 10 through 13 for N equal to 1, 2, 4, and 8 for a few values of ϕ_o . For these plots $\mu_\ell = \mu$ and $\sigma = 0$. Note that for $\lambda/a \gg 1$ the normalized external admittance is small compared to one and thus, small compared to the normalized internal admittance. As a limiting case we define

$$Y_{\text{ext}}(\infty) = \lim_{N \rightarrow \infty} Y_{\text{ext}}(N) = \frac{\mu_\ell}{\mu} \frac{ka}{2} Y_{\text{ext}_o} \quad (43)$$

which is independent of ϕ_o and is included in the graphs for comparison. Note that as N is increased, $Y_\ell(N)$ approaches $Y_\ell(\infty)$, which we might consider the ideal case.

D. Cable Admittance

The admittance per unit length associated with the signal cables is defined as g_c . This is calculated from

$$g_c = \frac{1}{Z_c \ell} \quad (44)$$

where ℓ is the length of the cylinder and Z_c is the cable impedance at the loop gaps, the gaps being considered as driven in series. Thus, Z_c is the sum of the cable impedances associated with each loop gap, or N times the impedance associated with any one loop gap.

In normalized form define

$$G_c = j\omega\mu_\ell\pi a^2 g_c \quad (45)$$

which we call the normalized cable conductance. Rewrite G_c as

$$G_c = j \frac{\mu_\ell}{\mu} \pi k a \left(\frac{g_c a}{Y} \right) \quad (46)$$

where

$$Y = \frac{1}{Z} \quad (47)$$

and is the wave admittance. For the special case of $\epsilon_\ell = \epsilon = \epsilon_0$, $\mu_\ell = \mu = \mu_0$, and $\sigma_\ell = \sigma = 0$ which is used for the plots, we have a normalized cable conductance of the form

$$G_c = j\pi \left(\frac{\chi}{a} \right)^{-1} \left(\frac{g_c a}{Y_0} \right) \quad (48)$$

where $g_c a/Y_0$ is a convenient dimensionless parameter and Y_0 is the wave admittance of free space.

IV. Frequency Response Characteristics

As an intermediate step in obtaining the frequency response curves for the multi-gap cylindrical loop define a response function which includes only the admittances as

$$R_y(N) = \left[Y_\ell(N) + Y_{\text{ext}}(N) + G_c \right]^{-1} \quad (49)$$

This is graphed versus χ/a in figures 14 through 17 for an N of 1, 2, 4, and 8 with $g_c a/Y_0$ as a parameter for the curves. For $g_c a/Y_0 = 0$ note that as N is increased the first peak (in order of decreasing χ/a) in the response curve is both made smaller and moved to smaller χ/a . Increasing N would then seem to improve the frequency response characteristics of the cylindrical loop. We choose $\phi_0 = .1$ for these and subsequent response curves.

Including the short circuit current transfer function, define the response function for the multi-gap cylindrical loop as

$$R(\phi_1, N) = T(\phi_1, N) R_y(N) \quad (50)$$

For comparison consider the limiting case of

$$\begin{aligned}
R(\infty) \Big|_{g_c=0} &= \lim_{N \rightarrow \infty} R(\phi_1, N) \Big|_{g_c=0} \\
&= T_o \left[Y_\ell(\infty) + Y_{\text{ext}}(\infty) \right]^{-1} \\
&= \left[-j \frac{\pi k a}{2} H_1^{(2)}(ka) \right]^{-1} \left\{ \frac{k a}{2} \left[\frac{J_o(ka)}{J_1(ka)} - \frac{H_o^{(2)}(ka)}{H_1^{(2)}(ka)} \right] \right\}^{-1} \\
&= \frac{2}{k a} \left\{ -j \frac{\pi k a}{2} \frac{J_o(ka) H_1^{(2)}(ka) - H_o^{(2)}(ka) J_1(ka)}{J_1(ka)} \right\}^{-1} \\
&= \frac{2}{k a} J_1(ka) \tag{51}
\end{aligned}$$

where for this response function we have used $\epsilon_\ell = \epsilon$, $\mu_\ell = \mu$, and $\sigma_\ell = \sigma$. Note the relatively simple form for this last response function; for $\sigma = 0$ this function is a purely real number.

Before considering the dependence of $R(\phi_1, N)$ on ϕ_1 , let us consider just its dependence on λ/a , $g_c a/Y_o$, and N . To do this we consider an artificial response function of the form, $T_o R_y(N)$. Referring to figures 2 through 5 note that T_o (or $T(\infty)$) approximates $T(\phi_1, N)$ above some λ/a of the order of one and that as N increases the approximation improves, holding down to smaller λ/a . Also if we were to average $T(\phi_1, N)$ over ϕ_1 for $0 \leq \phi_1 \leq 2\pi$ we would have precisely T_o . In figures 18 through 21 there is plotted $T_o R_y(N)$ versus λ/a for an N of 1, 2, 4, and 8 with $g_c a/Y_o$ as a parameter for the curves. The comparison function from equation (51) is also included in these figures. Note for $g_c a/Y_o = 0$ that as N is increased the response curves approach $R(\infty)$ closer and closer and the frequency response of the loop increases.

Based on $T_o R_y(N)$ we define an upper frequency response as the maximum value of λ/a for which

$$|T_o R_y(N)| = \frac{1}{\sqrt{2}} \tag{52}$$

Referring to figures 18 through 21 note that for sufficiently small $g_c a/Y_o$, then $|T_o R_y(N)|$ has a significant peak (in the vicinity of $\lambda/a = 1$) before it falls off for decreasing λ/a . For sufficiently large $g_c a/Y_o$ this peak is removed, giving a smoother response curve. There is a smallest value of $g_c a/Y_o$ for which $|T_o R_y(N)|$ does not rise above one before falling off. We call such a condition a maximally flat frequency response. In figure 22 the λ/a for upper frequency response (as defined in equation (52)) is plotted versus $g_c a/Y_o$. Two values of ϕ_o and four values of N are used for these curves, and each curve is arbitrarily ended at approximately that value of $g_c a/Y_o$ corresponding to a maximally flat frequency response for the particular ϕ_o and N . Note that as N is increased and/or ϕ_o is increased one can use smaller values of $g_c a/Y_o$ to obtain a larger frequency response for a given loop radius.

Finally, we have $R(\phi_1, N)$ plotted in figures 23 through 26, illustrating the dependence of the loop response on ϕ_1 . For these graphs $\phi_0 = .1$ and $g_c a / Y_0$ is chosen for each N to give an approximately maximally flat frequency response, based on the previous calculations with $T_{O R_y}(N)$. As with the short circuit current transfer function we choose ϕ_1 in the range $0 < \frac{N\phi_1}{\pi} < 1$.

Note that for an N of 1 or 2 the loop response is significantly dependent on ϕ_1 for frequencies for which the response is still significant (i.e., for $|R(\phi_1, N)|$ near one). For an N of 4, however, the region of significant dependence on ϕ_1 is confined to smaller λ/a where $|R(\phi_1, 4)|$ is significantly lower than one. Finally, for an N of 8, the dependence on ϕ_1 is essentially absent from the response for frequencies for which the response is significant. Thus increasing N can significantly reduce the dependence of the loop response on ϕ_1 .

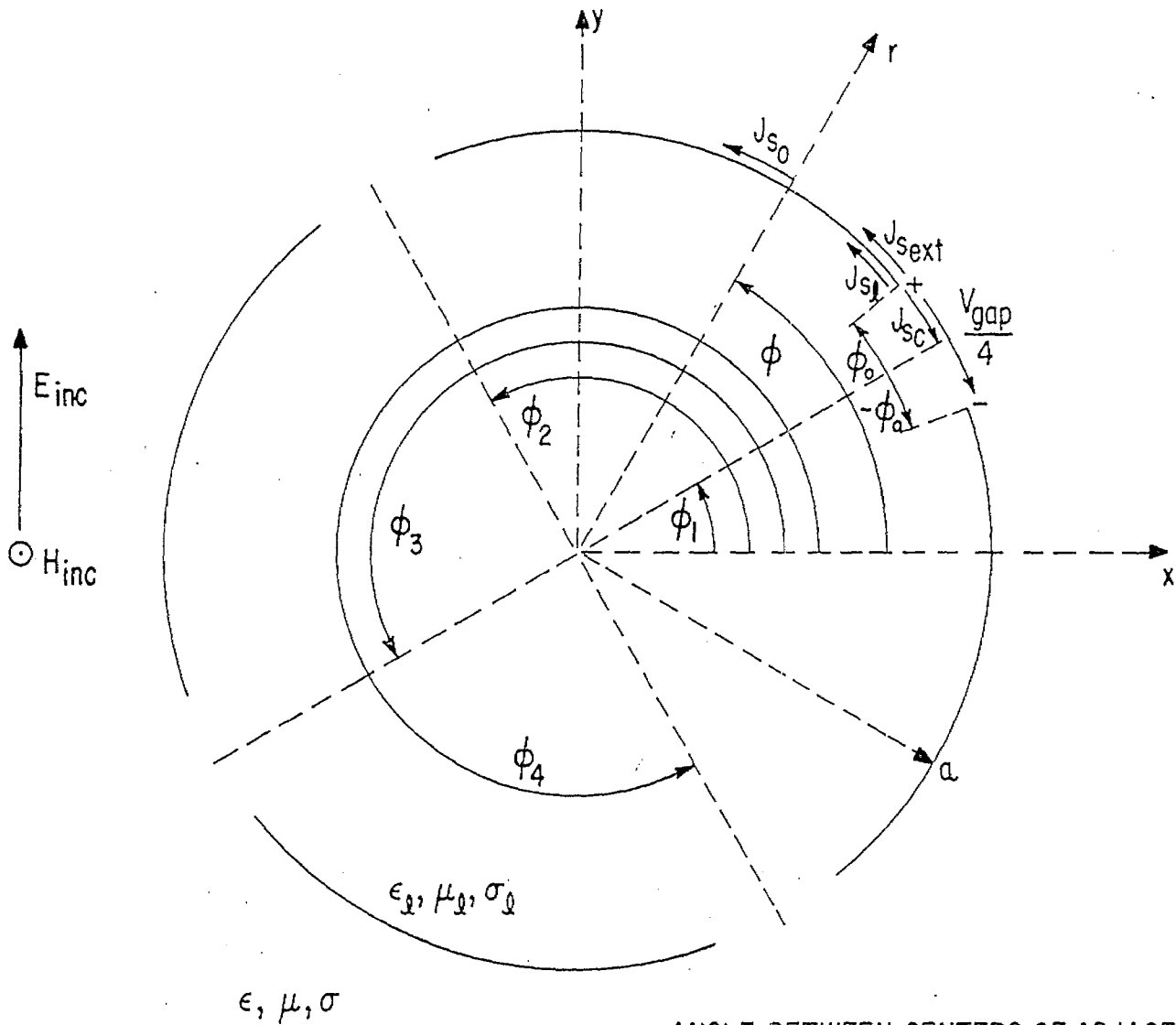
V. Summary

We have considered the response characteristics of the multi-gap cylindrical loop under some simplifying assumptions. The incident wave is considered propagating perpendicular to the loop axis and the length of the loop is assumed much larger than the radius so as to leave a two-dimensional problem. For the same reason the resistive loading is assumed to be uniformly distributed along the loop gaps. The loop response is also assumed to be insignificantly affected by close proximity to other field scatterers such as signal cables connected to the loop. One should be cautious because these various assumptions are often only very approximately correct.

The response of the multi-gap cylindrical loop is analyzed based on a Norton equivalent circuit. The short circuit current transfer function is first obtained, followed by the admittances. The multi-gap cylindrical loop is constrained to be periodic in ϕ with a period of $\frac{2\pi}{N}$ where N is the number of loop gaps; the loop gaps are evenly spaced around the loop and all loop gaps have the same width, resistive loading, etc. This periodicity in the loop structure simplifies the mathematical forms of the short circuit current transfer function and the normalized internal and external admittances. As N is increased two significant effects on the loop response are observed for frequencies of interest (for λ/a of the order of one): the dependence of the loop response on the direction of the wave incidence is decreased, and the upper frequency response (presuming sufficiently small $g_c a / Y_0$) is increased.

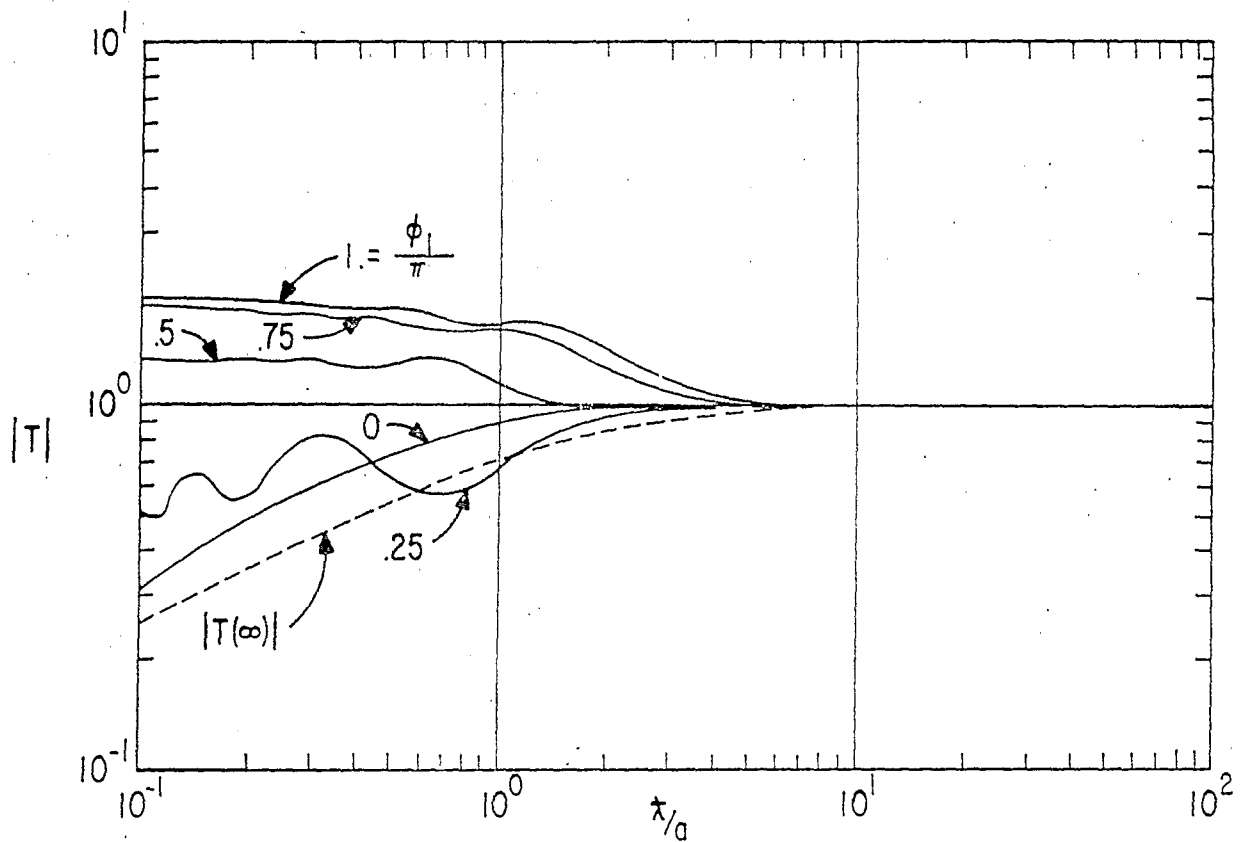
The mathematical expressions developed in this note are very similar to those in reference 1. For $N > 1$ certain terms are merely not included in the sums. As a result the accuracies in the computations are essentially the same as for the corresponding computations in the previous note on the single-gap cylindrical loop. Thus, one may refer to the appendix of reference 1 for a more detailed discussion of these accuracies, which are held to a few percent as in this previous case.

LENGTH OF THE LOOP (INTO AND OUT OF THE PAGE) IS Q .

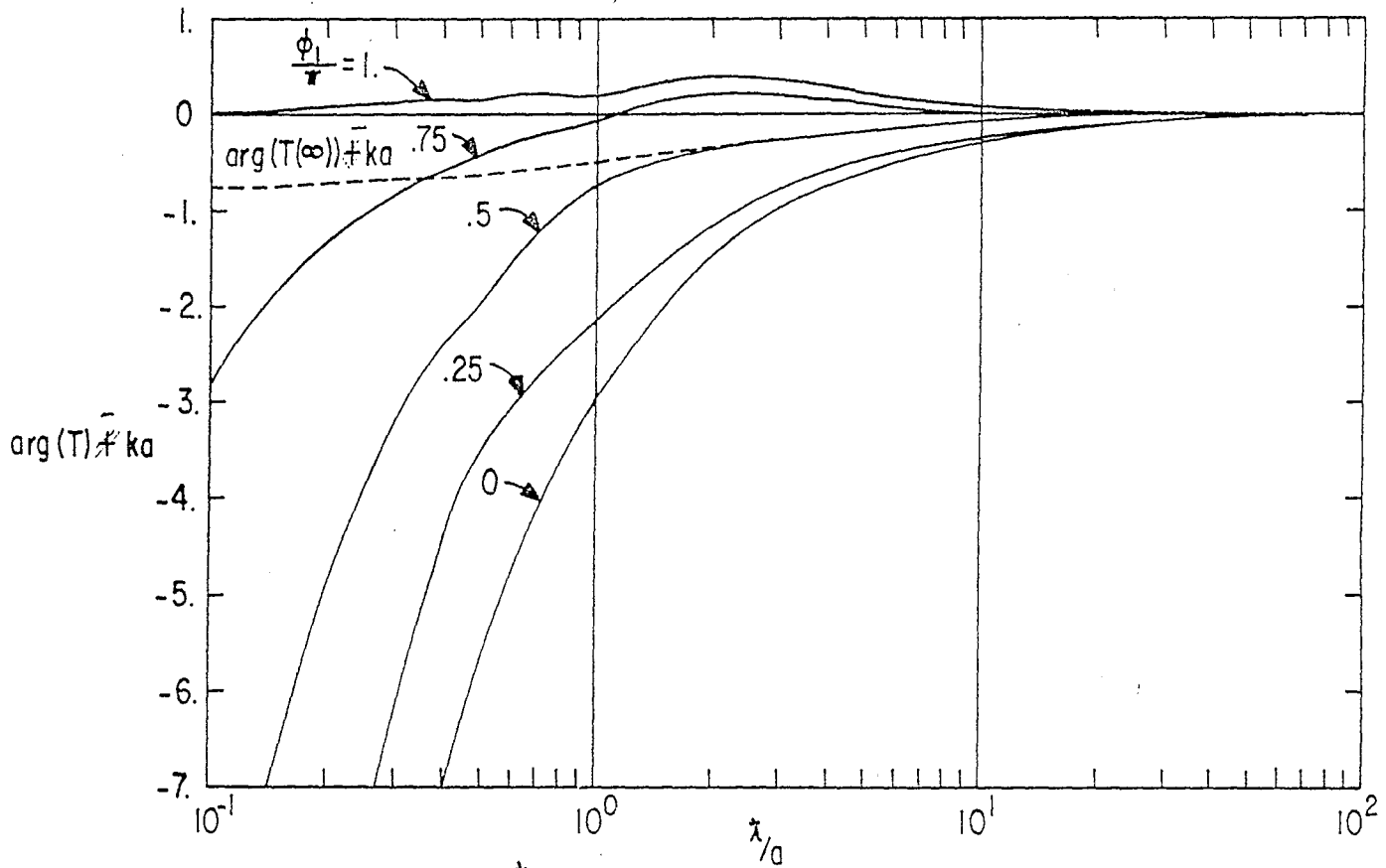


ANGLE BETWEEN CENTERS OF ADJACENT LOOP GAPS IS $\frac{2\pi}{N}$. ALL LOOP GAPS HAVE THE SAME ANGULAR WIDTH.

FIGURE 1. MULTI-GAP CYLINDRICAL LOOP, ILLUSTRATED FOR $N = 4$: CROSS SECTION VIEW

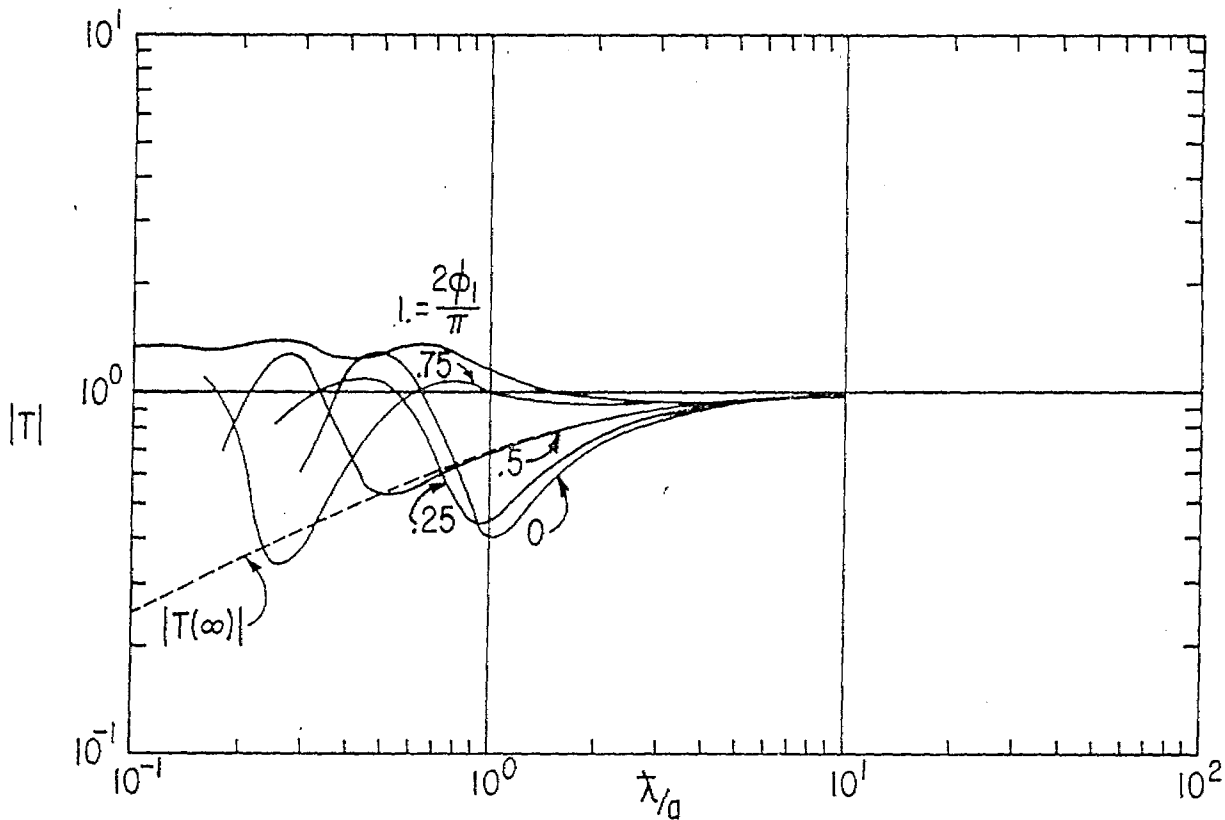


A. MAGNITUDE OF $T(\phi_1, l)$ vs. λ/a WITH ϕ_1 , AS A PARAMETER

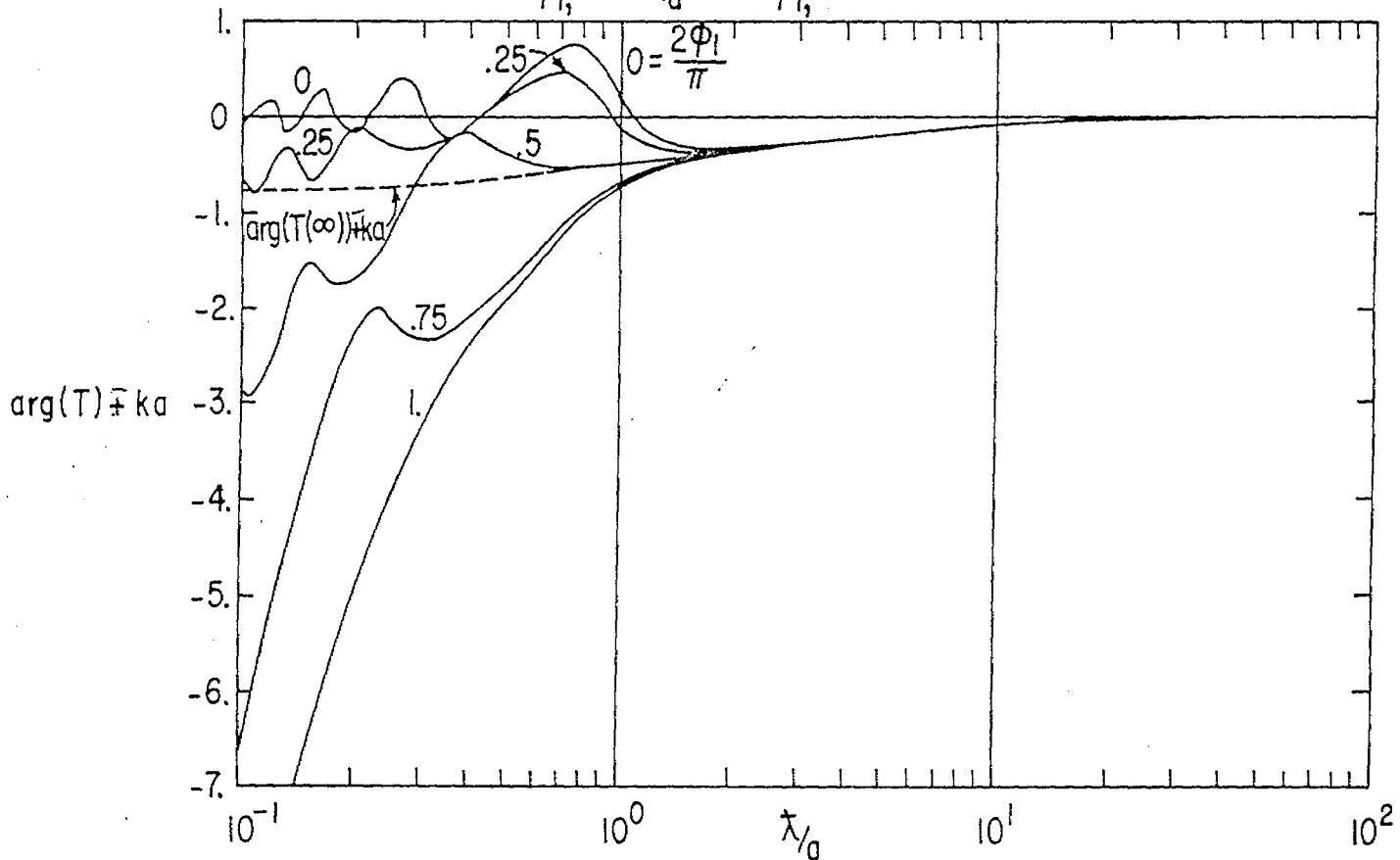


B. PHASE OF $T(\phi_1, l)$ vs. λ/a WITH ϕ_1 AS A PARAMETER

FIGURE 2. SHORT CIRCUIT CURRENT TRANSFER FUNCTION: $N=1$

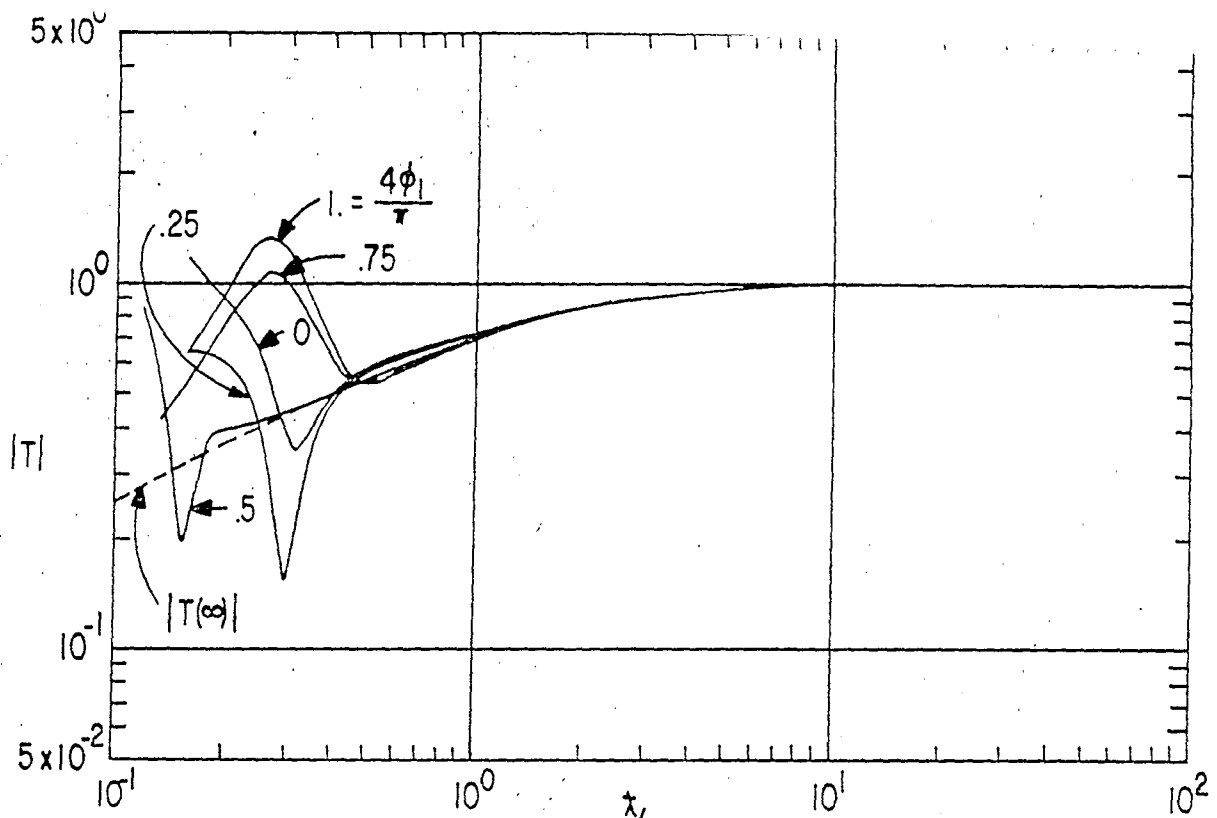


A. MAGNITUDE OF $T(\phi_1, 2)$ vs. λ/a WITH ϕ_1 AS A PARAMETER

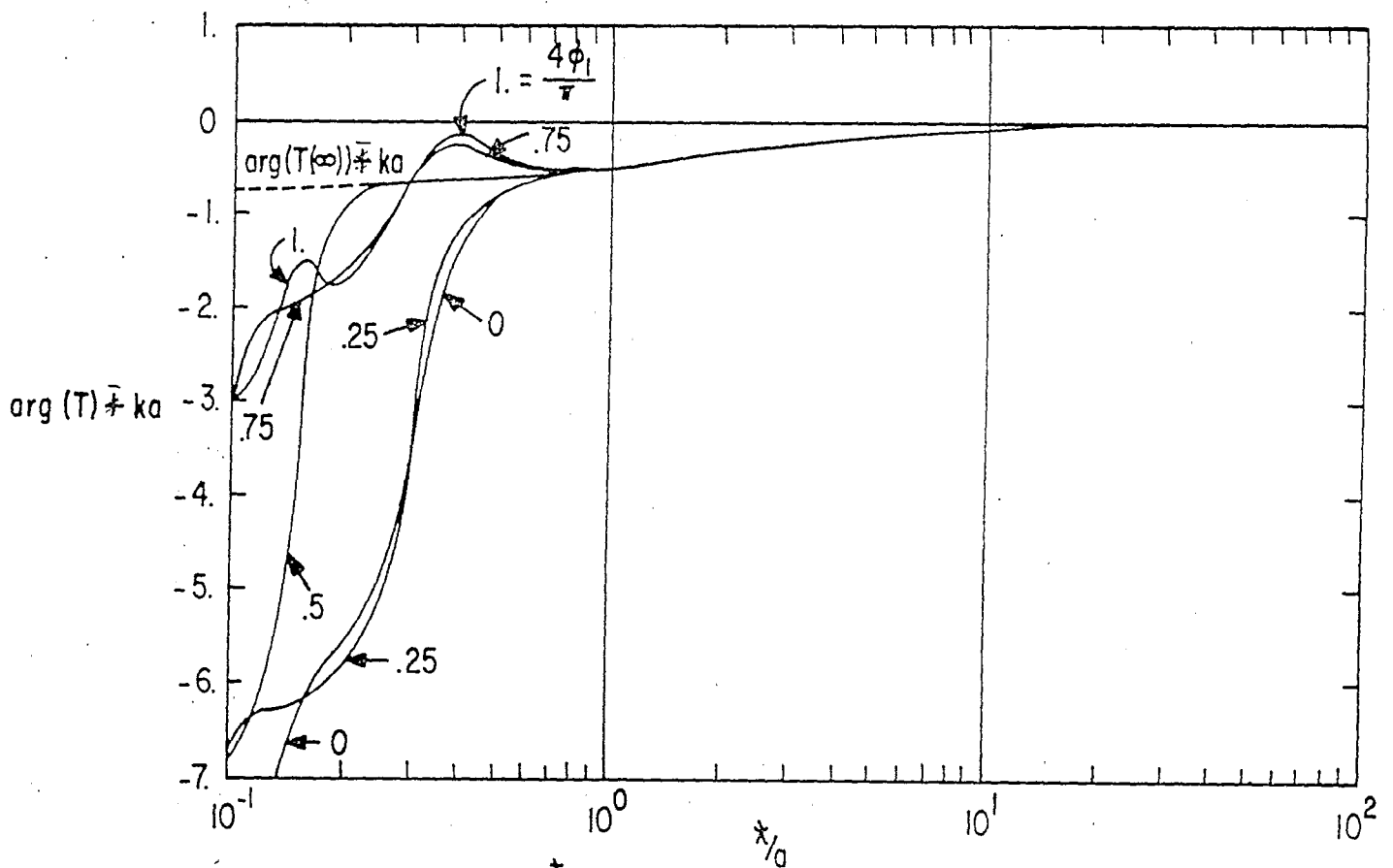


B. PHASE OF $T(\phi_1, 2)$ vs. λ/a WITH ϕ_1 AS A PARAMETER

FIGURE 3. SHORT CIRCUIT CURRENT TRANSFER FUNCTION: $N = 2$

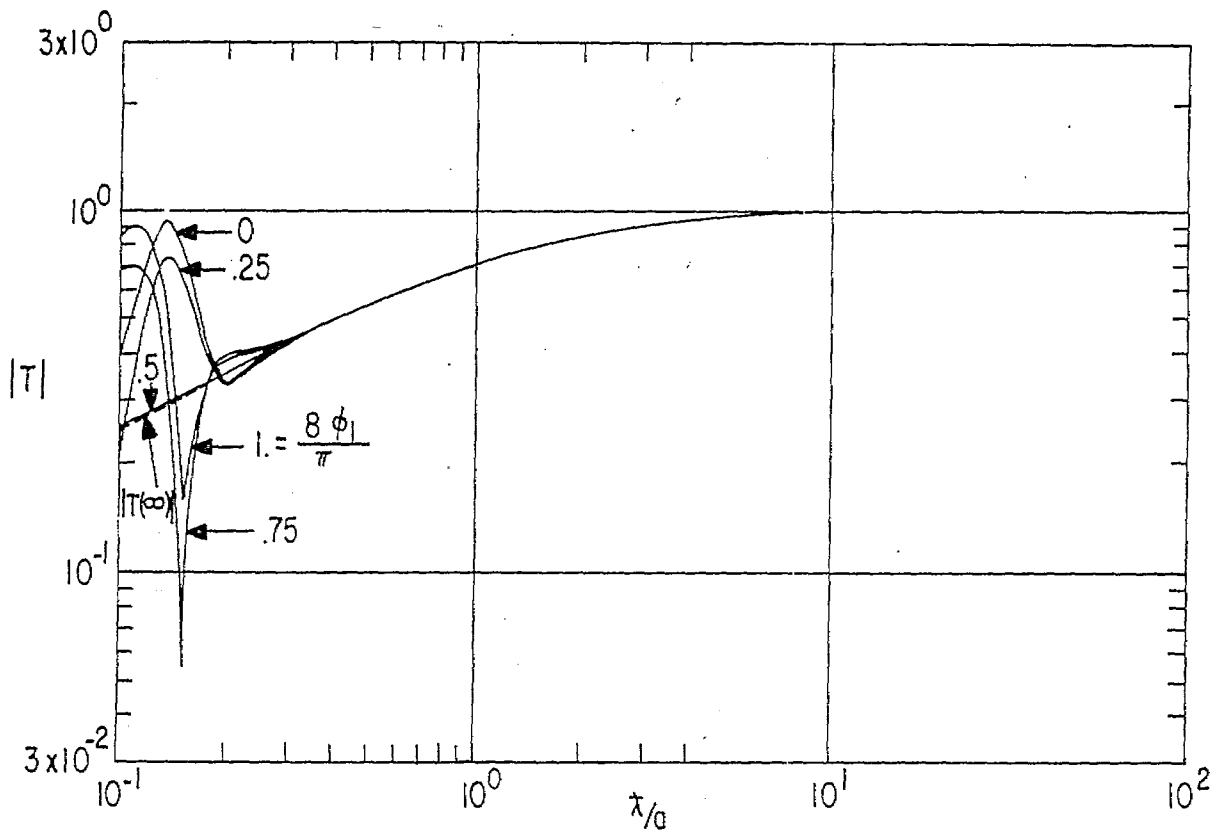


A. MAGNITUDE OF $T(\phi_1, 4)$ vs. x/a WITH ϕ_1 AS A PARAMETER

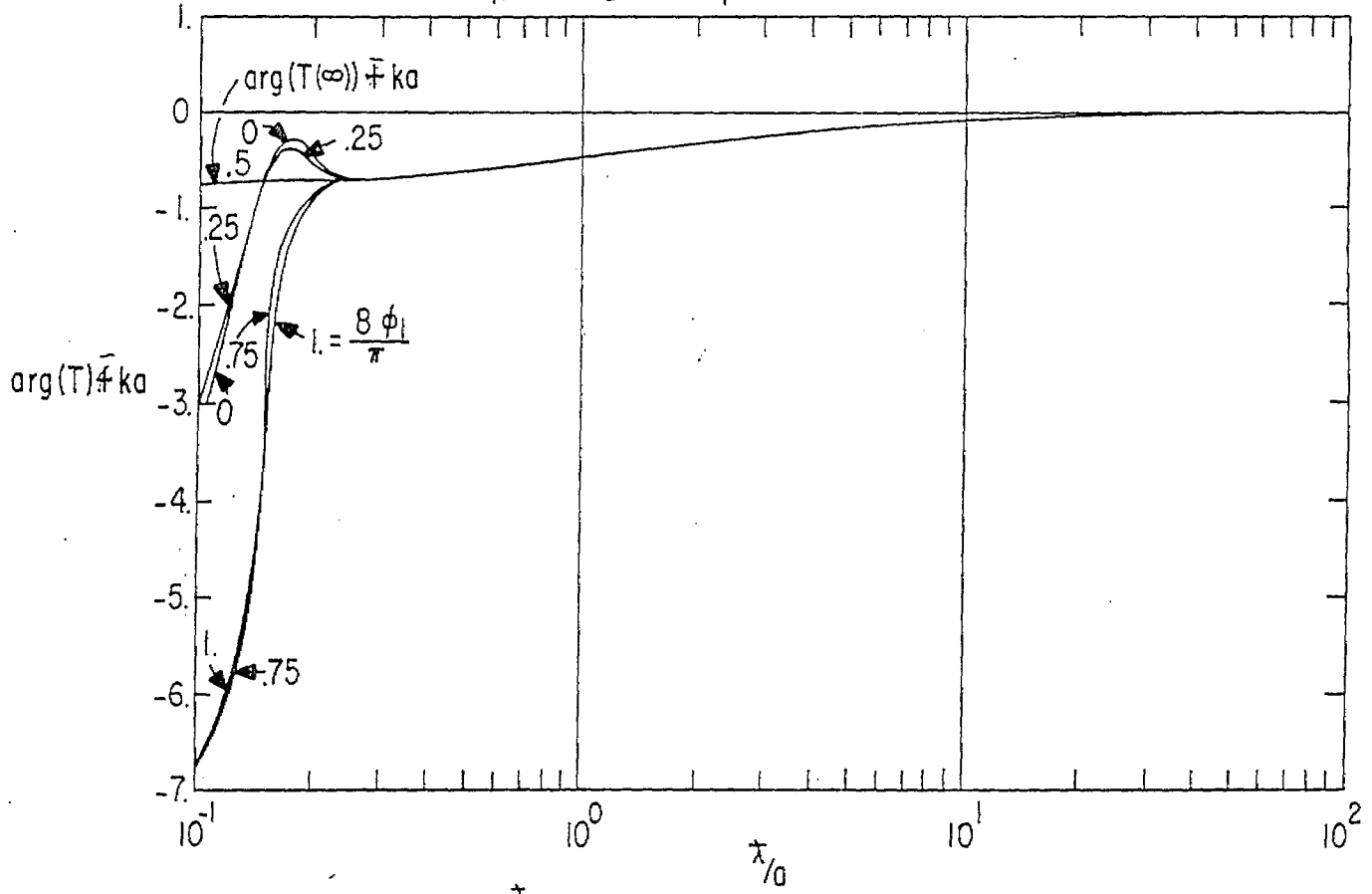


B. PHASE OF $T(\phi_1, 4)$ vs. x/a WITH ϕ_1 AS A PARAMETER

FIGURE 4. SHORT CIRCUIT CURRENT TRANSFER FUNCTION: $N=4$



A. MAGNITUDE OF $T(\phi_1, 8)$ vs. λ/g WITH ϕ_1 AS A PARAMETER



B. PHASE OF $T(\phi_1, 8)$ vs. λ/g WITH ϕ_1 AS A PARAMETER

FIGURE 5. SHORT CIRCUIT CURRENT TRANSFER FUNCTION: $N=8$

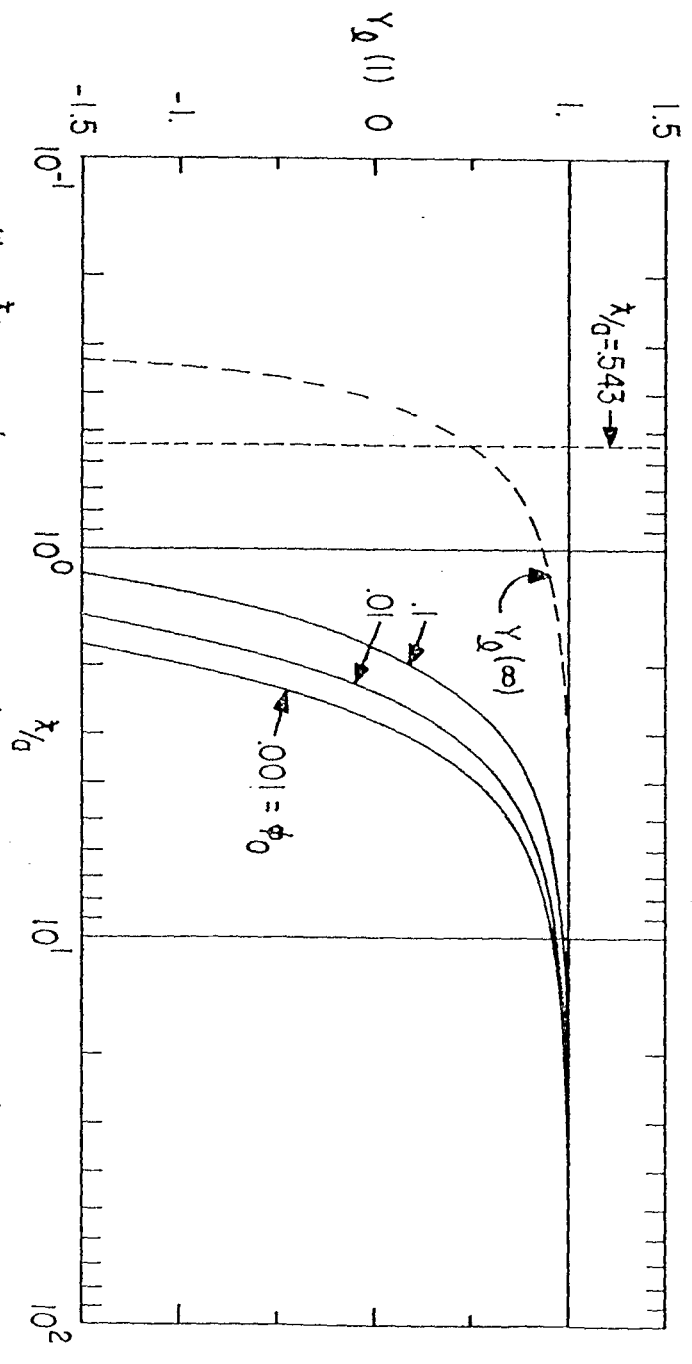
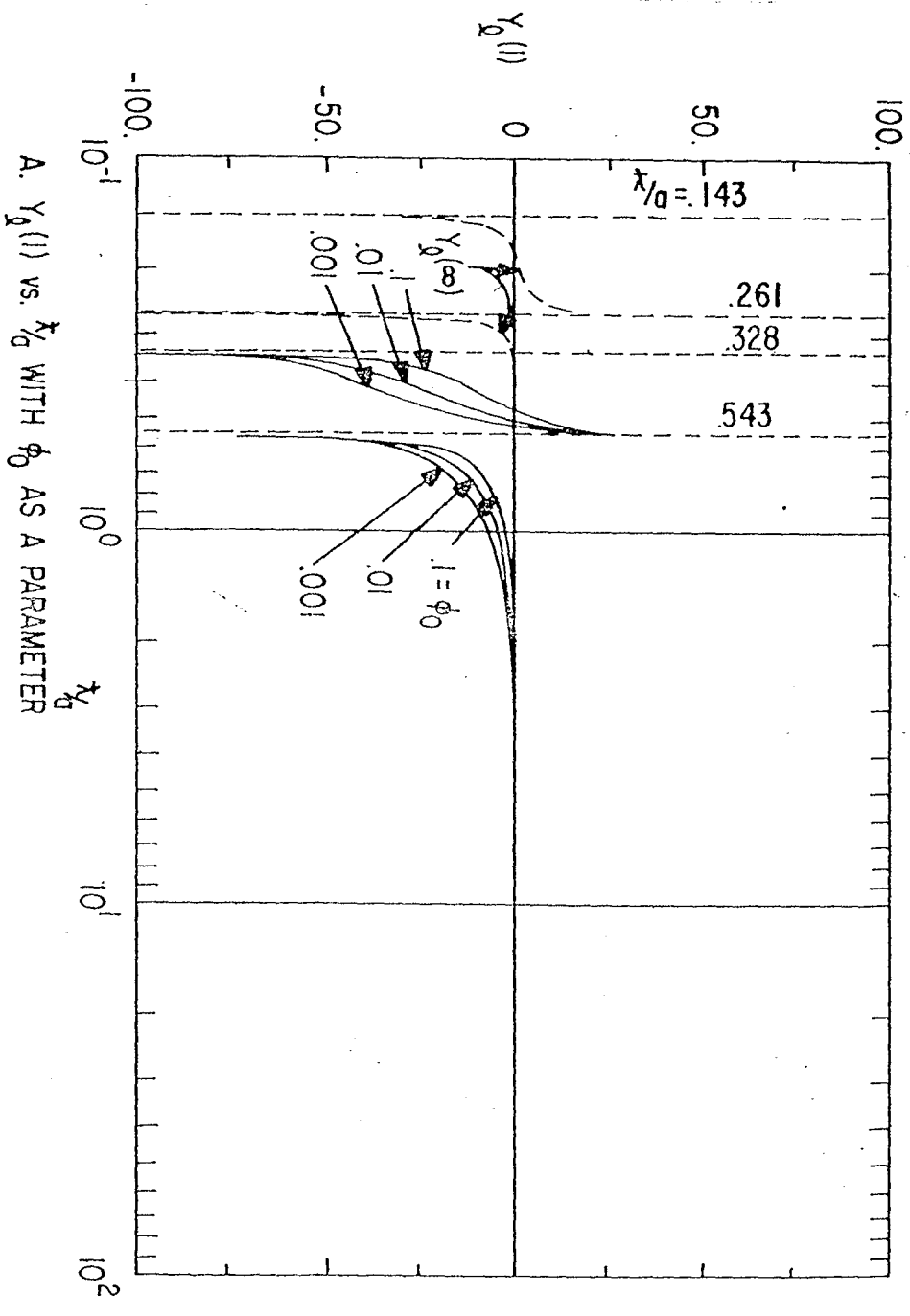
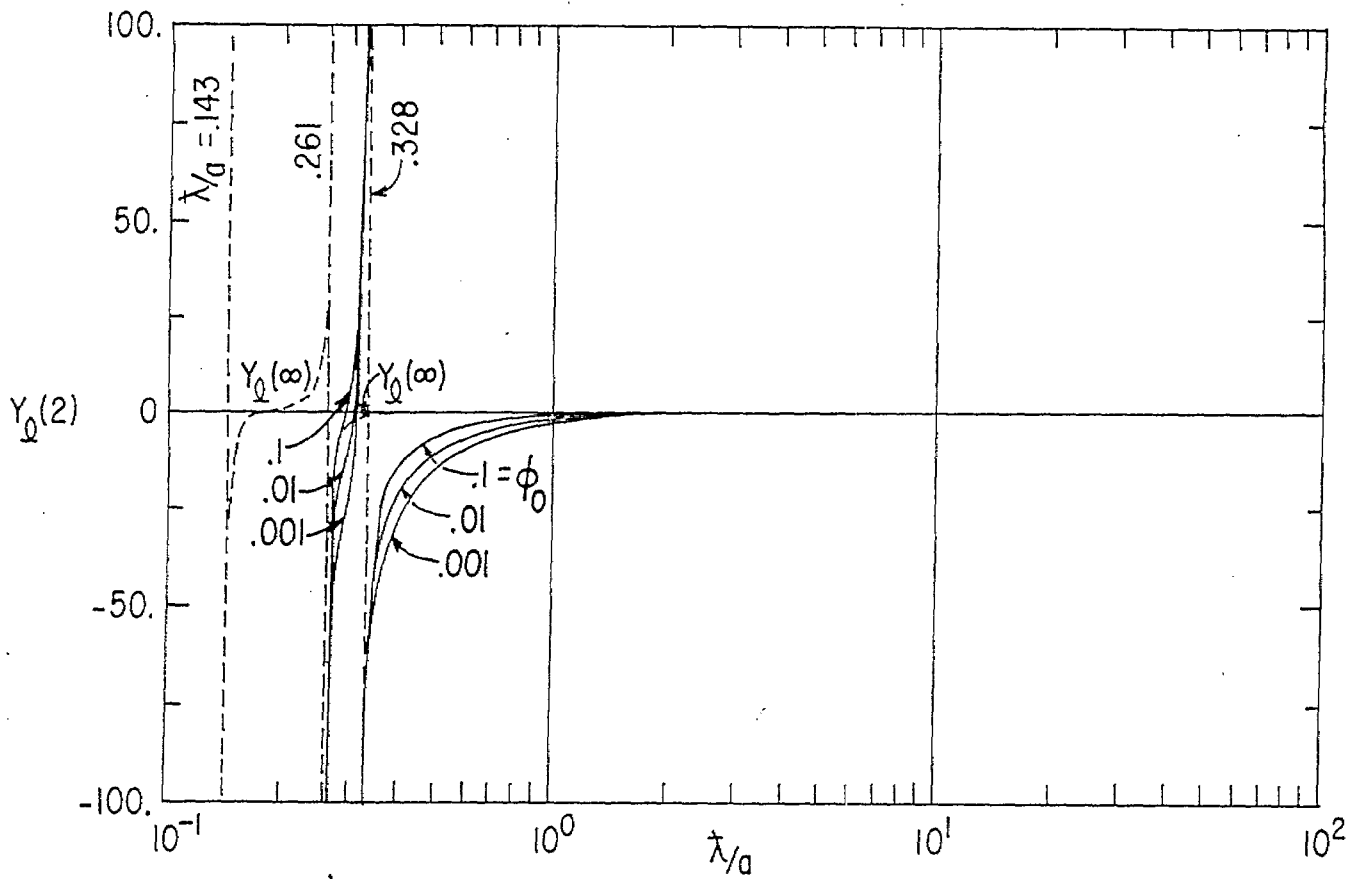
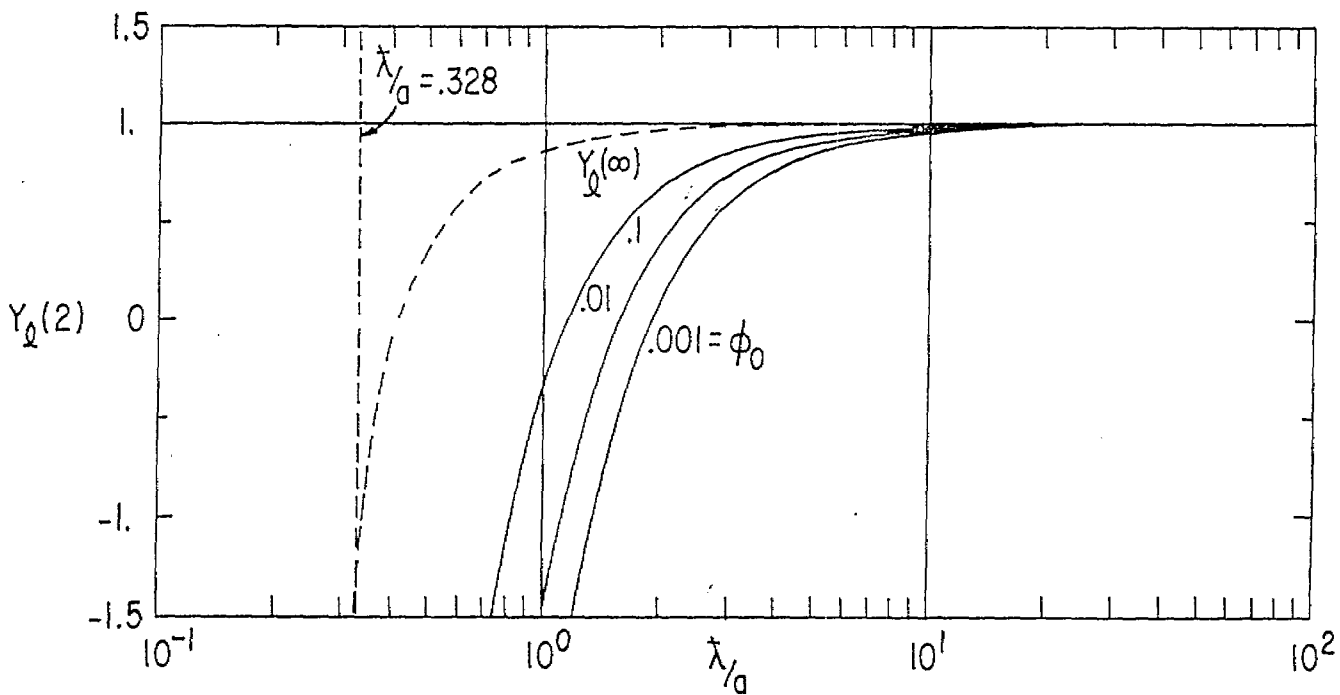


FIGURE 6. NORMALIZED INTERNAL ADMITTANCE: $N=1$

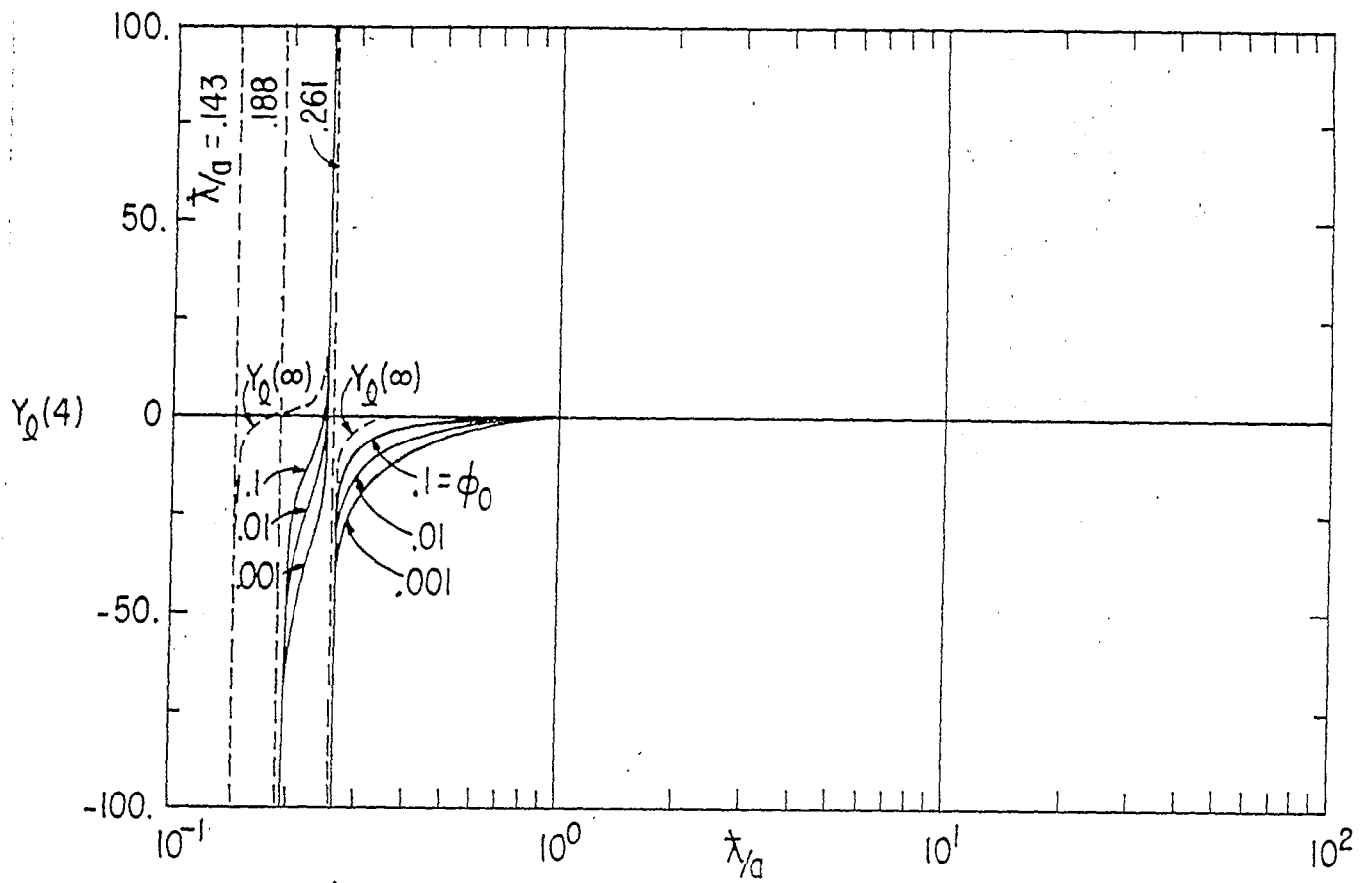


A. $Y_Q(2)$ vs. λ/γ_a WITH ϕ_0 AS A PARAMETER

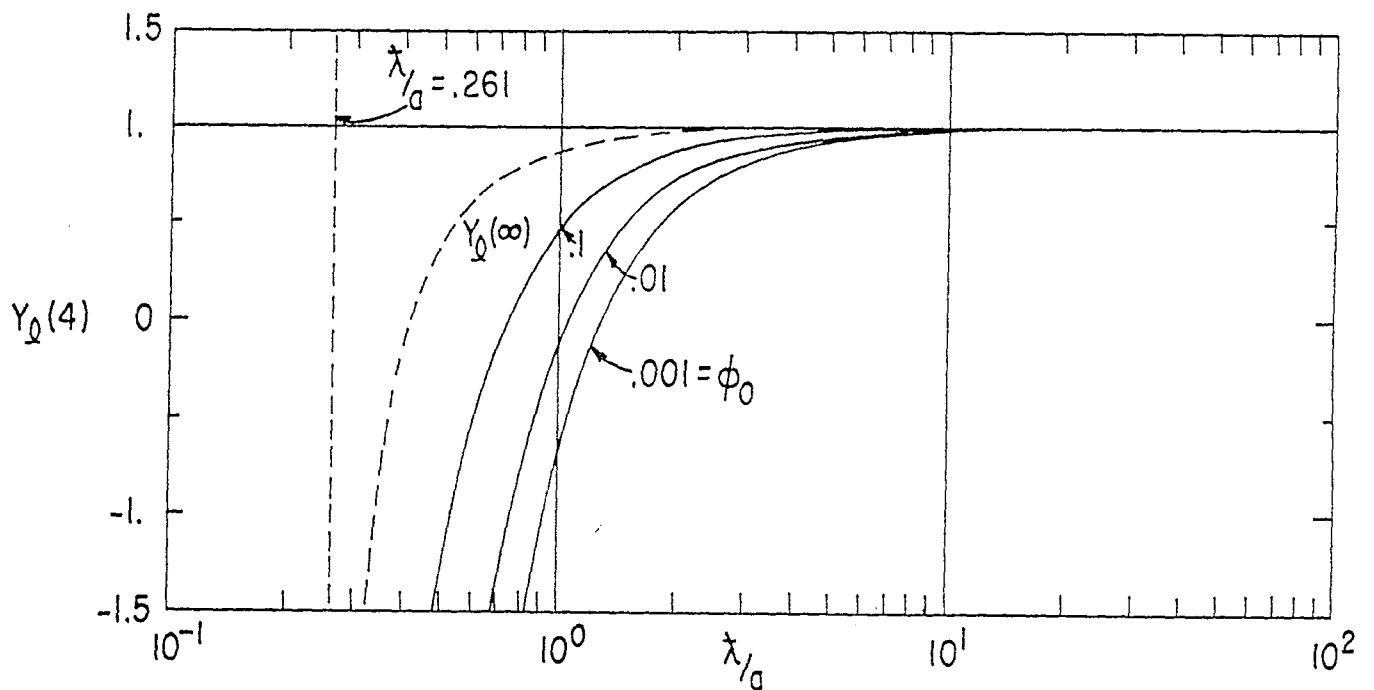


B. $Y_Q(2)$ vs. λ/γ_a WITH ϕ_0 AS A PARAMETER (SCALE OF A EXPANDED)

FIGURE 7. NORMALIZED INTERNAL ADMITTANCE: N=2

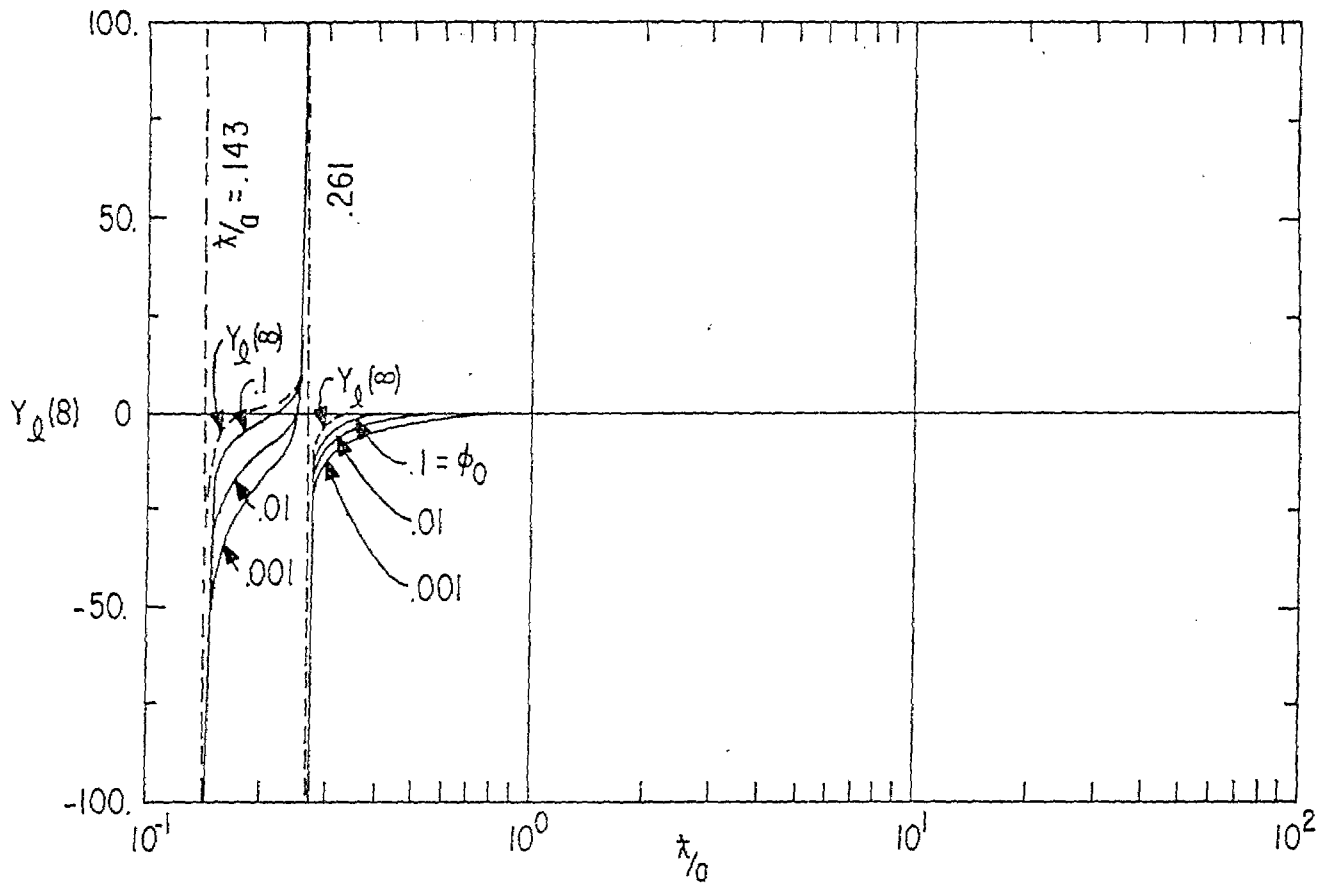


A. $Y_Q(4)$ vs. λ/γ_a WITH ϕ_0 AS A PARAMETER

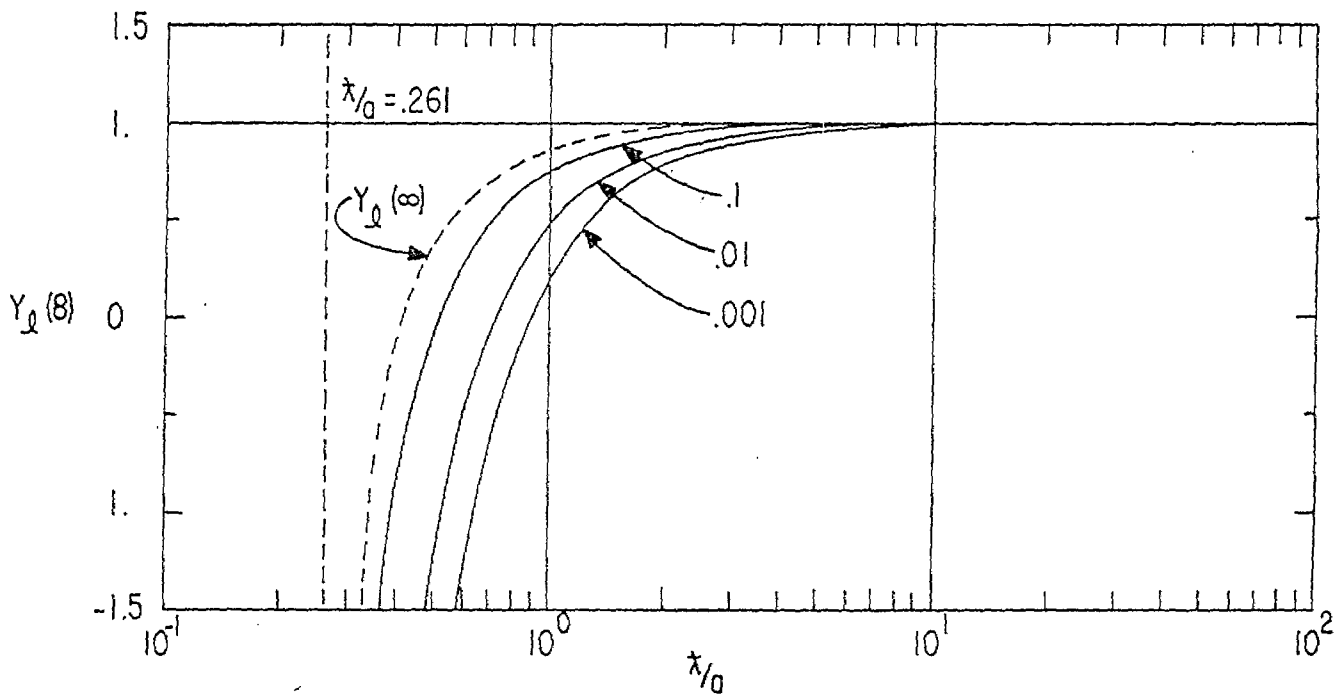


B. $Y_Q(4)$ vs. λ/γ_a WITH ϕ_0 AS A PARAMETER (SCALE OF A EXPANDED)

FIGURE 8. NORMALIZED INTERNAL ADMITTANCE: $N=4$

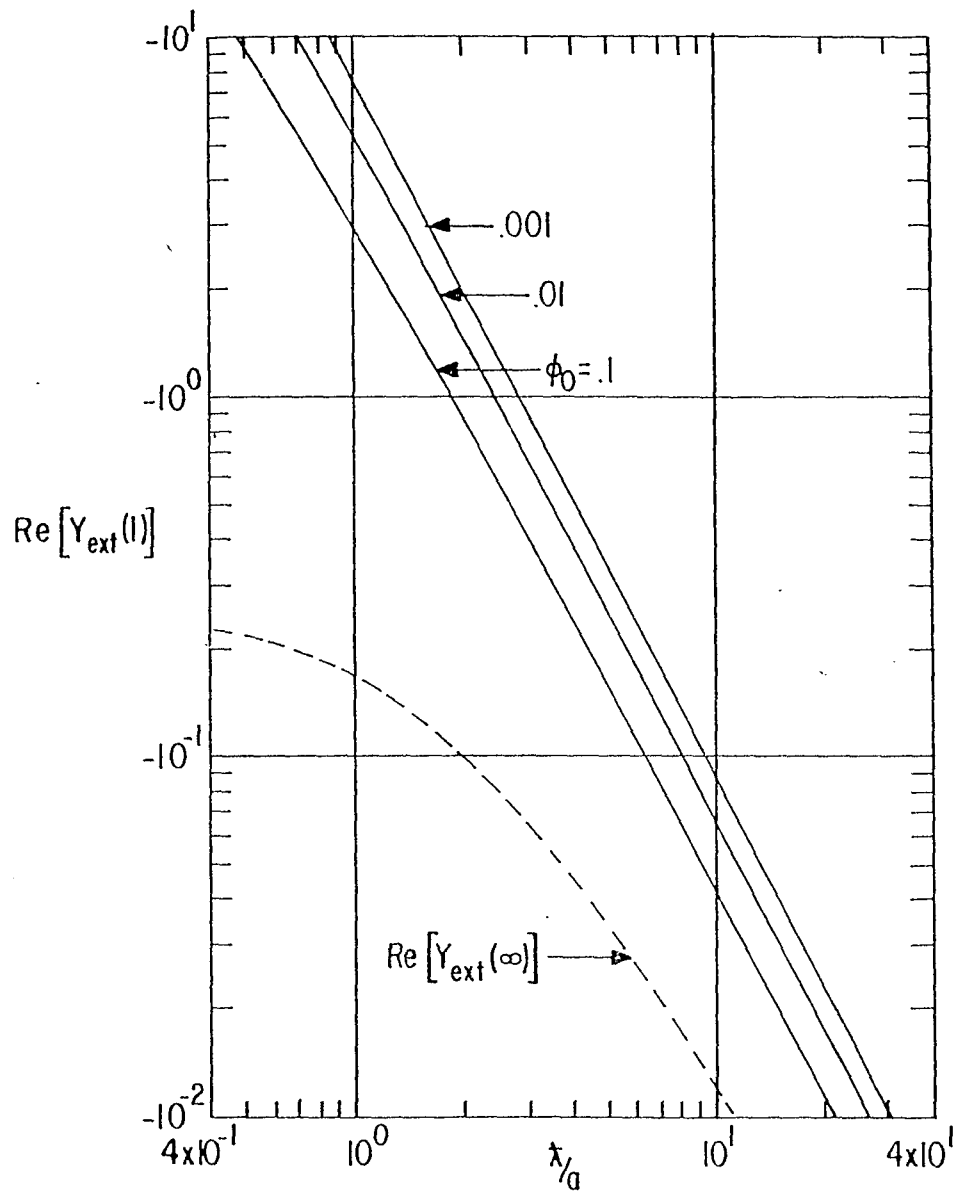


A. $Y_q(8)$ vs. k_0/a WITH ϕ_0 AS A PARAMETER

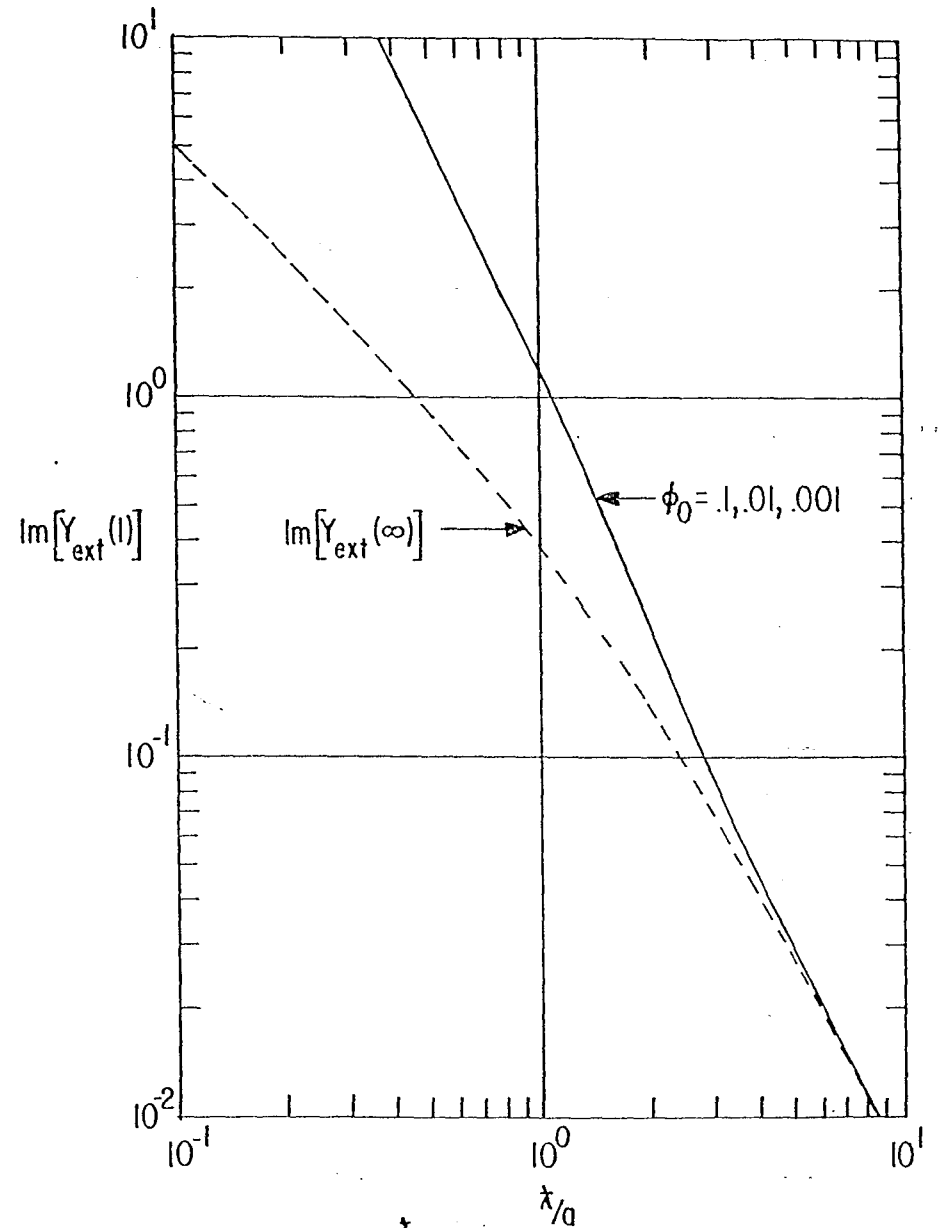


B. $Y_q(8)$ vs. k_0/a WITH ϕ_0 AS A PARAMETER (SCALE OF A EXPANDED)

FIGURE 9. NORMALIZED INTERNAL ADMITTANCE: $N=8$

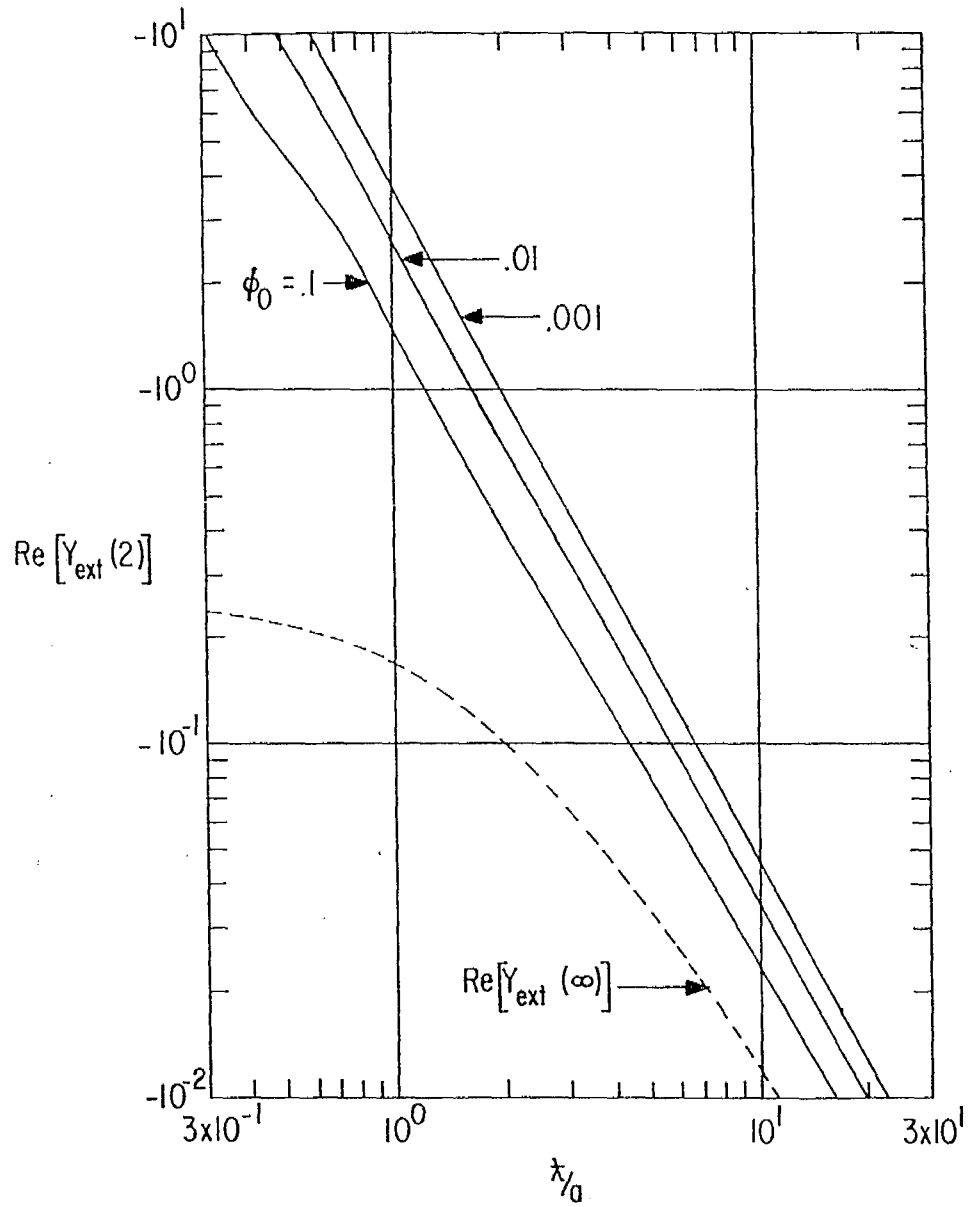


A. $\text{Re}[Y_{\text{ext}}(l)]$ vs. λ_g WITH ϕ_0 AS A PARAMETER

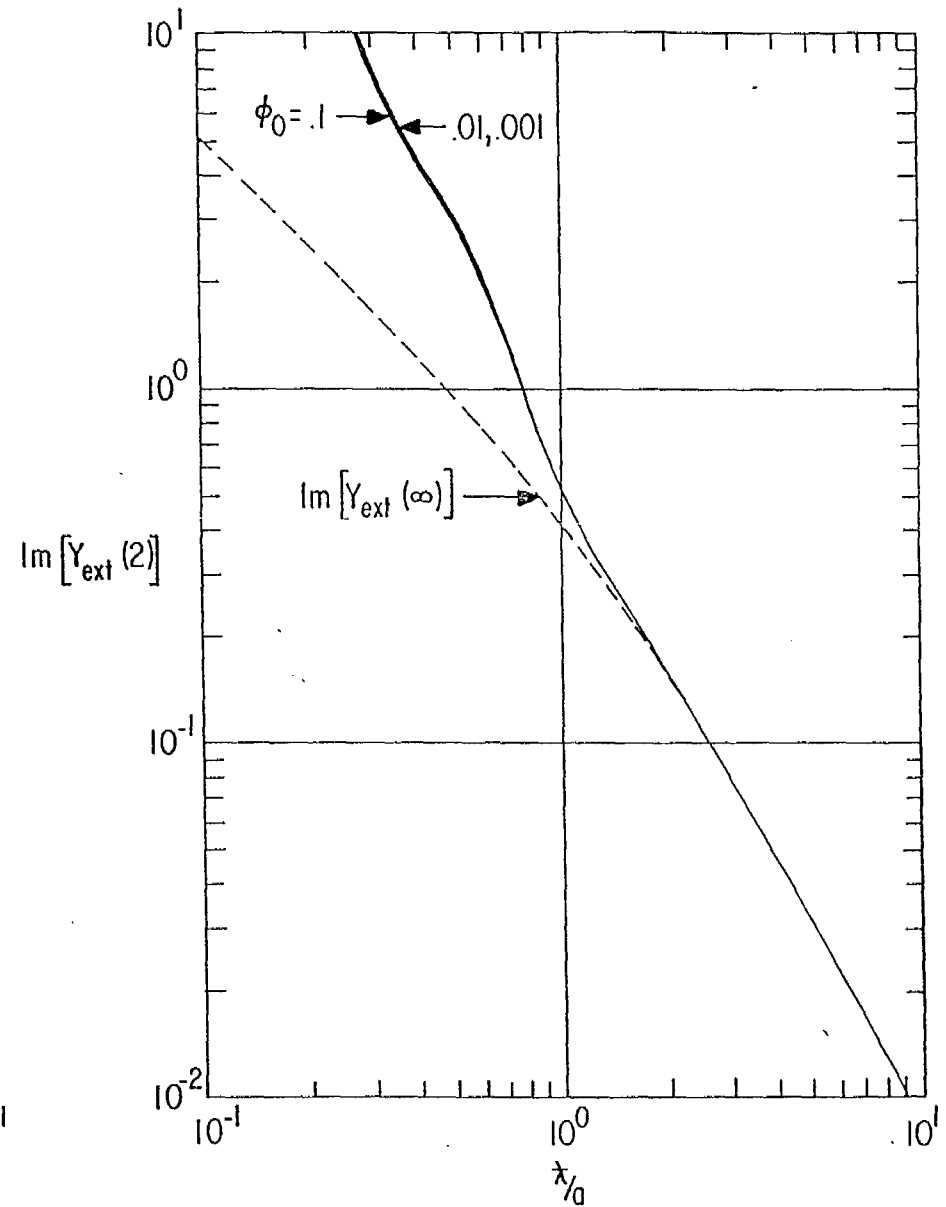


B. $\text{Im}[Y_{\text{ext}}(l)]$ vs. λ_g WITH ϕ_0 AS A PARAMETER

FIGURE 10. NORMALIZED EXTERNAL ADMITTANCE: $N=1$

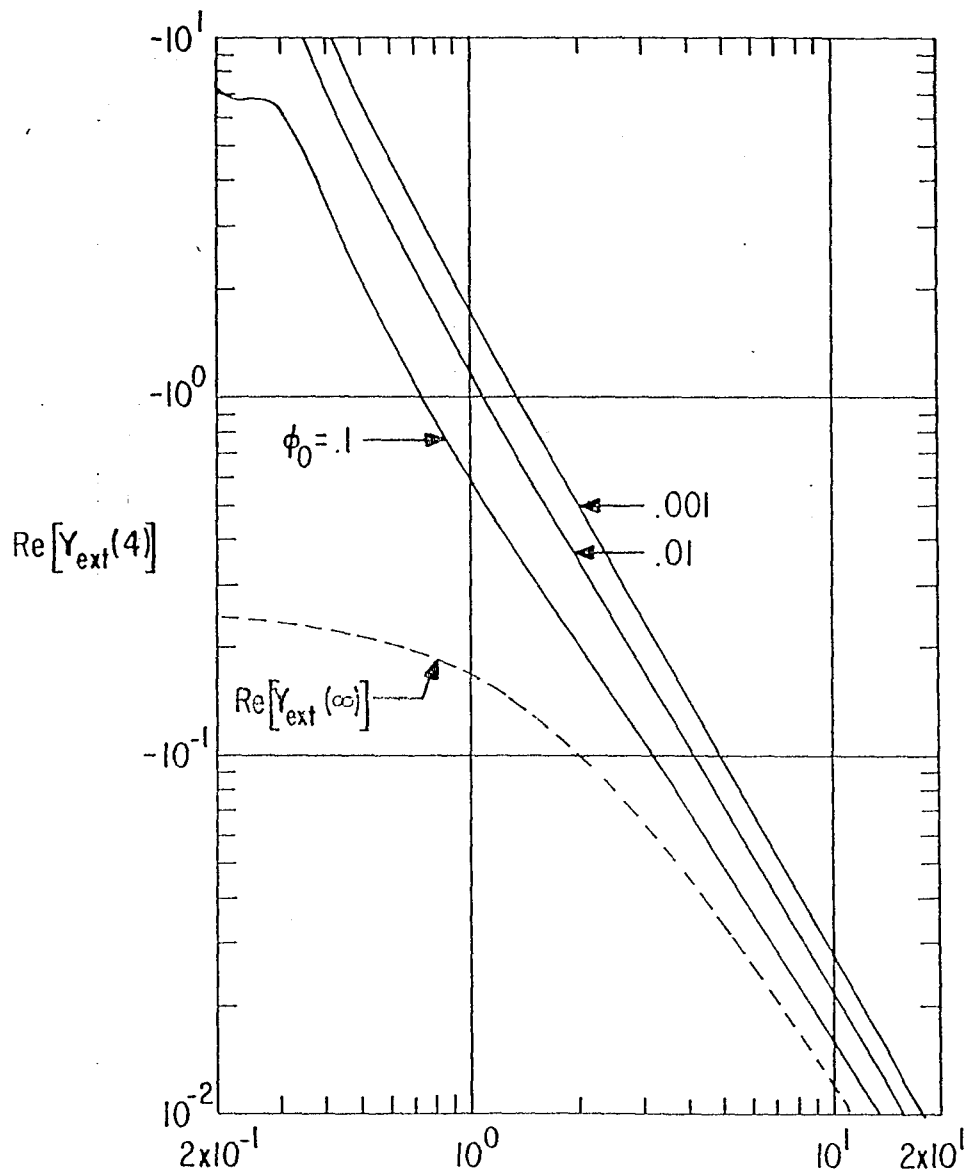


A. $\text{Re}[Y_{\text{ext}}(2)]$ vs. x/γ_a WITH ϕ_0 AS A PARAMETER

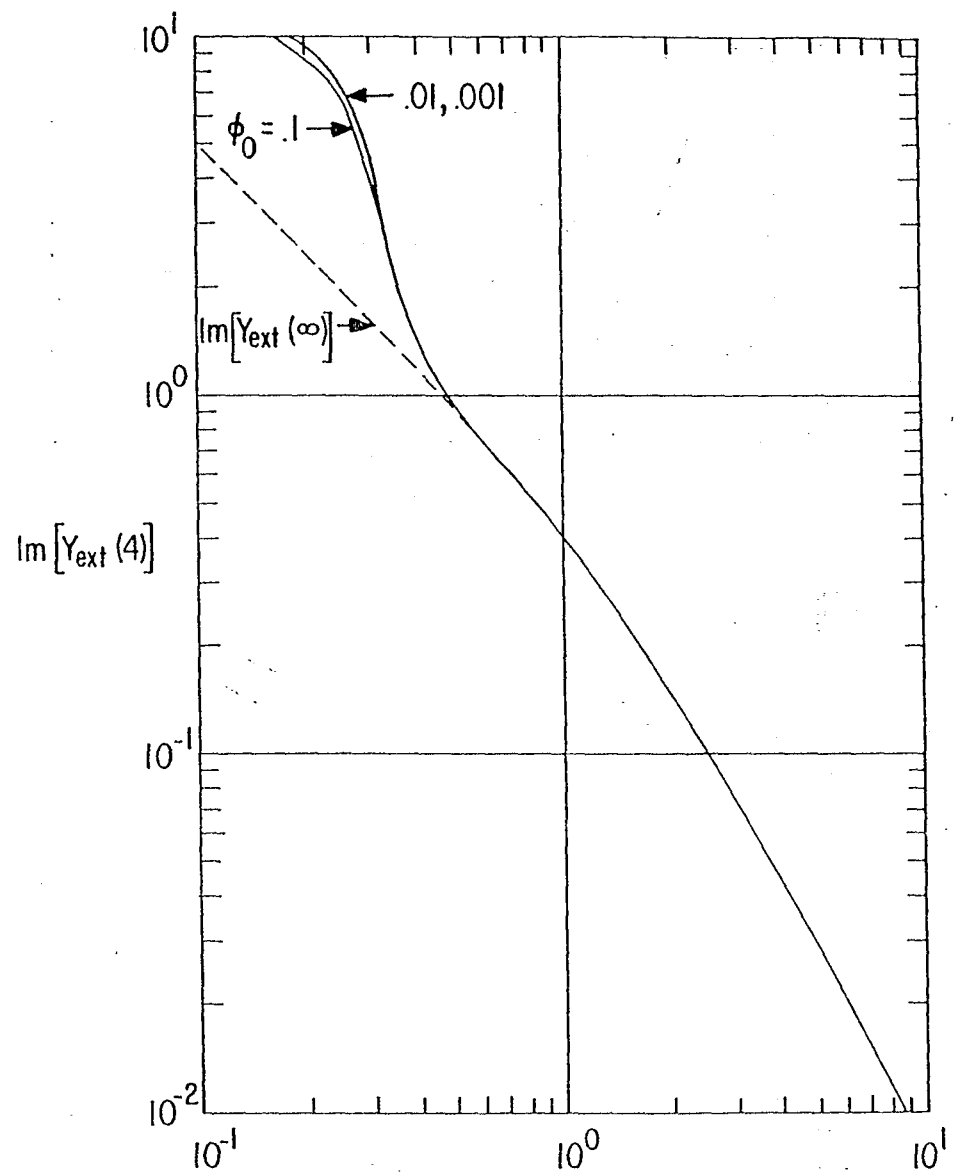


B. $\text{Im}[Y_{\text{ext}}(2)]$ vs. x/γ_a WITH ϕ_0 AS A PARAMETER

FIGURE 11. NORMALIZED EXTERNAL ADMITTANCE: N=2

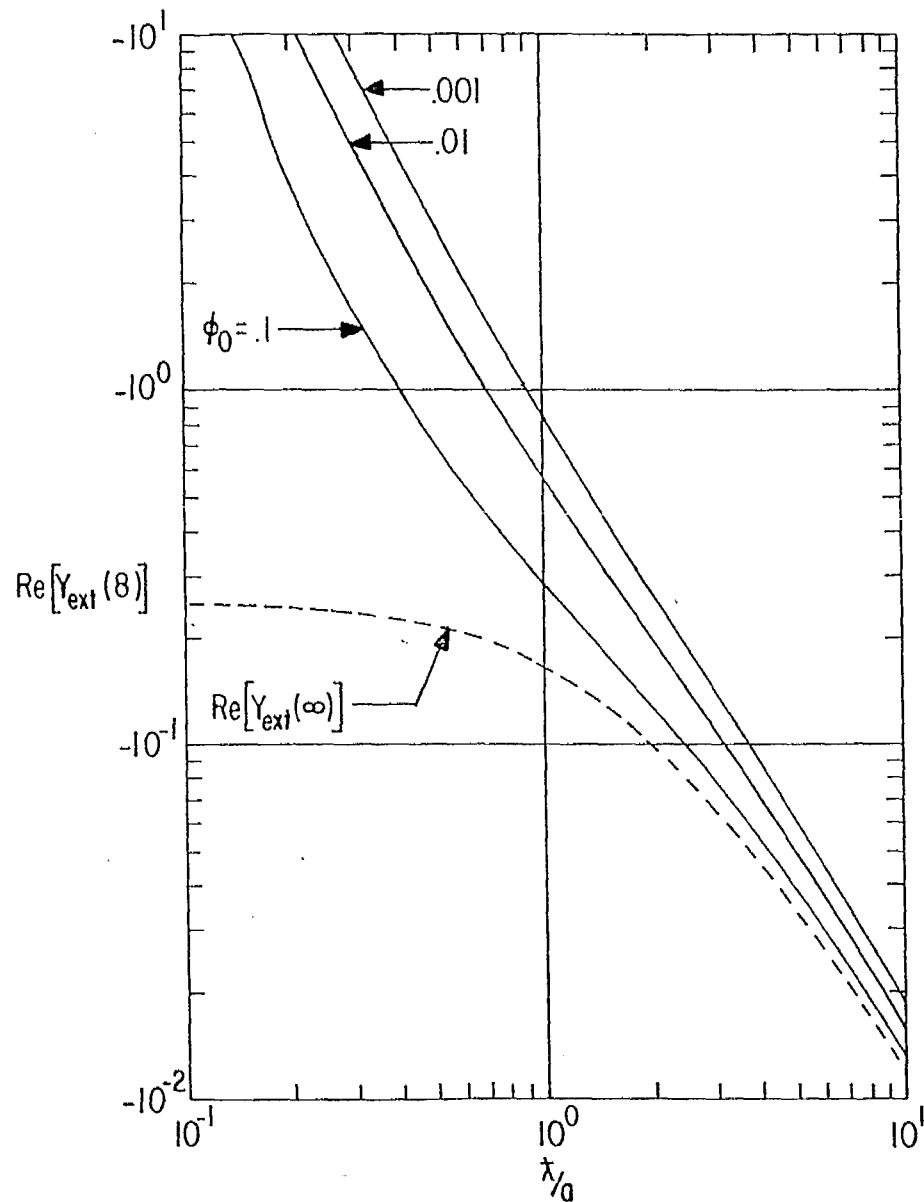


A. $\text{Re}[Y_{\text{ext}}(4)]$ vs. λ/a WITH ϕ_0 AS A PARAMETER

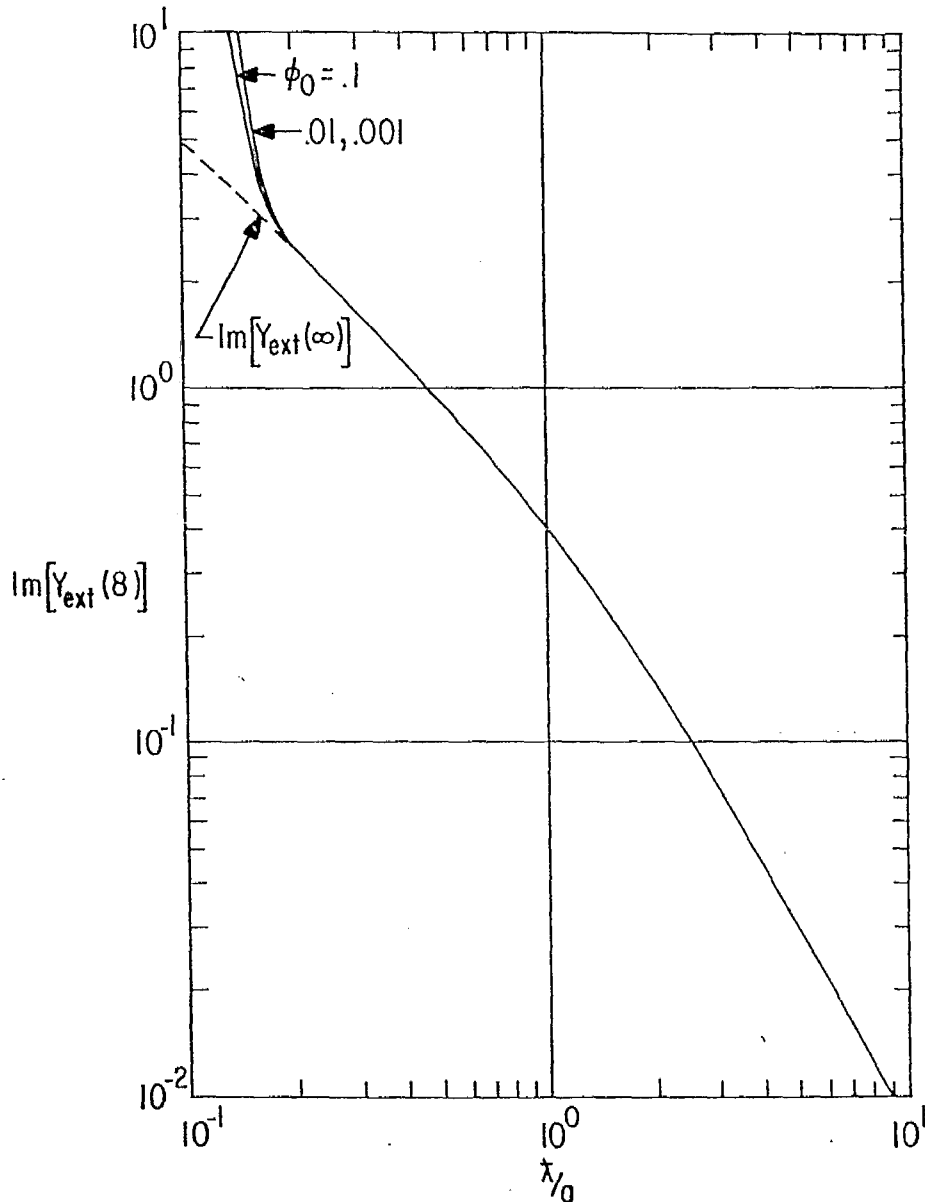


B. $\text{Im}[Y_{\text{ext}}(4)]$ vs. λ/a WITH ϕ_0 AS A PARAMETER

FIGURE 12. NORMALIZED EXTERNAL ADMITTANCE: N=4

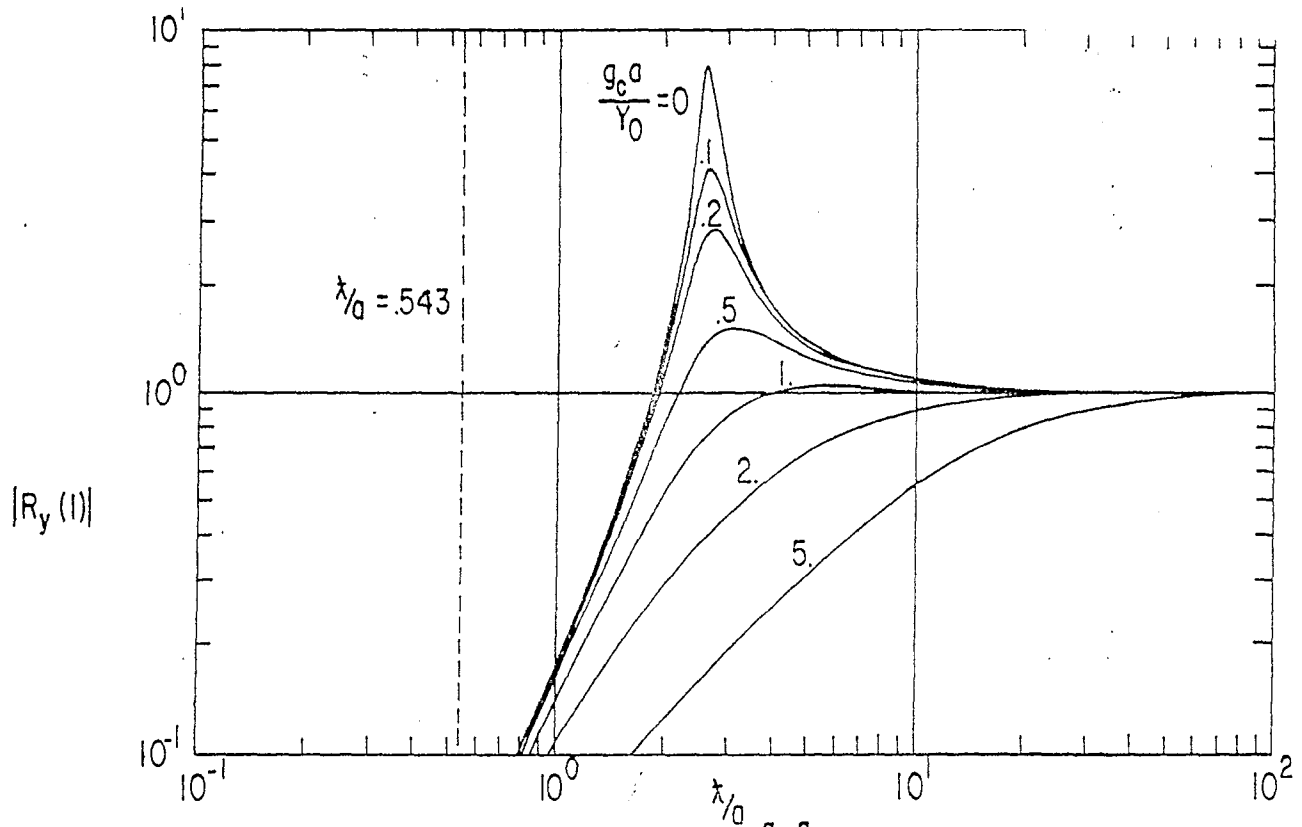


A. $\text{Re}[Y_{\text{ext}}(s)]$ vs. λ/a WITH ϕ_0 AS A PARAMETER

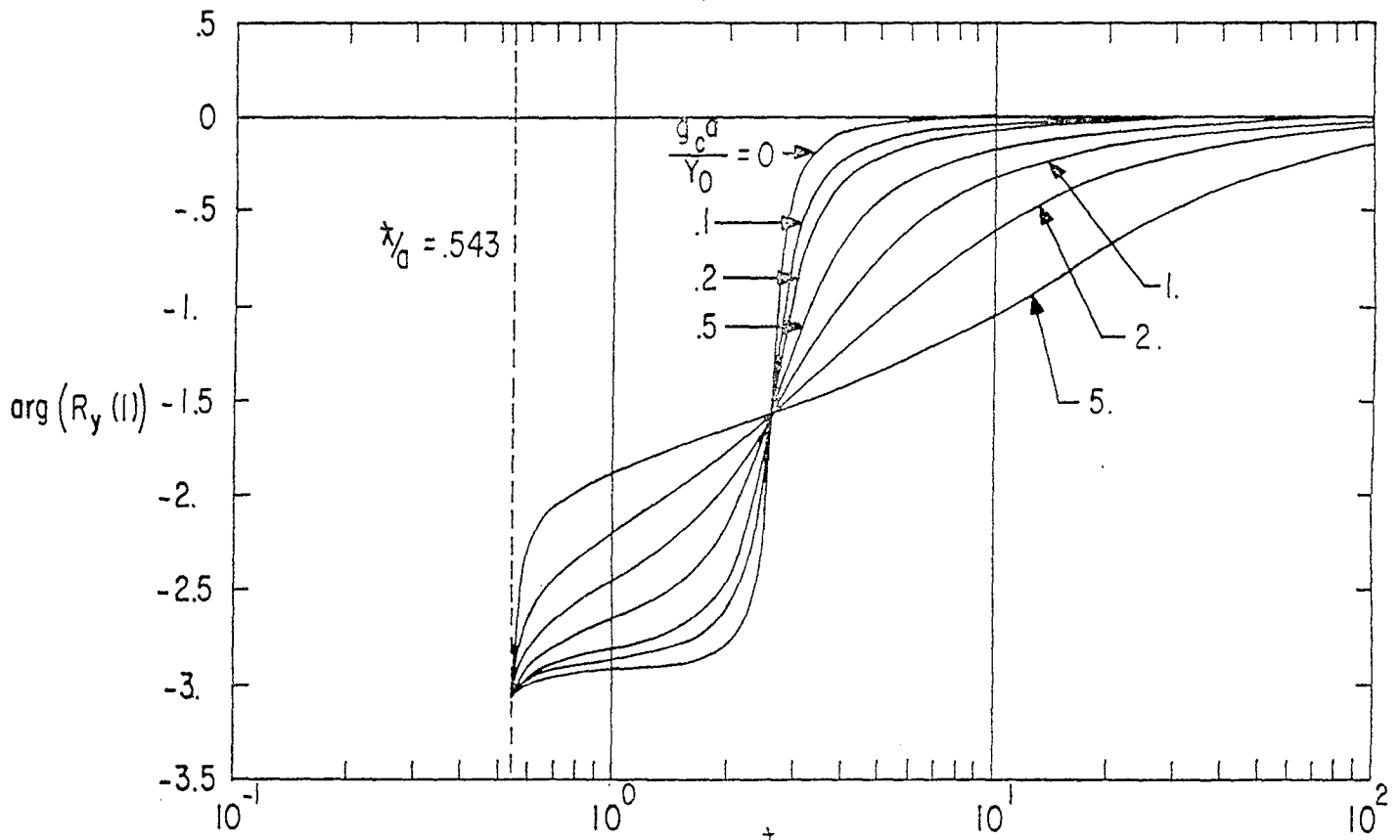


B. $\text{Im}[Y_{\text{ext}}(s)]$ vs. λ/a WITH ϕ_0 AS A PARAMETER

FIGURE 13. NORMALIZED EXTERNAL ADMITTANCE: $N = 8$

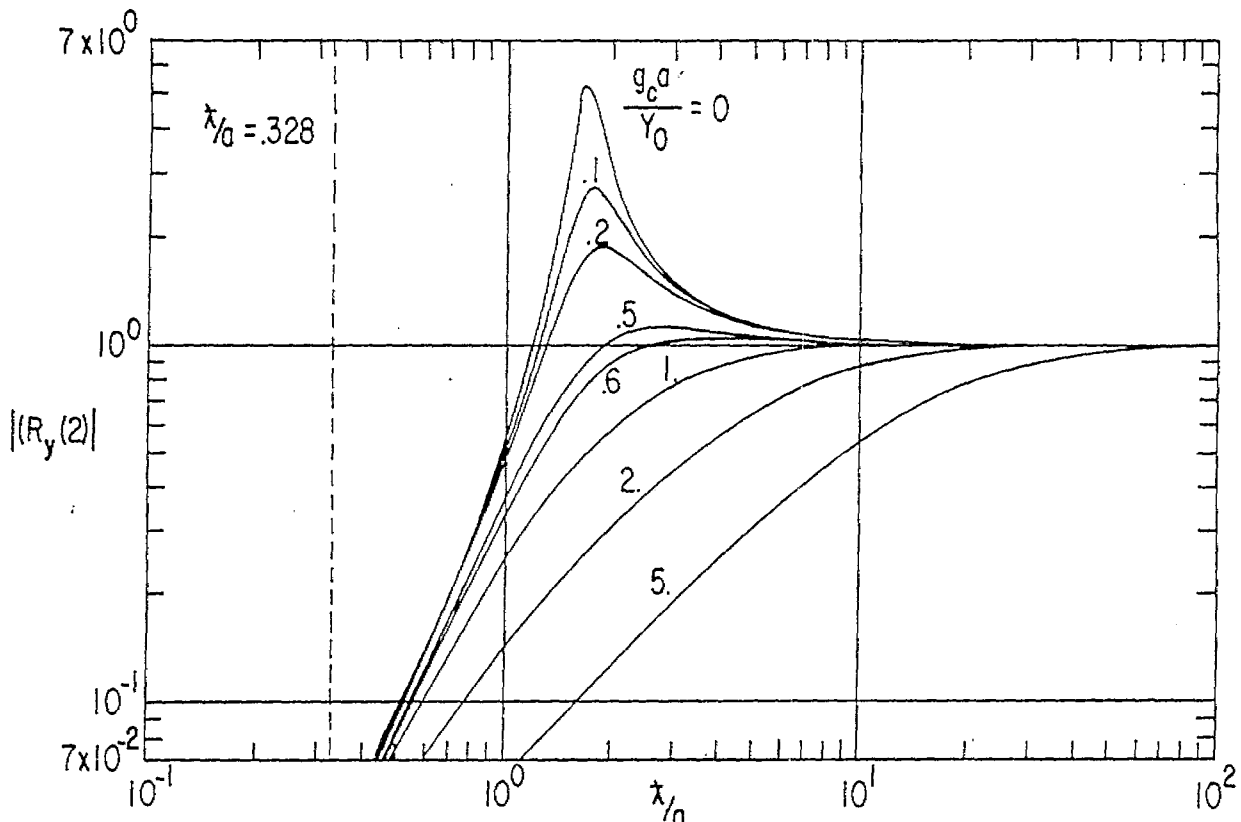


A. MAGNITUDE OF $R_y(1)$ vs. λ/d WITH $\frac{g_c a}{Y_0}$ AS A PARAMETER

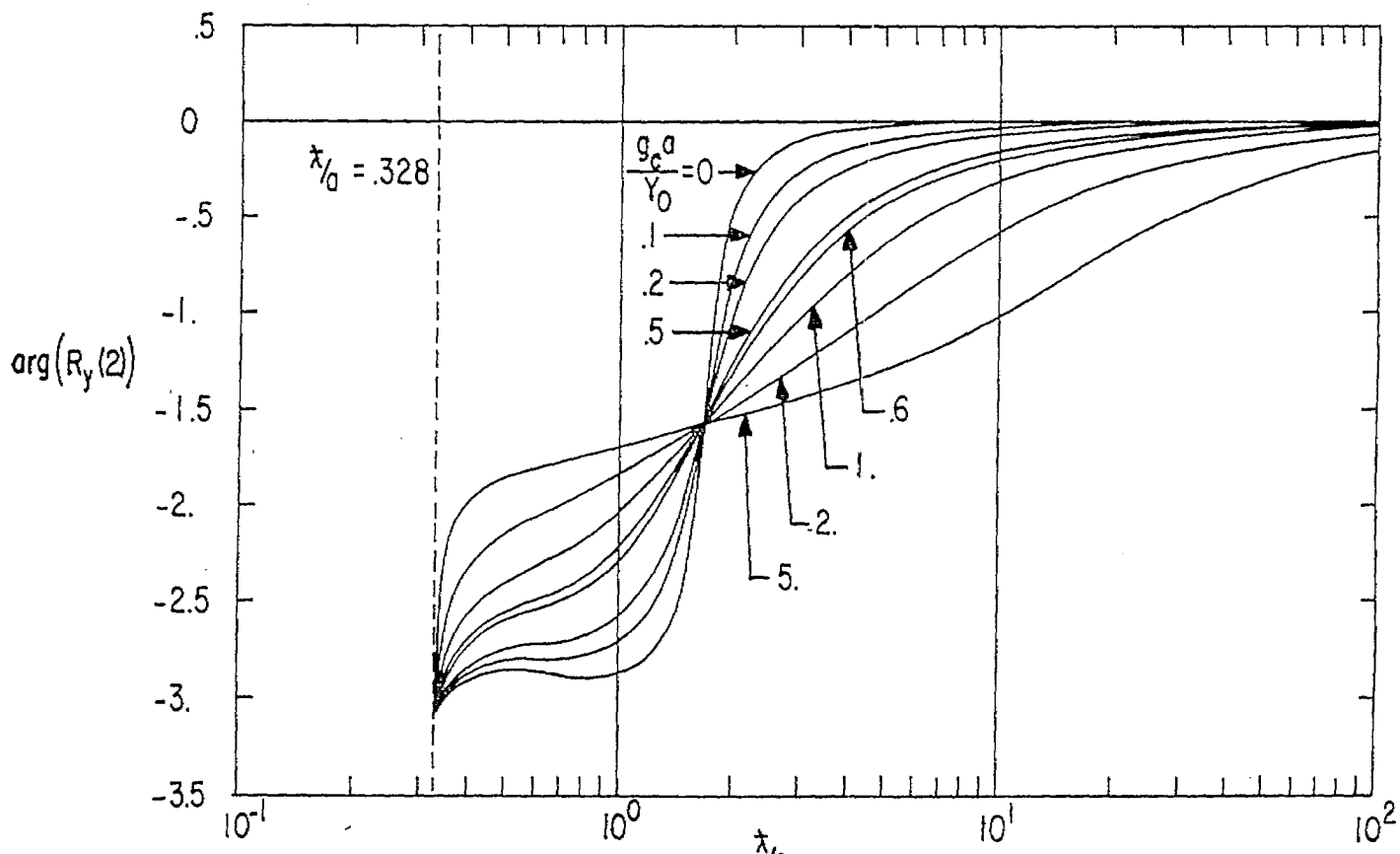


B. PHASE OF $R_y(1)$ vs. λ/d WITH $\frac{g_c a}{Y_0}$ AS A PARAMETER

FIGURE 14. EFFECT OF ADMITTANCES ON RESPONSE: $N=1$, $\phi_0=.1$

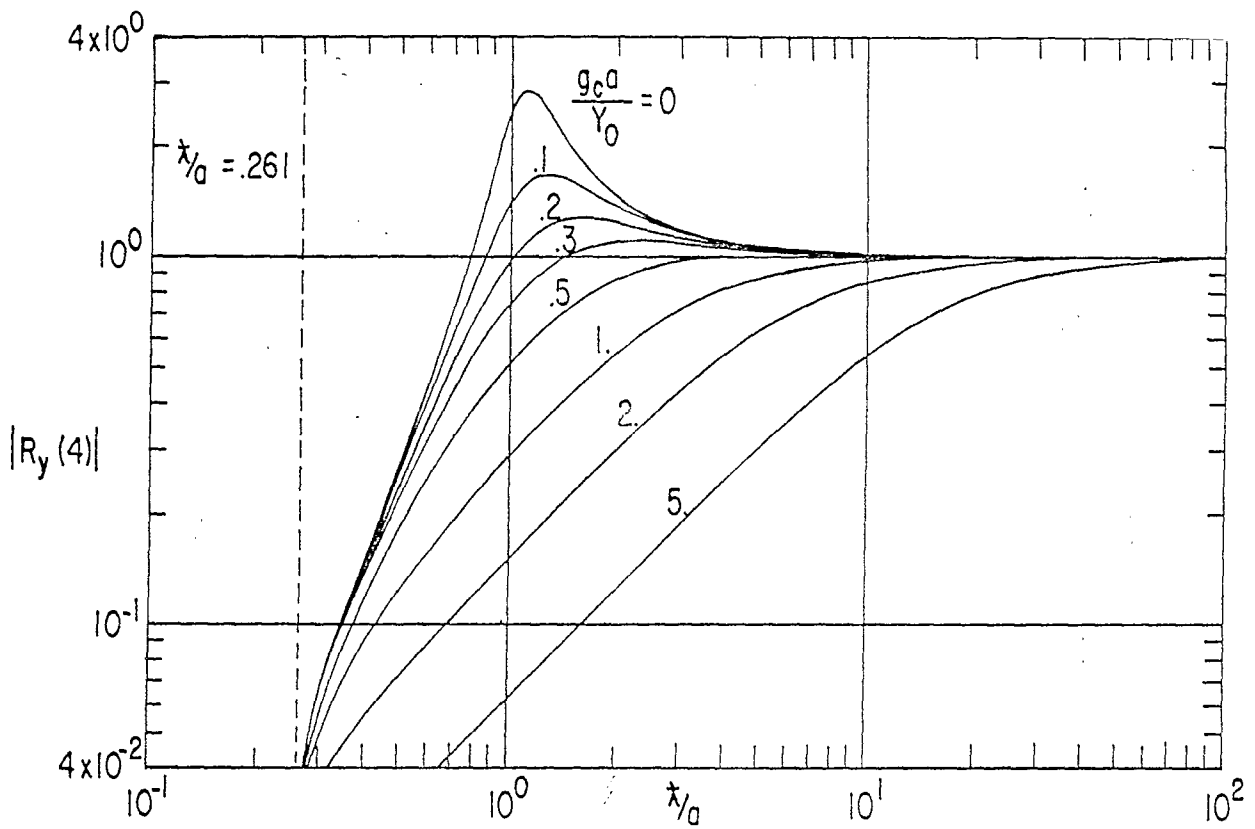


A. MAGNITUDE OF $R_y(2)$ vs. λ/a WITH $\frac{g_c a}{Y_0}$ AS A PARAMETER

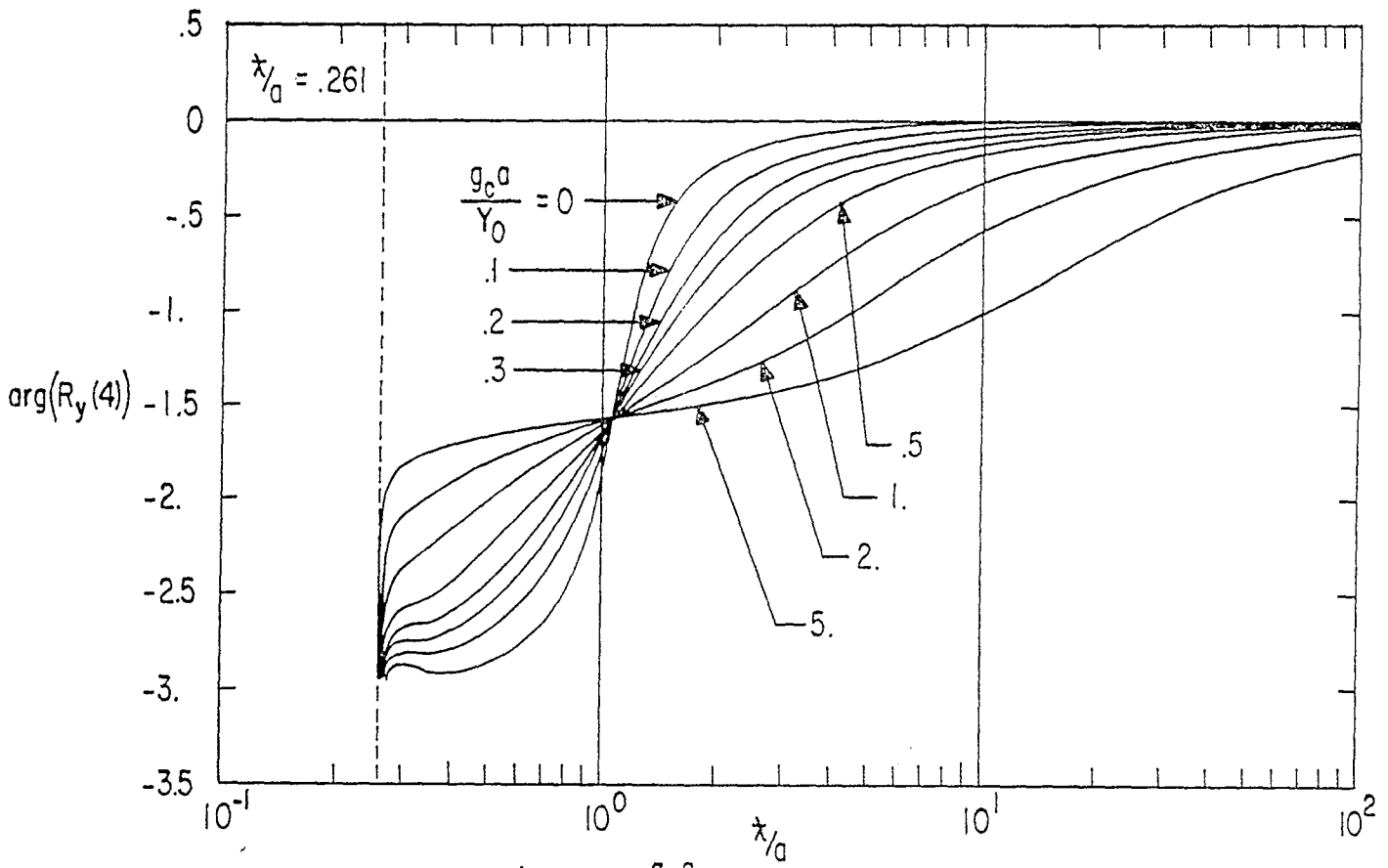


B. PHASE OF $R_y(2)$ vs. λ/a WITH $\frac{g_c a}{Y_0}$ AS A PARAMETER

FIGURE 15. EFFECT OF ADMITTANCES ON RESPONSE: $N=2, \phi_0=.1$

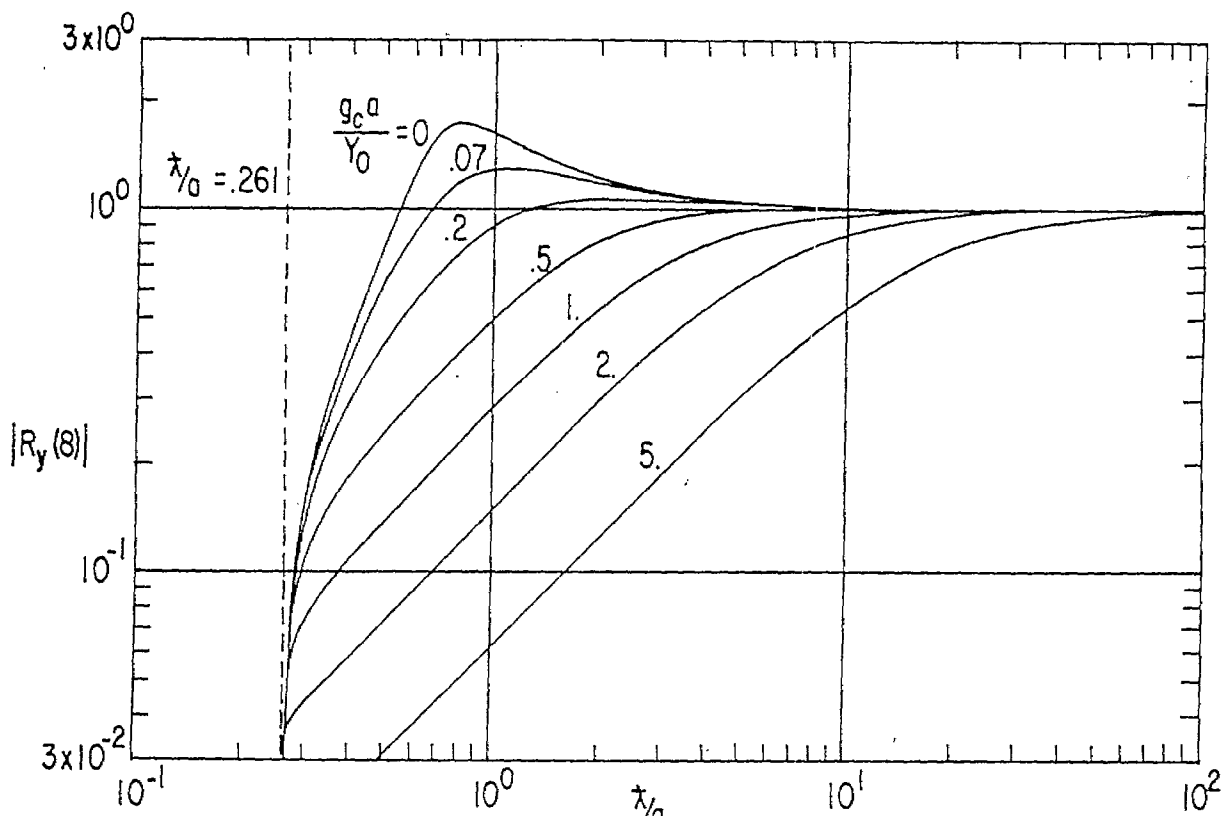


A. MAGNITUDE OF $R_y(4)$ vs. x/a WITH $\frac{g_c a}{Y_0}$ AS A PARAMETER

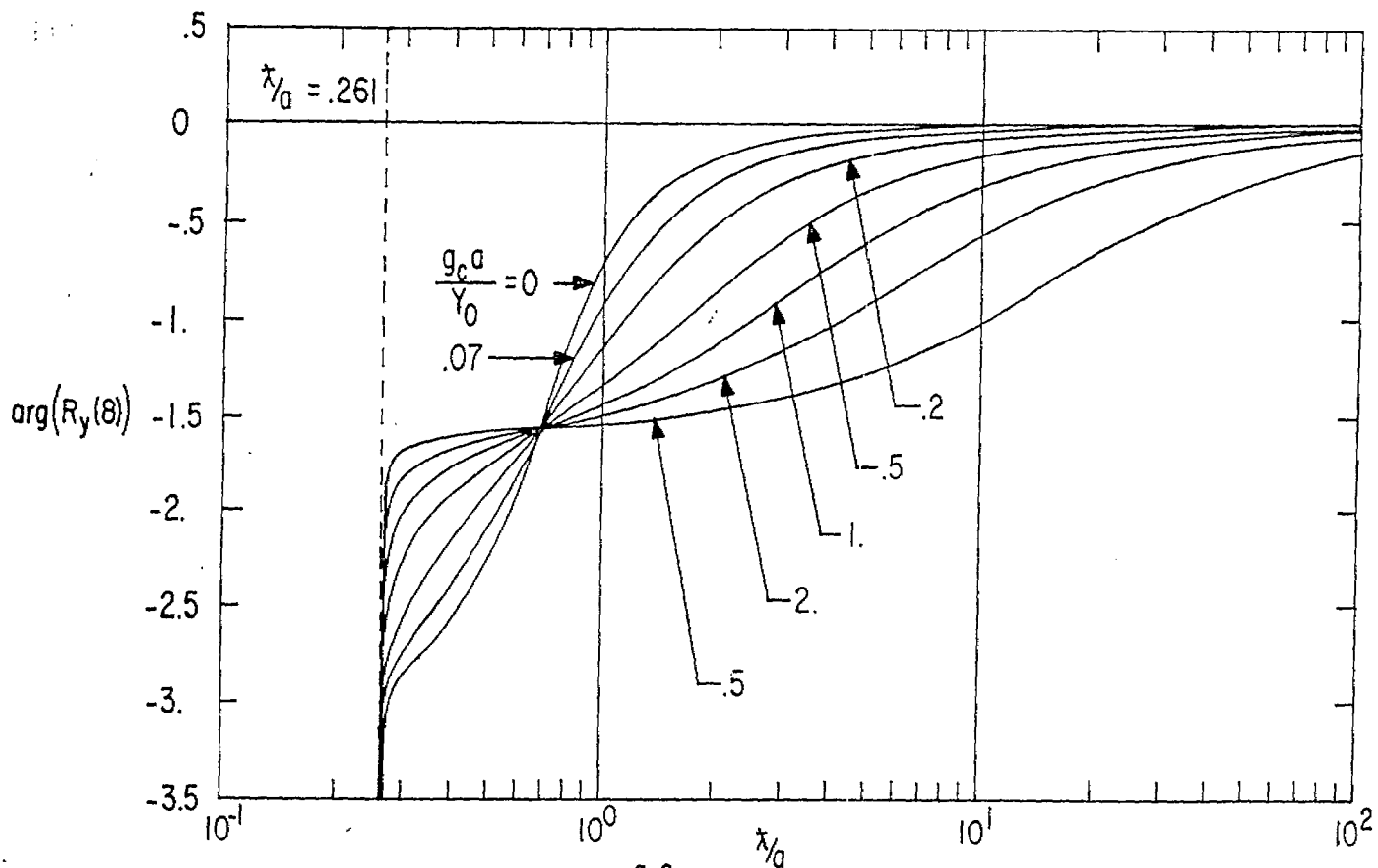


B. PHASE OF $R_y(4)$ vs. x/a WITH $\frac{g_c a}{Y_0}$ AS A PARAMETER

FIGURE 16. EFFECT OF ADMITTANCES ON RESPONSE: $N=4$, $\phi_0 = .1$



A. MAGNITUDE OF $R_y(s)$ vs. λ/a WITH $\frac{g_c^a}{Y_0}$ AS A PARAMETER



B. PHASE OF $R_y(s)$ vs. λ/a WITH $\frac{g_c^a}{Y_0}$ AS A PARAMETER

FIGURE 17. EFFECT OF ADMITTANCES ON RESPONSE: $N=8, \phi_0 = .1$

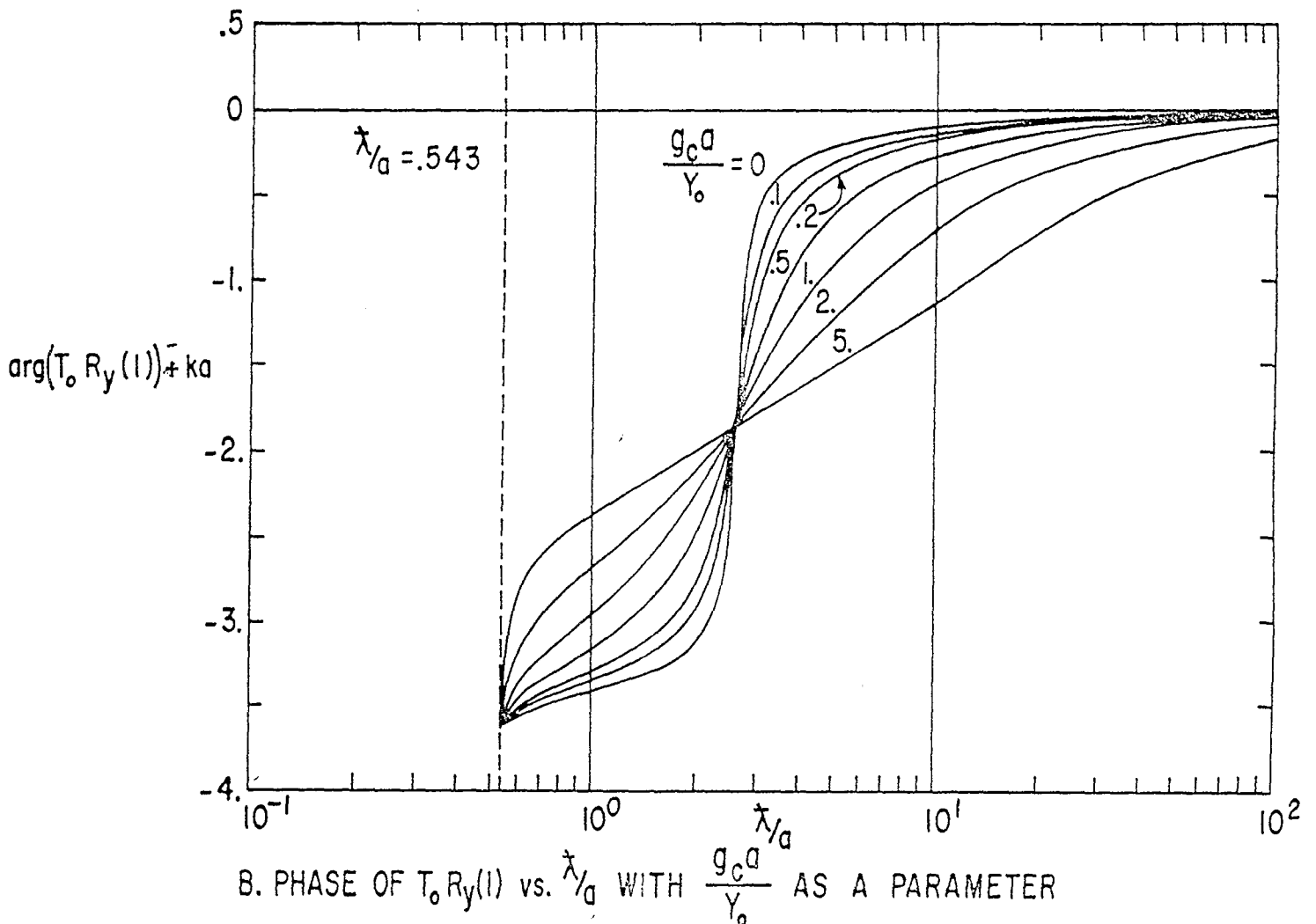
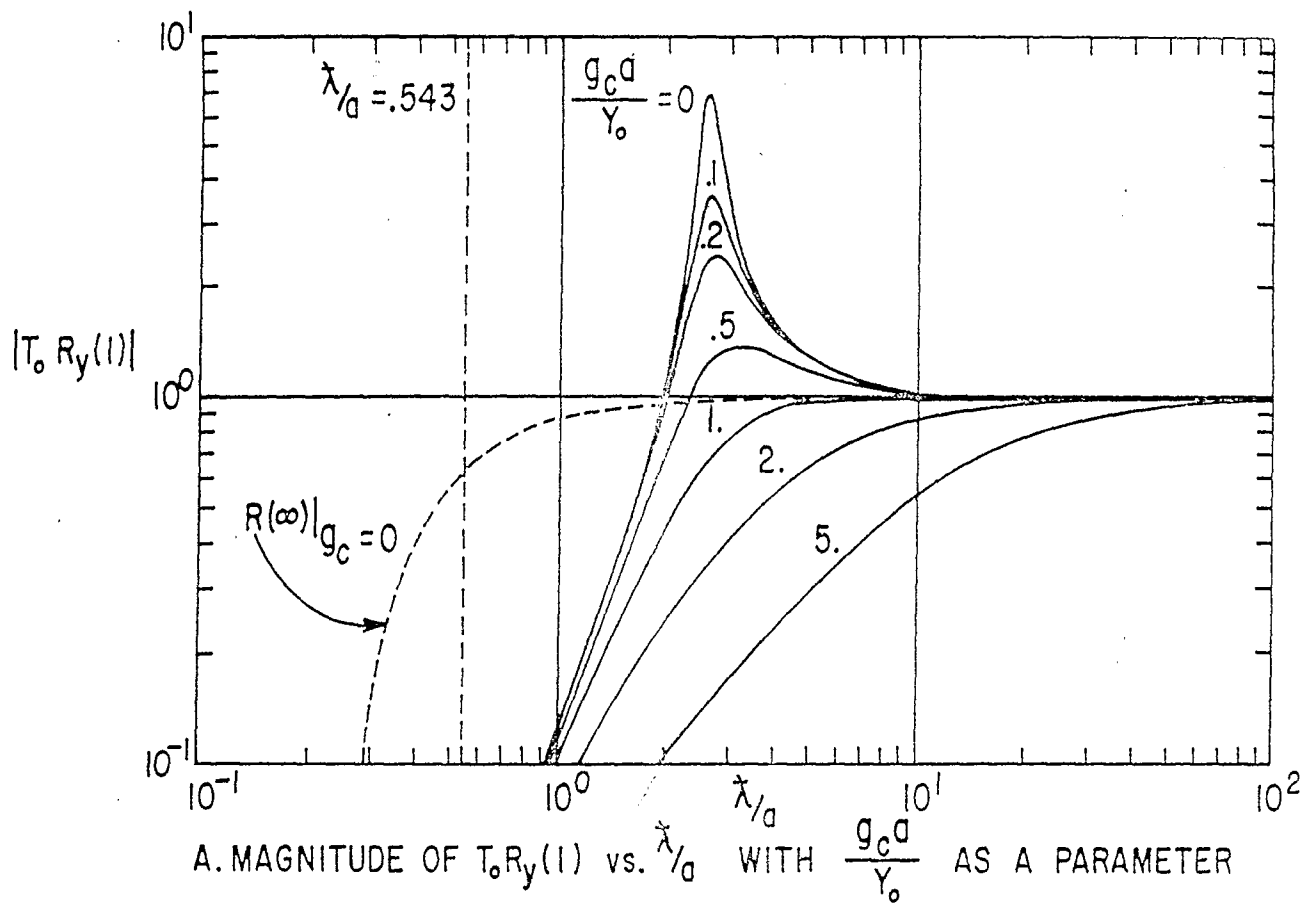
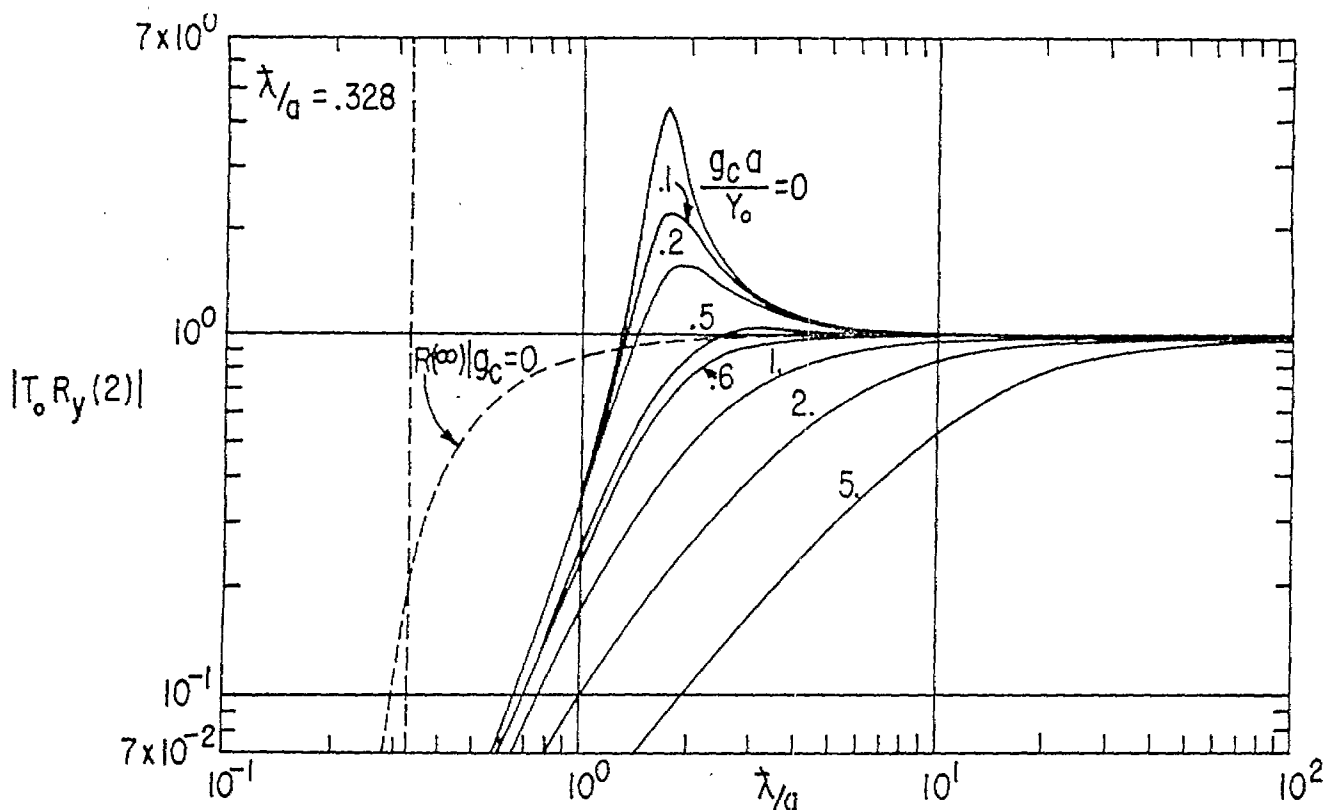
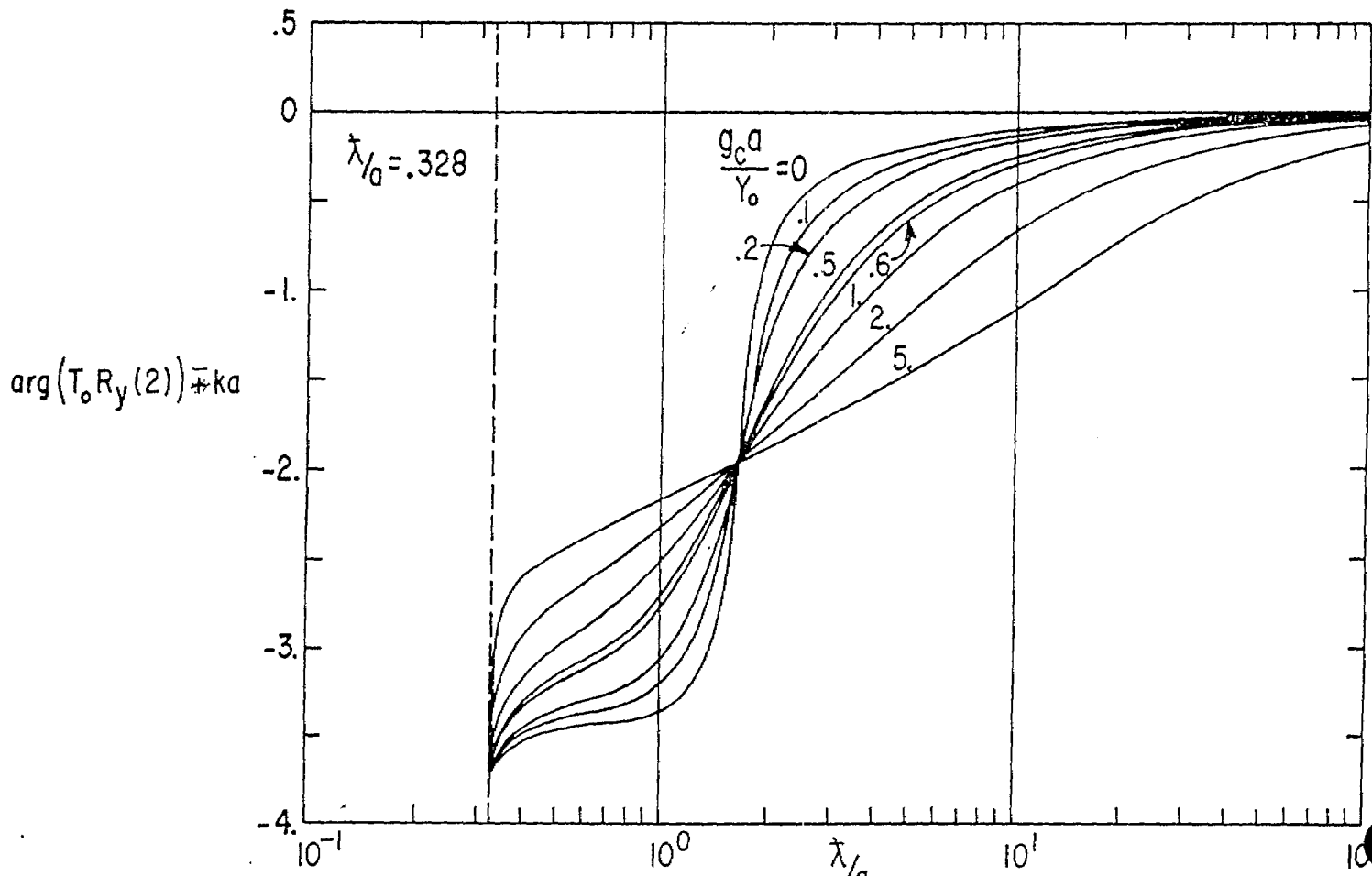


FIGURE 18. ARTIFICIAL RESPONSE CHARACTERISTICS: $N = 1, \phi_o = .1$

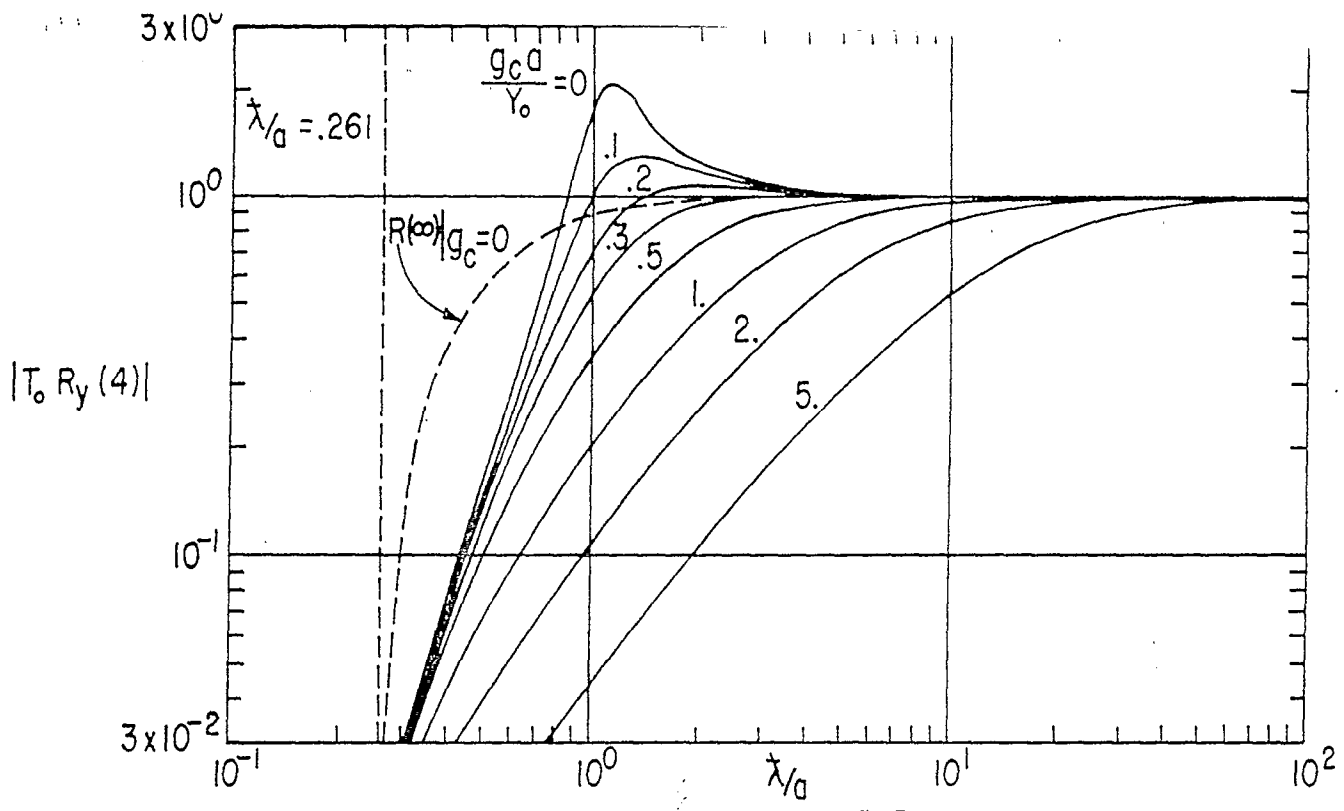


A. MAGNITUDE OF $T_o R_y(2)$ vs. λ/a WITH $\frac{g_c a}{Y_o}$ AS A PARAMETER

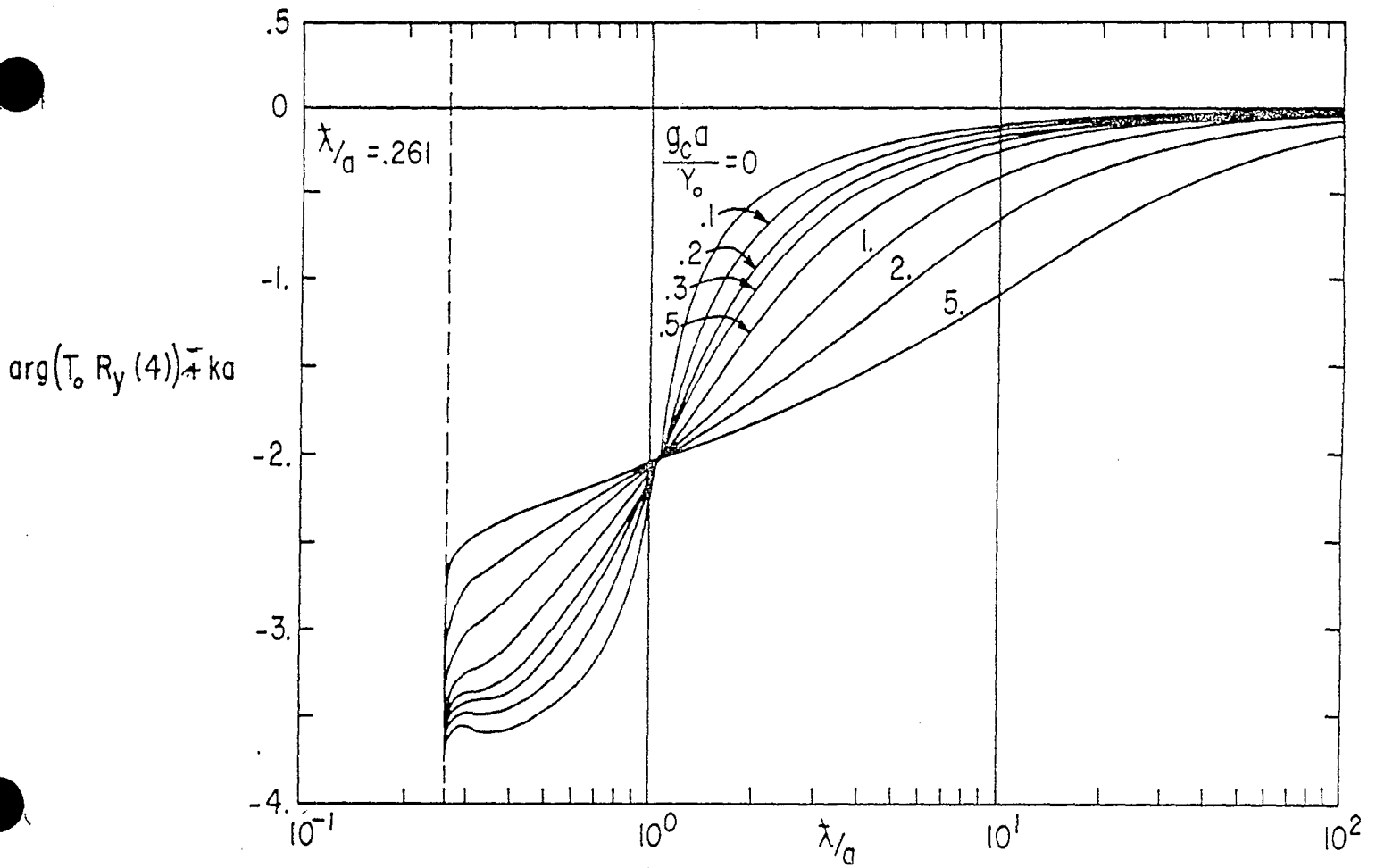


B. PHASE OF $T_o R_y(2)$ vs. λ/a WITH $\frac{g_c a}{Y_o}$ AS A PARAMETER

FIGURE 19. ARTIFICIAL RESPONSE CHARACTERISTICS: $N=2$, $\phi_o = .1$

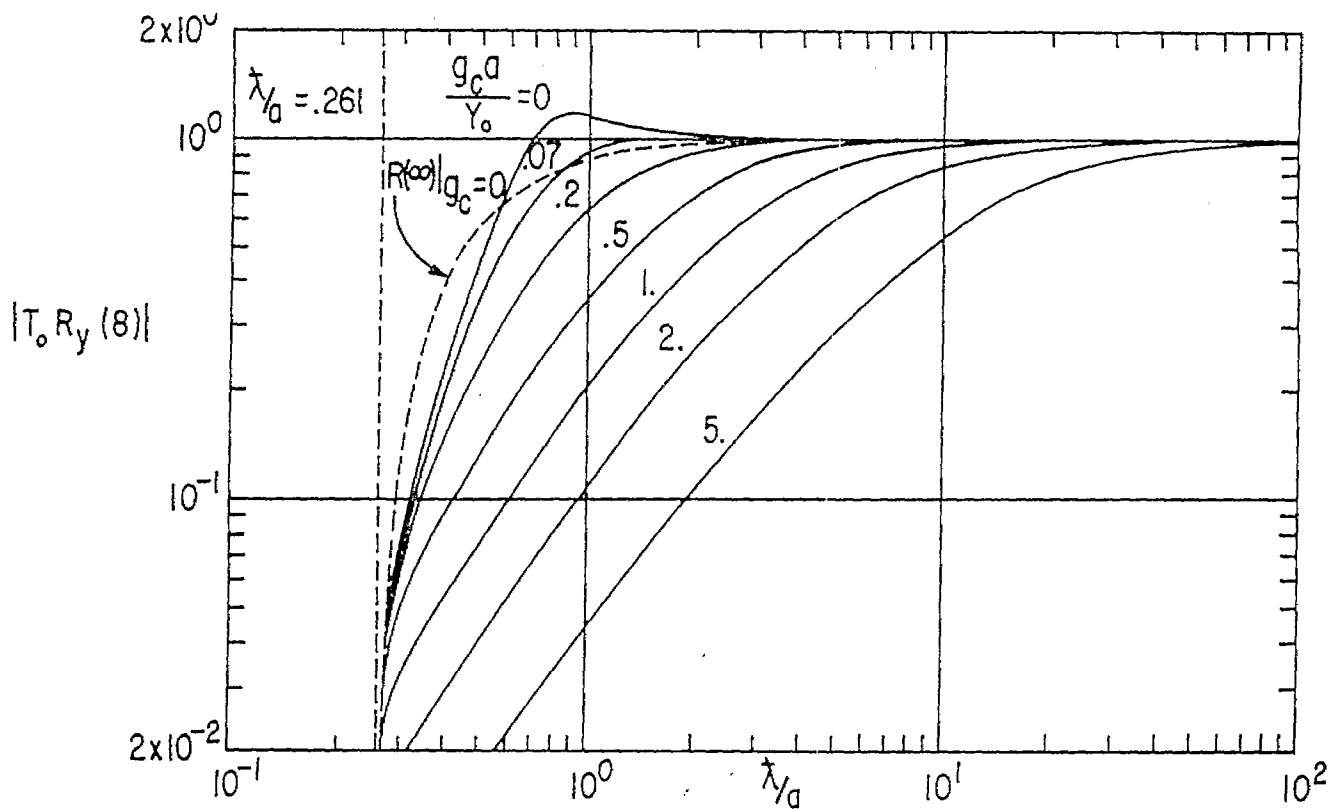


A. MAGNITUDE OF $T_0 R_y(4)$ vs. λ/a WITH $\frac{g_c a}{Y_0}$ AS A PARAMETER

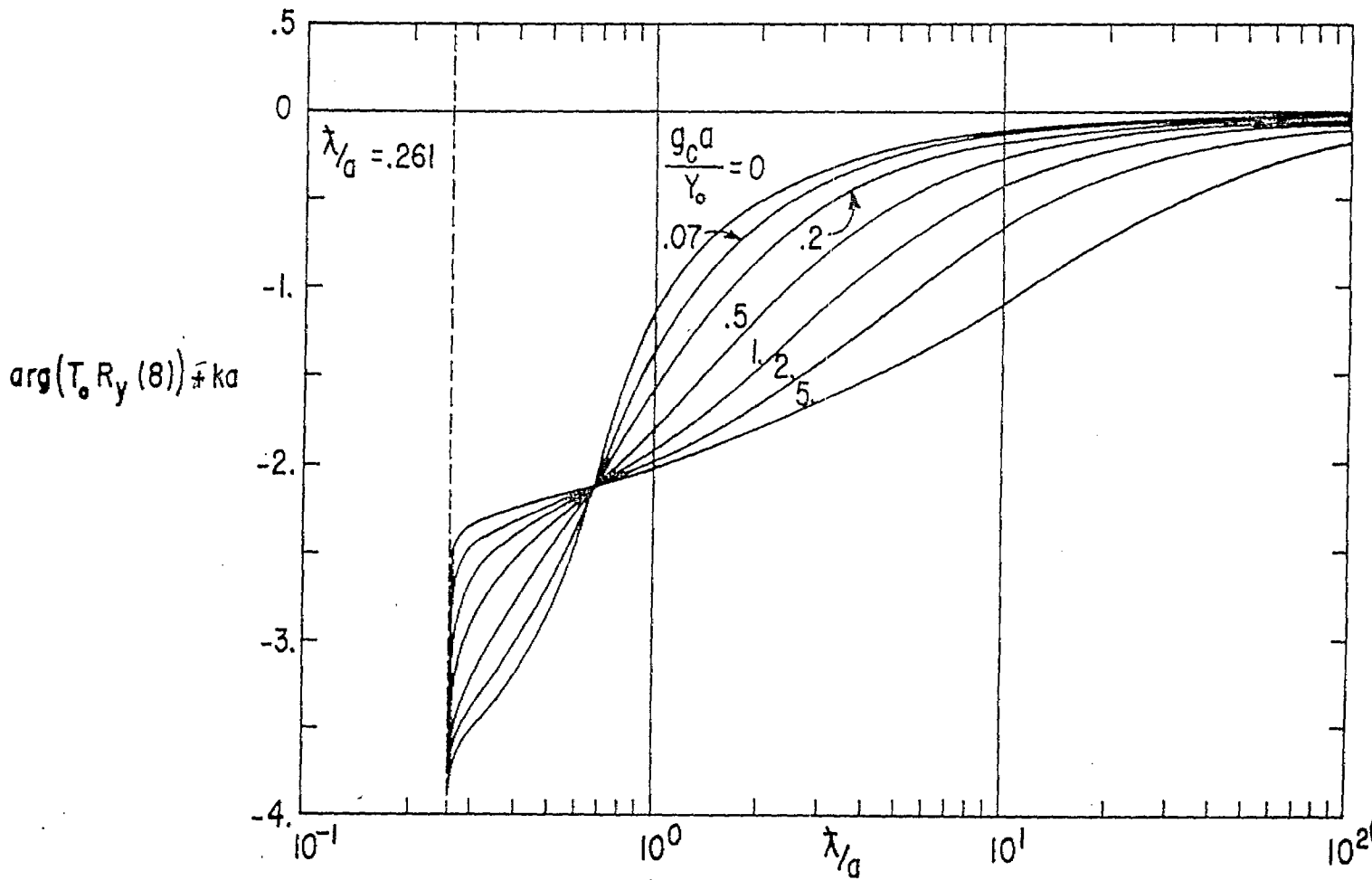


B. PHASE OF $T_0 R_y(4)$ vs. λ/a WITH $\frac{g_c a}{Y_0}$ AS A PARAMETER

FIGURE 20. ARTIFICIAL RESPONSE CHARACTERISTICS: $N=4$, $\phi_0 = .1$



A. MAGNITUDE OF $T_o R_y(s)$ vs. λ/γ_a WITH $\frac{g_c^a}{\gamma_o}$ AS A PARAMETER



B. PHASE OF $T_o R_y(s)$ vs. λ/γ_a WITH $\frac{g_c^a}{\gamma_o}$ AS A PARAMETER

FIGURE 21. ARTIFICIAL RESPONSE CHARACTERISTICS: $N=8, \phi_o=.1$

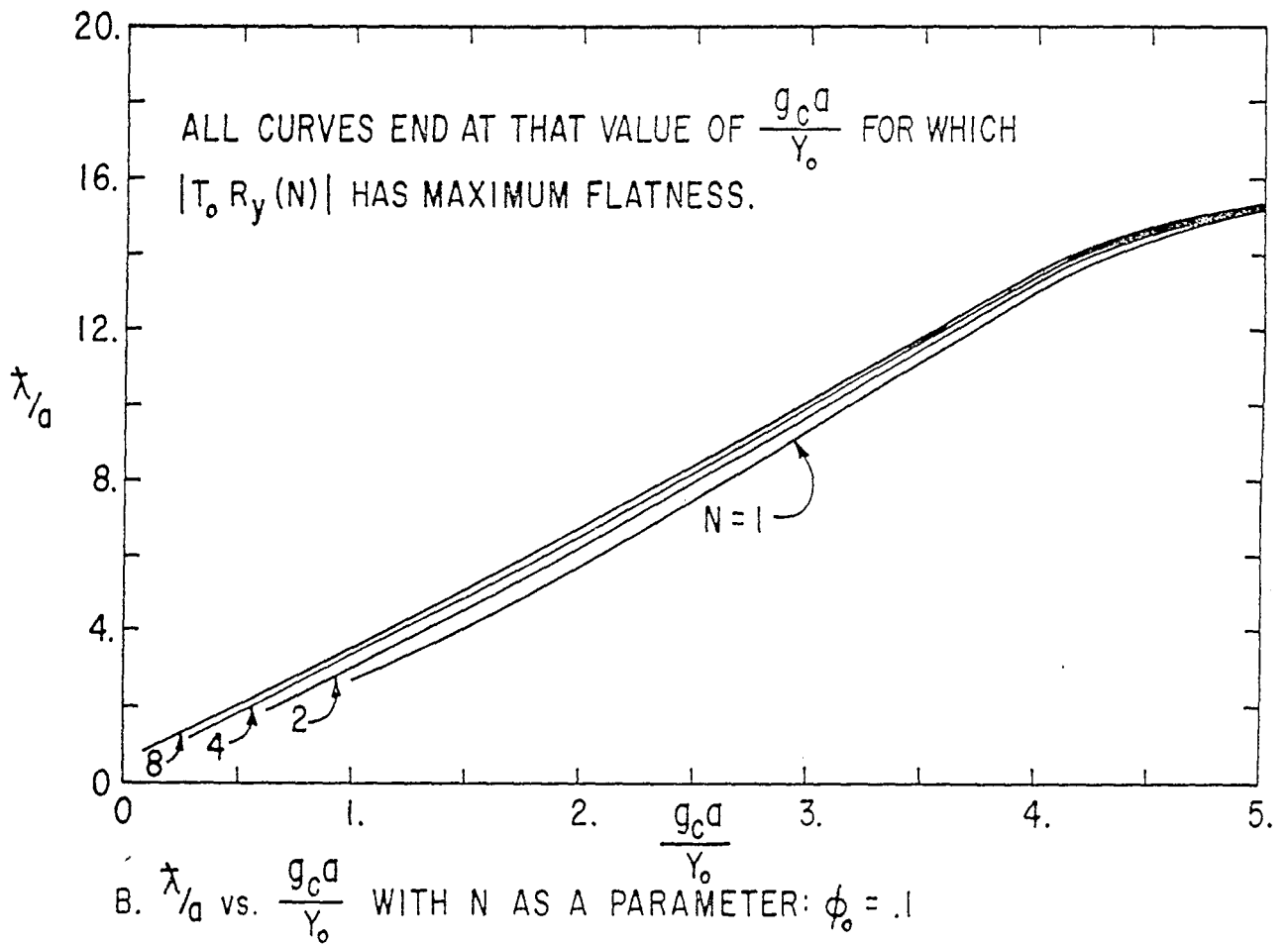
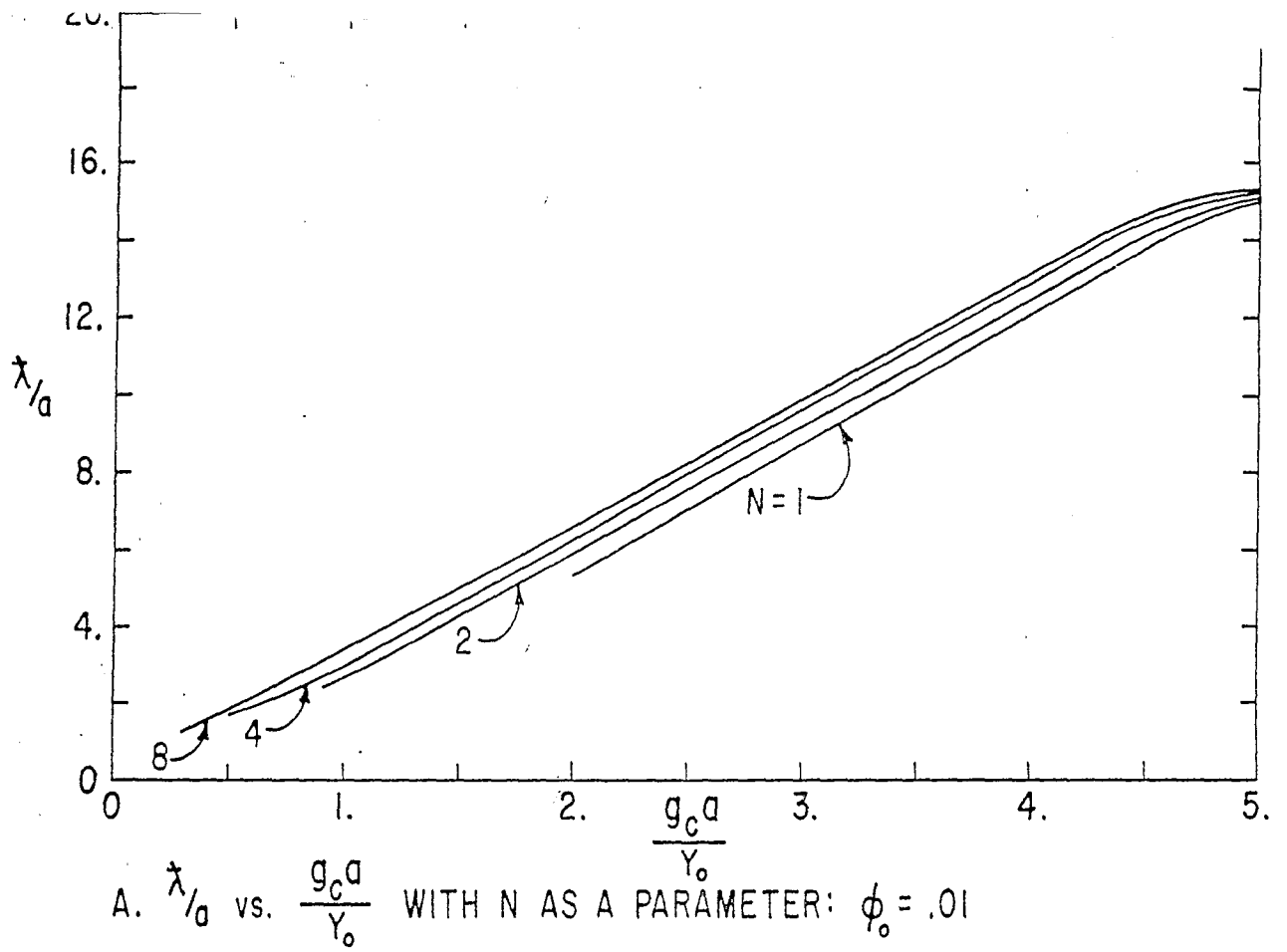


FIGURE 22. DEPENDENCE OF FREQUENCY RESPONSE ON CABLE CONDUCTANCE:
 $|T_0 R_y(N)| = 1/\sqrt{2}$

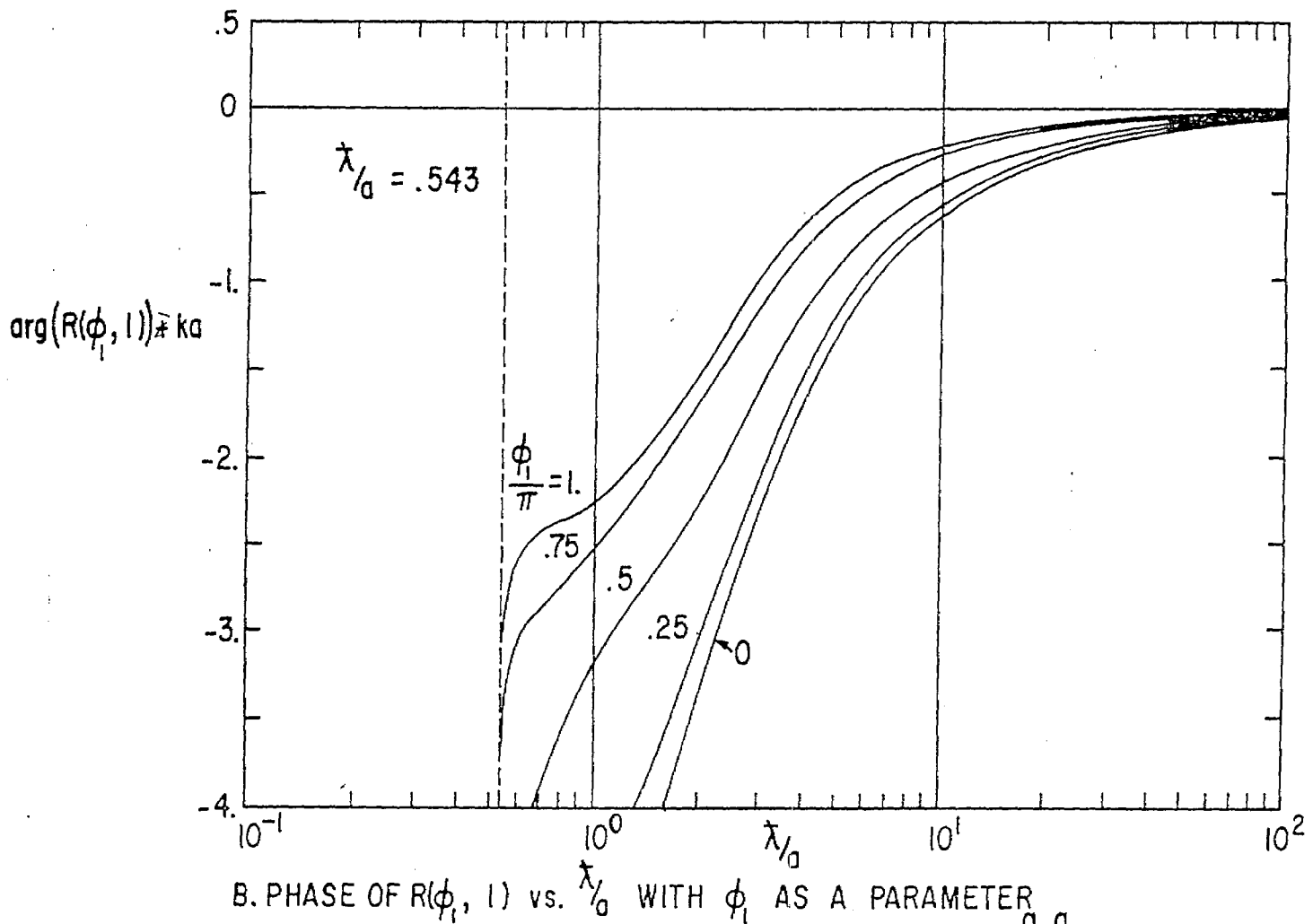
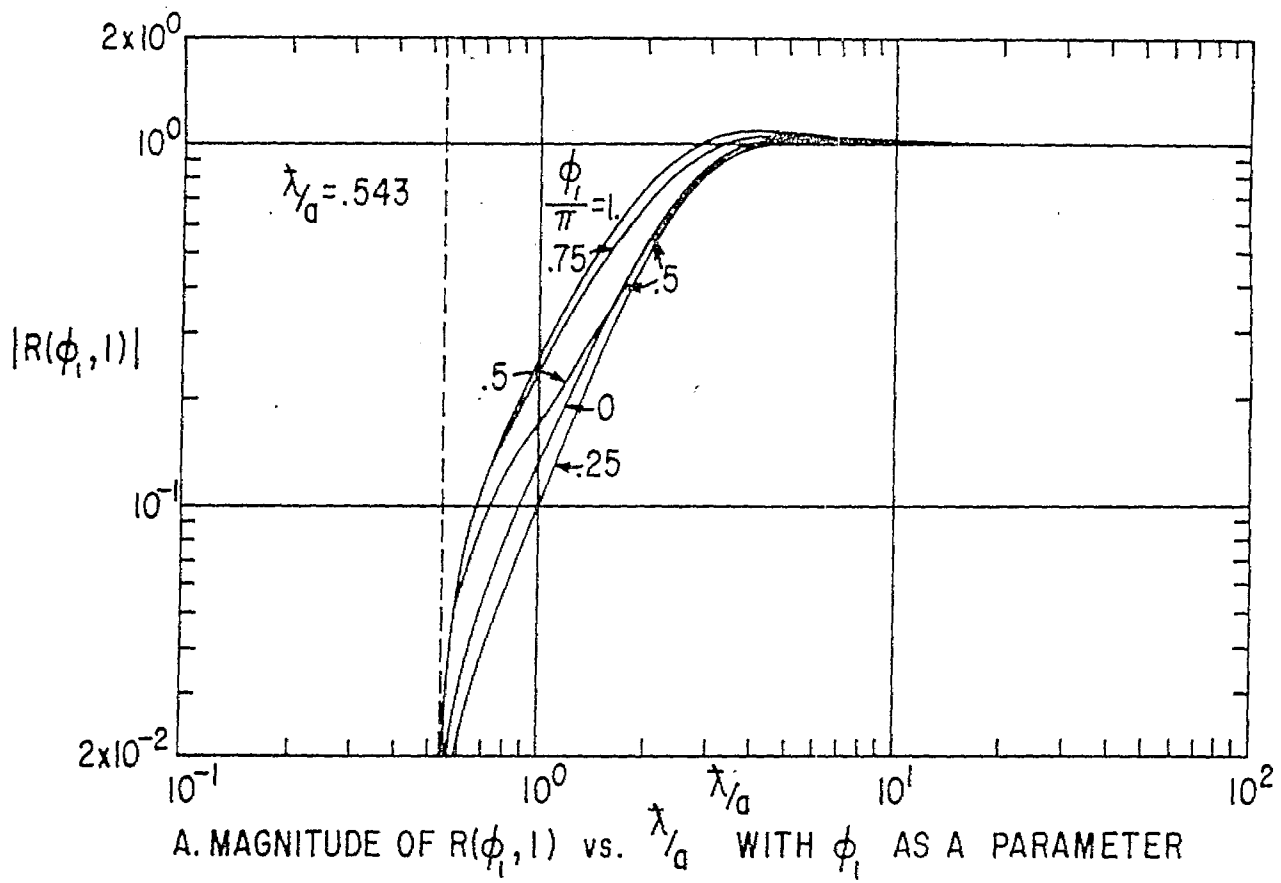
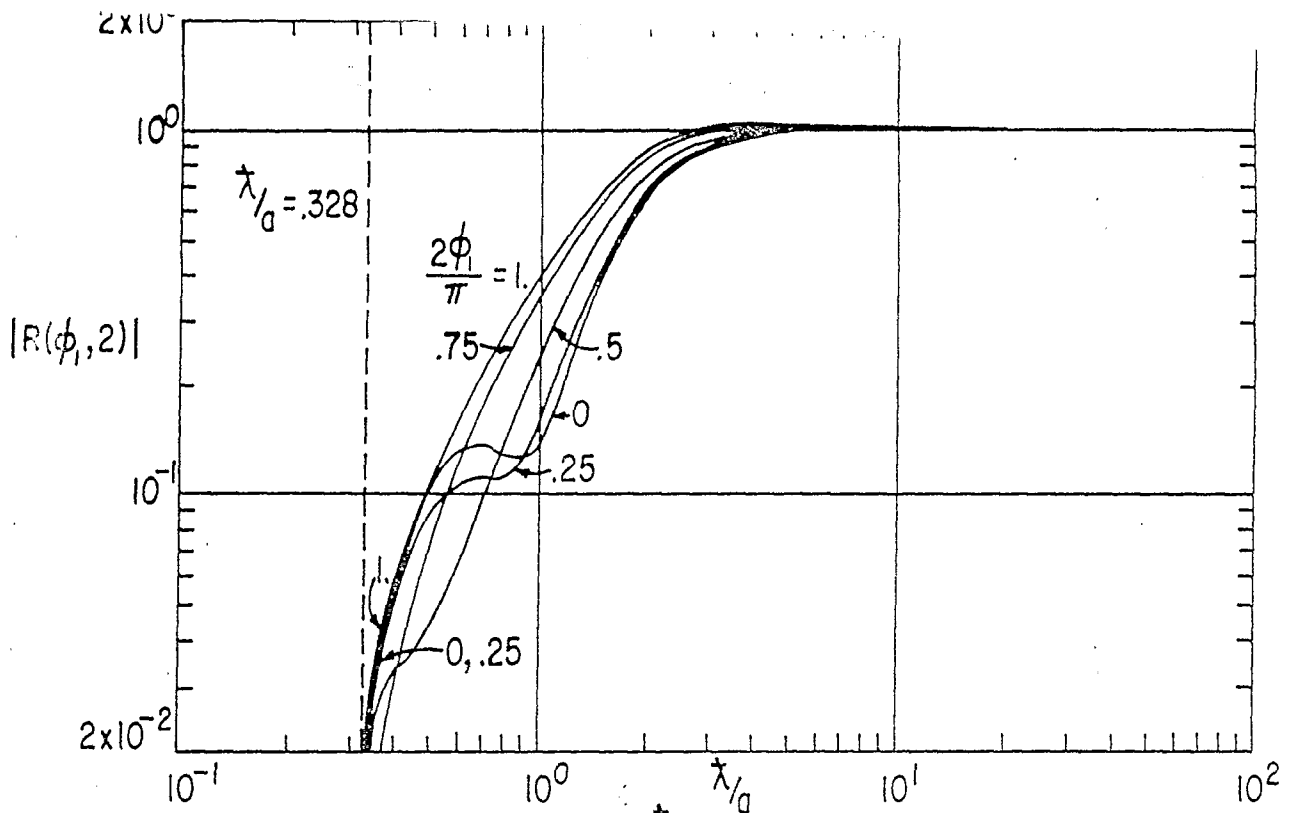
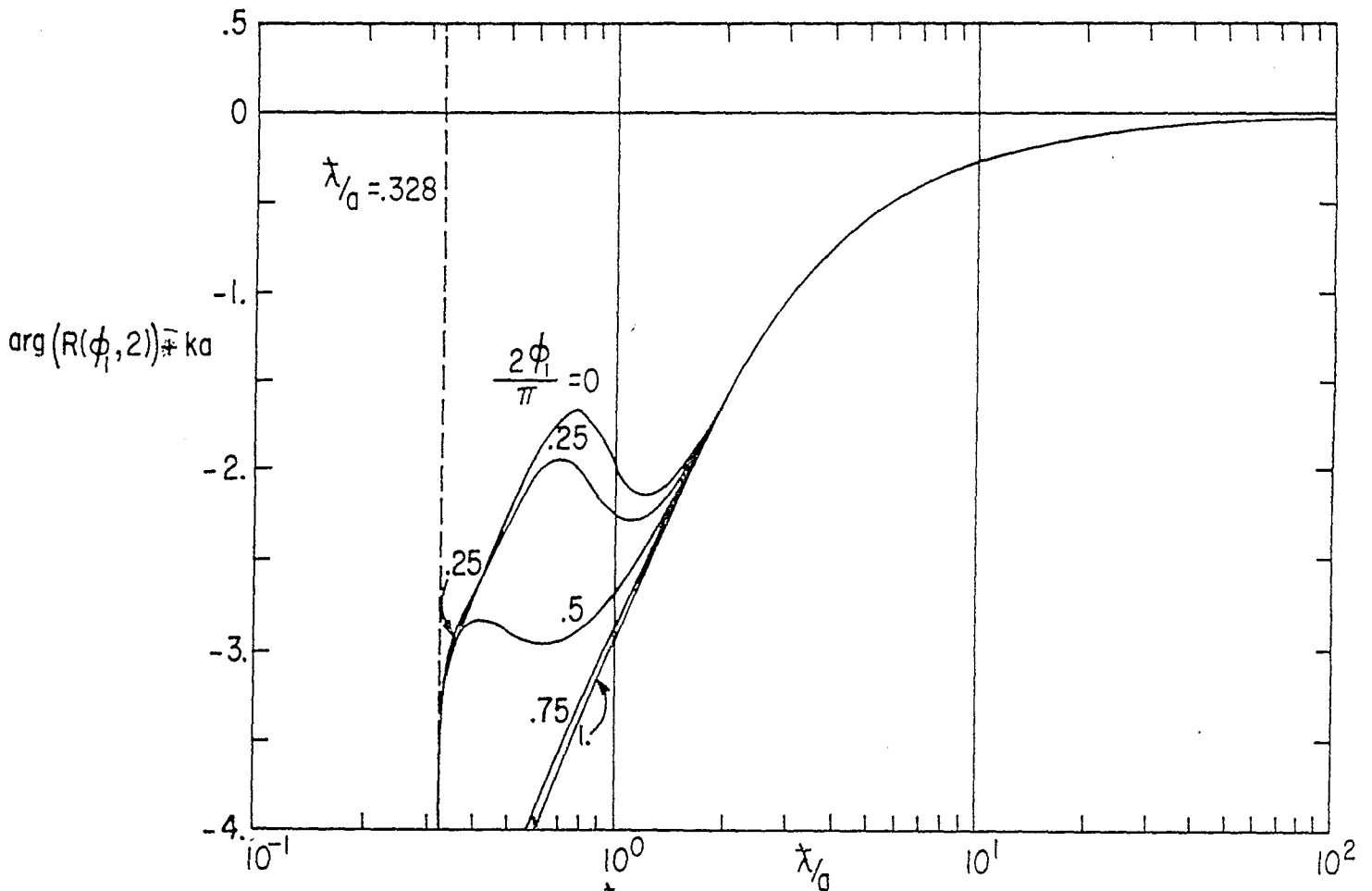


FIGURE 23. RESPONSE CHARACTERISTICS: $N = 1, \phi_0 = .1, \frac{g_c a}{Y_0} = 1.$



A. MAGNITUDE OF $R(\phi_1, 2)$ vs. λ/a WITH ϕ_1 AS A PARAMETER



B. PHASE OF $R(\phi_1, 2)$ vs. λ/a WITH ϕ_1 AS A PARAMETER

FIGURE 24. RESPONSE CHARACTERISTICS: $N=2, \phi_0 = .1, \frac{g_c a}{\gamma_0} = .6$

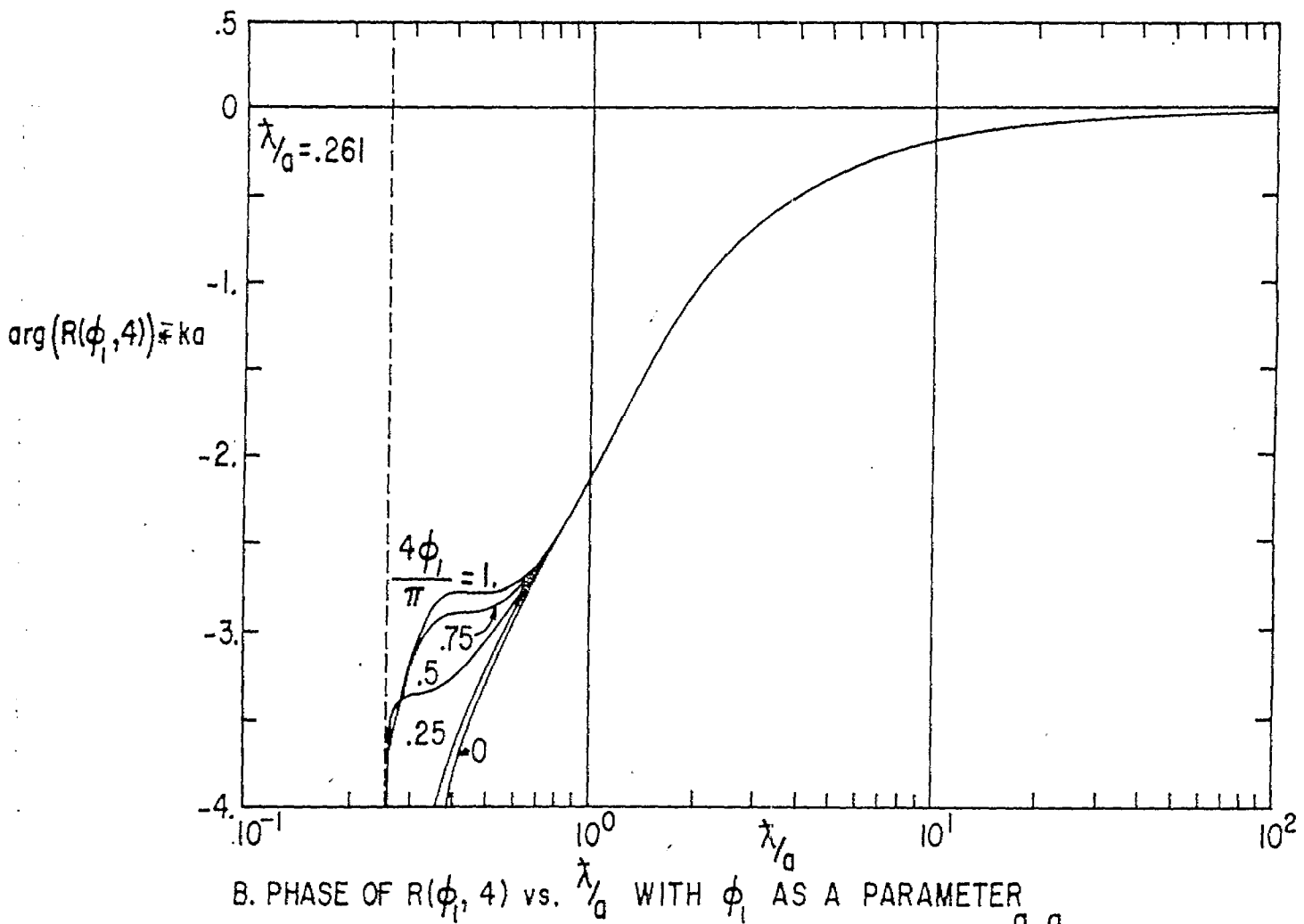
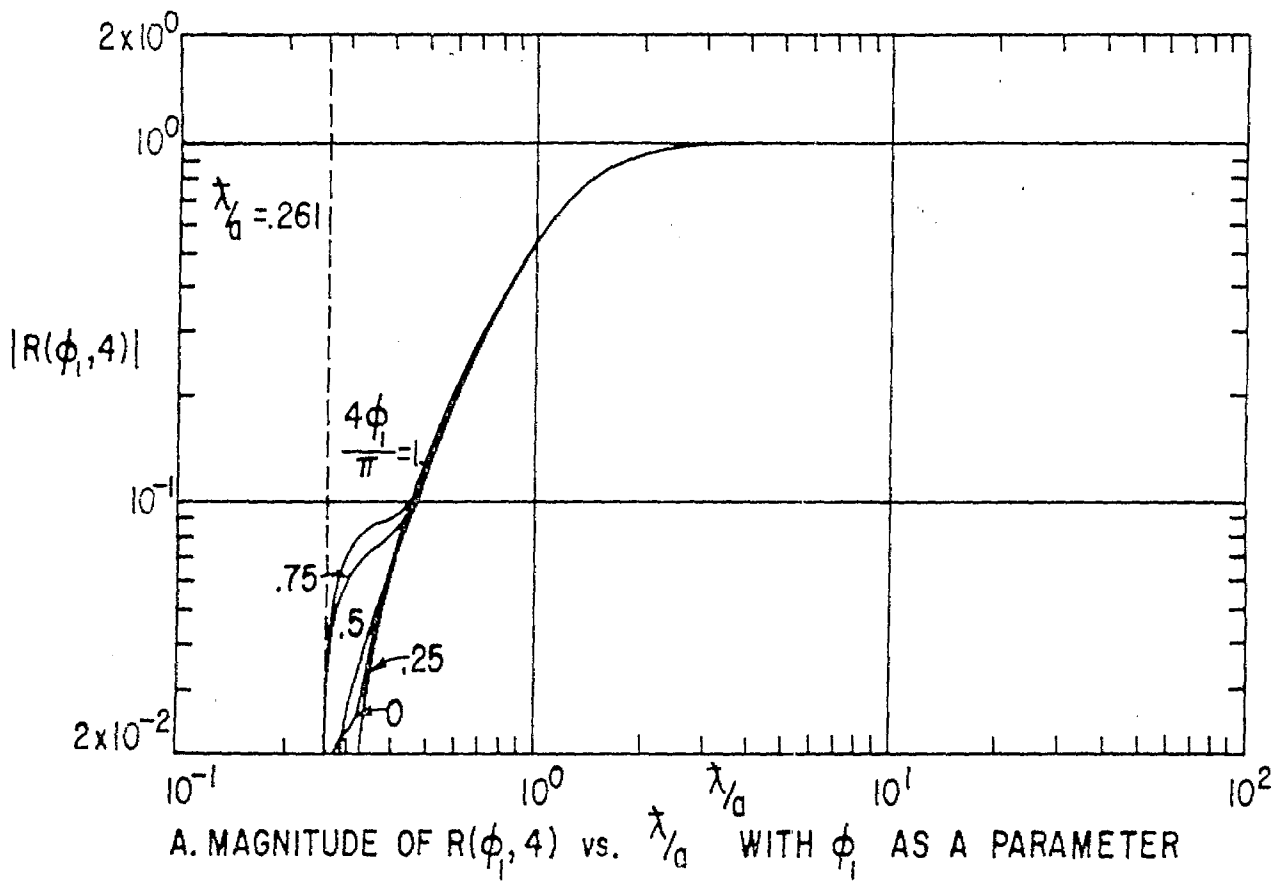
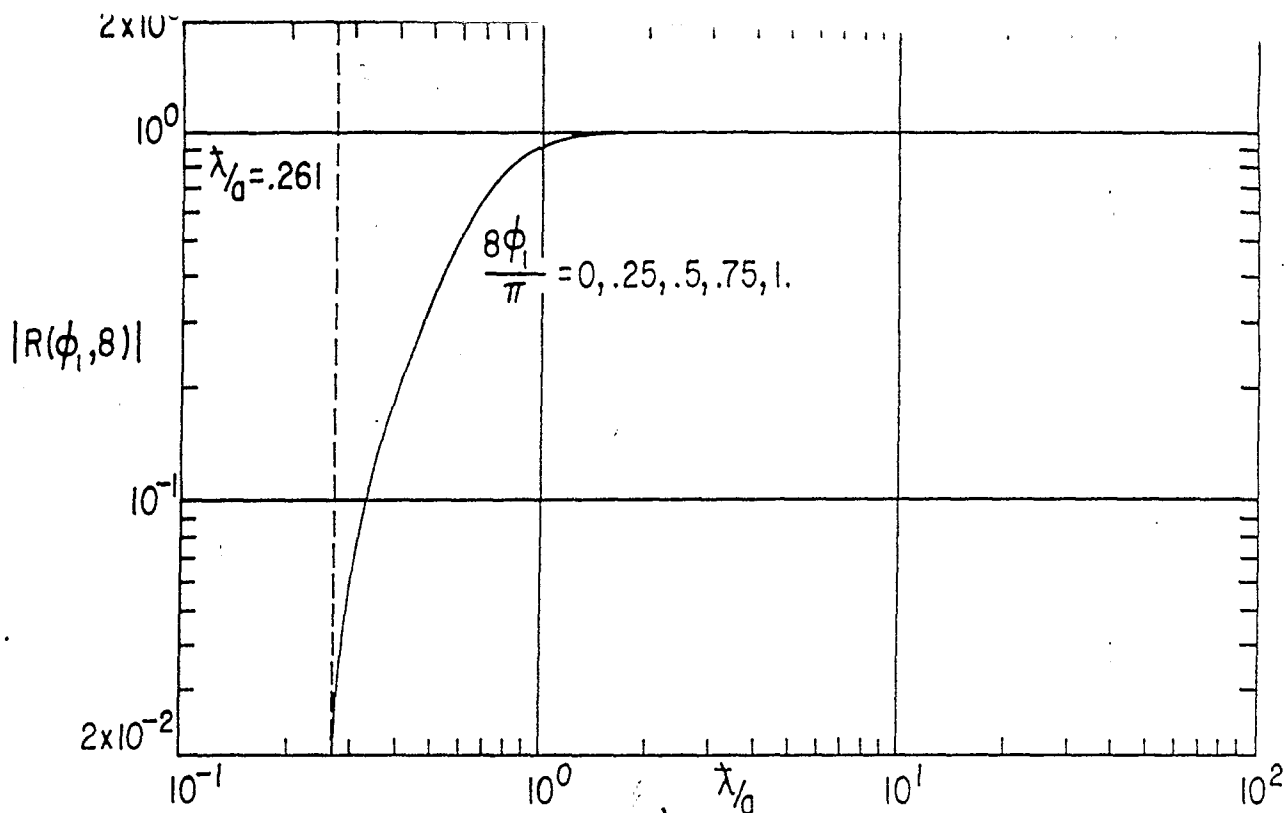
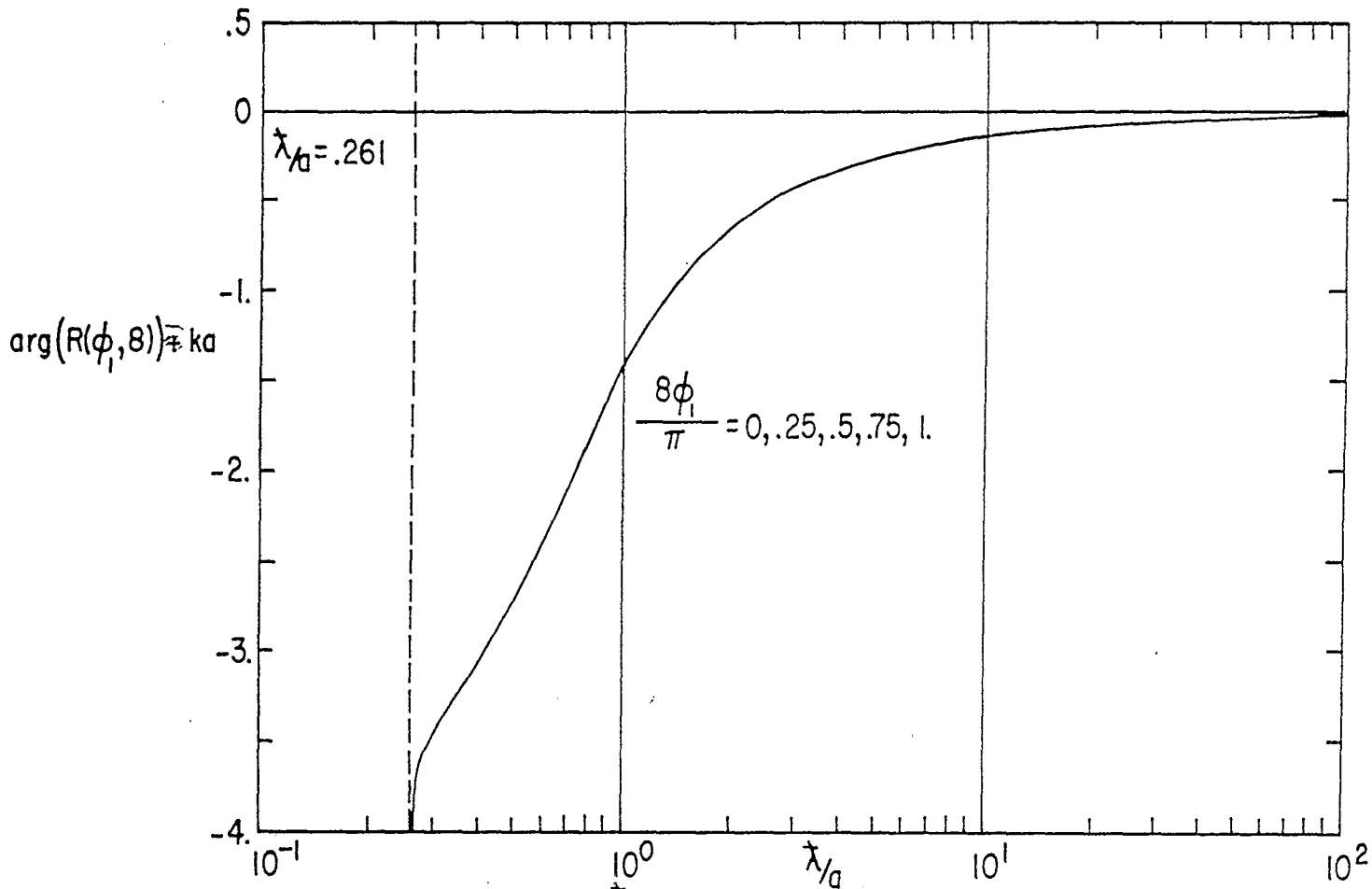


FIGURE 25. RESPONSE CHARACTERISTICS: $N=4$, $\phi_0 = .1$, $\frac{g_c a}{Y_0} = .3$



A. MAGNITUDE OF $R(\phi_1, 8)$ vs. λ/λ_0 WITH ϕ_1 AS A PARAMETER



B. PHASE OF $R(\phi_1, 8)$ vs. λ/λ_0 WITH ϕ_1 AS A PARAMETER

FIGURE 26. RESPONSE CHARACTERISTICS: $N = 8$, $\phi_0 = .1$, $\frac{g_{ca}}{Y_0} = .07$